Fines are charged at 50p per hour

28 MAR 2002

5·00

INVESTIGATIONS OF THE OPTOELECTRONIC

BEHAVIOUR OF NOVEL PHTHALOCYANINE

LANGMUIR-BLODGETT FILMS

by

ANDREW J. HIBBERD   BSc

A thesis submitted in partial fulfilment of the requirements of Sheffield Hallam

University for the degree of Doctor of Philosophy

January 1996

Collaborating Organisation: Health and Safety Executive

Department of Engineering Information Technology

Sheffield Hallam University

Sheffield, England.

DECLARATION

I hereby declare that this thesis is entirely my own work and that it has not been

submitted as an exercise for a degree at any other University.

(signature)

Andrew J. Hibberd

ACKNOWLEDGEMENT

ABSTRACT

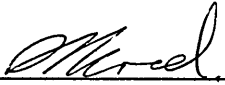A review of phthalocyanine materials is presented, their history, properties, applications, and potential. The two materials under investigation in this thesis (A410 H_2 and A40iso6 H_2) are introduced as metal free, non-peripheral octa-substituted phthalocyanines, molecularly engineered for Langmuir-Blodgett deposition by M. Cook at the University of East Anglia.

The Langmuir-Blodgett method is used to deposit the two materials in the Y-form, onto substrates of glass and gold plated glass, and on quartz with interdigitated platinum electrodes.

Optical absorption spectra are obtained for the materials, and the linear relation between the absorption intensity and thickness confirmed. The variation in optical absorption with polarisation and angle of incidence is used to obtain the molecular orientation of the two phthalocyanines. The polarisation results confirm earlier observations. The molecular orientation angles (with respect to the substrate) obtained in this thesis are novel for these materials, and confirm the Herringbone alignment of molecular pairs.

Surface Plasmon resonance is used to obtain a refractive index of 1.629, and a thickness of 17.2 nm for a 6 layer film of the A410 material.

The electrical properties were measured using samples of the film deposited on substrates with interdigitated electrodes. The spectral photocurrent, conductivity, and activation energy under illumination were investigated for both materials.

The electrical response of the films to temperature, voltage and gaseous environment is presented with the time dependent photocurrent response.

The characterisation measurement techniques are discussed and suggestions for improvements and further work are made.

CONTENTS

v

CHAPTER 1

INTRODUCTION

1.1 Organic materials

Until recently, inorganic materials, such as single crystal silicon, have been largely relied on by the microelectronics and optoelectronics industry. However, as the perceived limitations of these inorganics begin to restrict the realisation of more complex system designs, more attention is being focused on the organic solid state. The range and variety of organic materials available, and the possibilities achievable through molecular engineering offers enormous potential for fabricating advanced structures.

The best known application of organic materials is that of liquid crystals and their use in displays. New materials and phenomena are being discovered and seem likely to lead to much improved devices. Other examples are piezoelectric polymers, photoconducting polymers for photocopying, and photochromic molecules for reversible high density optical storage and signal processing. Biosensors and chemical sensors for converting specific biochemical or chemical interactions into electrical signals for use in industry or medical applications are further applications. All of these applications have in common their engineered organic molecular component performing an active function; thus using molecular engineering to optimise molecular electronics (Roberts 1985).

1.2   Langmuir-Blodgett Deposition

Certain organic substances have the ability to form a film of one molecule in thickness when placed on the surface of water. These materials invariably consist of amphiphillic molecules, i.e. molecules that posses both hydrophobic and hydrophillic chemical groups. This phenomenon has been known for many hundreds of years. The first application is believed to be the Japanese printing art called *sumi-nagashi*. In this century Irving Langmuir and Katharine Blodgett extensively investigated the transfer of fatty acid monolayers from a water surface to a solid substrate. This was performed by withdrawing the substrate through the air water interface dragging the monolayer from the water surface onto the substrate. This work has left their names firmly associated with the resulting films.

As Langmuir-Blodgett deposition is performed at a molecular level, the immediate environment must be maintained under very clean conditions. The presence of contaminants can easily disrupt the process. The advantages of this film forming technique are the high degree of ordering, and the precise control of the film thickness. Also the ability to manufacture films with a thickness of one monolayer or alternating sandwich structures of two molecular components has clear device benefits (Petty 1987).

1.3   Optical Absorption

The phthalocyanine material group is most commonly known as a dark blue dye in the clothing and paint industries. As the perceived colour of a material is dependant upon the electronic configuration of its molecules, it follows that such coloured materials should be investigated using optical interrogation. The usual technique is to study the optical absorption properties of the material. This is performed by measuring the light attenuation of a sample material as a function of light wavelength. The resulting spectrum is used to identify the electronic structure of the material. Light photons of energy $E_l = hc/\lambda$ incident on the material are absorbed if the energy shift between levels of the molecule $E_g = E_l$. The atomic band structure of the solid material, can be obtained by relating the wavelength of the absorption peaks to an electronic band gap model.

A further application of optical absorption is the use of polarised light interrogation at varying angles of incidence. The absorption process is dependant on the orientation of the dipole moments in the material. A material with un-symmetrical charge distribution (dipole moment) will have a strong or weak light absorption depending on whether the direction of the dipole coincides with the direction of polarisation of the incident light. Clearly it is possible to obtain an indication of the orientation of these dipoles, and hence the molecules themselves, by measuring the light absorption as a function of polarising direction and incident angle of the light source.

1.4   Surface Plasmon Resonance

Surface Plasmon Resonance (SPR) has received much attention recently for its application in gas sensors. This optical detection method investigates the effect organic films have on the surface plasmon resonance properties of a thin metal film. The excitation is ensured by using the principle of total internal reflection of a prism to amplify the monochromatic light source. A surface plasmon is a surface charge density wave at a metal surface. If the metal is sandwiched between two materials of different dielectric constant, placed in intimate contact with the back of the prism, then resonance can occur. Resonance is observed as sharp minimum in the reflectance, R, when measured as a function of incidence angle (θ). The resonance angle (θ_r) is ultra-sensitive to variations in the refractive index of the medium adjacent to the metal film. For example, the small change in an organic film due to a gas absorption can easily be monitored even if the active gas is of concentrations in the parts-per-billion range.

The gas active film is ideally thin and of high ordering. The Langmuir-Blodgett film deposition technique is ideally suited to this application.

As SPR is sensitive to the properties of the organic medium adjacent to the metal film, it is possible to obtain the refractive index and thickness of this organic medium.

1.5   Optoelectronics

The natural orientation properties and degree of control over molecular structure are good reasons for utilising organic Langmuir-Blodgett films in optoelectronics. In this field, materials with interesting non-centrosymmetric structures are required. In order to avoid the symmetry inherent in multilayer Langmuir-Blodgett films, it would appear that each alternate layer should be of a different inactive material to retain the permanent polarisation of the active component. This is achieved using a Langmuir-Blodgett alternate-layer-deposition trough. Highly efficient non-linear optics materials would permit functions such as frequency conversion, parametric amplification, switching and modulation to be performed in a totally optical manner without the need for electron-phonon conversion processes. This optical analogue of electronics is sometimes referred to as "photonics" (Truong et al. 1994).

The use of copper phthalocyanine has been investigated as an optical storage medium (Chen et al. 1994). They indicated the potential of this material as a practical write-once, read-many recording medium.

Alternate Langmuir-Blodgett films of Docosanoyl Itaconate/1-Docosylamine were investigated by Tsibouklis et al (1991) who observed a pyroelectric coefficient of $1.4\mu Cm^{-2}K^{-1}$.

1.6   Outline of Thesis

The materials tested in this thesis are novel metal free phthalocyanines, molecularly engineered to be deposited by the Langmuir-Blodgett method. Their intended application is in the optoelectronics field. The properties of interest to device engineers are centred on the structure of the film, the optical properties of the film and the electrical properties of the film.

The molecular orientation of the film molecules was measured geometrically in chapter 3 from information obtained during the Langmuir-Blodgett deposition. The molecular orientation with respect to the substrate was investigated to a fuller extent in chapter 4 using polarised light optical spectroscopy.

Useful optical information can be gained from the optical spectra, the absorption wavelength range, the electronic transitions in the molecule and the molecule-molecule interactions can be surmised from the spectra. Further to this a measure of the refractive index of the film would be of importance for devices that require index matching of constituent materials and for modelling of the optical path. The Surface Plasmon method was chosen as it allows the measurement of the refractive index of a Langmuir-Blodgett film without knowing its thickness. The Surface Plasmon technique also enables calculation of the film thickness, and has potential as an imaging tool to observe defects in Langmuir-Blodgett films.

The relation between the photocurrent and applied voltage, temperature, wavelength of incident light and presence of ambient gases, together with the time dependence of the film to a change in the conditions, all provide important

information. This information would be used to anticipate the performance of the film in a given device situation. In addition to this an investigation into the conduction regime of these materials will be of use for modelling the conduction properties, and for comparison between similar materials.

In chapter 2 a review of the work undertaken on phthalocyanine materials is presented. Their historical development and current applications are described, together with a review of their structures and methods for manipulating these materials to form devices. The approach used in this thesis for selecting certain properties for investigation is explained.

Chapter 3 is an introduction to, and an in-depth examination of the Langmuir-Blodgett method for depositing thin monomolecular films onto solid substrates. A description of the techniques used to obtain the samples tested throughout this thesis is presented with examples of the isotherms produced and initial tests of the quality and structure of the film.

Chapter 4 presents initial optical tests performed on the samples. The physical process of absorption is described and a method of using polarised light to measure the orientation of the molecules in the film is investigated. The experimental techniques are described and a set of results is presented together with an analysis of the material tested and comparisons with other work in the field.

Chapter 5 is concerned with the surface plasmon method of measuring the refractive index and thickness of an organic film deposited on a thin metal layer. The theoretical aspects are described together with the presentation of the

procedure and an analysis of the results obtained. An interesting method of imaging the film using resonance contrast is discussed and a pair of trial pictures produced using this method are presented.

Chapter 6 contains electrical work performed on the phthalocyanines tested in this thesis. An investigation of the photocurrent response of the phthalocyanine films deposited on interdigitated electrodes is presented. A brief review of device applications of organic films is presented with the experimental techniques and proposed conduction mechanisms. The effects of temperature, vacuum, incident light wavelength and time on the photocurrent are investigated.

Chapter 7 summarises the thesis and draws together the individual investigations of these materials and presents the final conclusions. Suggestions for further work conclude this chapter.

Chapter 2

REVIEW OF PHTHALOCYANINES AND THEIR APPLICATION AS THIN FILMS

2.1 Historical Perspective.

In 1928, scientists discovered a new class of organic compound while preparing phtalimide by passing ammonia into molten phthalic anhydride in an iron vessel. The blue residue thus obtained was named "phthalocyanine" from the Greek naptha and cyanine meaning rockoil and dark blue respectively. Molecular similarity to chlorophyll and porphyrin molecules enabled the simulation of naturally occurring phenomena. Extensive research subsequently lead to an understanding of the electrical and photoelectric conduction mechanisms in phthalocyanine crystals. Observed semiconducting properties lead to the fabrication of thin films with a view to constructing electronic devices. More

recently phthalocyanine films have been utilised in the construction of gas sensors and photovoltaic cells. The highly ordered structures obtainable with the Langmuir-Blodgett method have been attributed as an important benefit to the performance of these devices. Due to the currently increasing interest in nanotechnology, the investigation of monomolecular films is of even more importance.

2.2 Properties of Phthalocyanines, including an introduction to the Phthalocyanines investigated in this Thesis.

Generally phthalocyanines are commonly used as dyes in industry because of their excellent light, heat and acid and alkali fastness. Cyanine dyes used in the photographic industry are used as sensitisers. Their suitability for this purpose has been investigated using optical absorption and electron diffraction techniques (Bliznyuk & Möhwald 1995).

Natural phthalocyanine occurs as highly coloured crystals varying from red-blue, green-blue to indigo blue. They are most commonly seen as the dark blue dyes used in paints, inks, plastics-manufacturing, rubber and cloths.

Structurally, phthalocyanines are derived from the porphyrin ring system. The square-flat structure of the phthalocyanine molecule has a central location that can be occupied by two hydrogen atoms or replaced by metals to form the metal phthalocyanines. Copper, iron, zinc, lead and platinum have all been incorporated as substituents in the phthalocyanine ring the location indicated by "M" in figure 2.1.
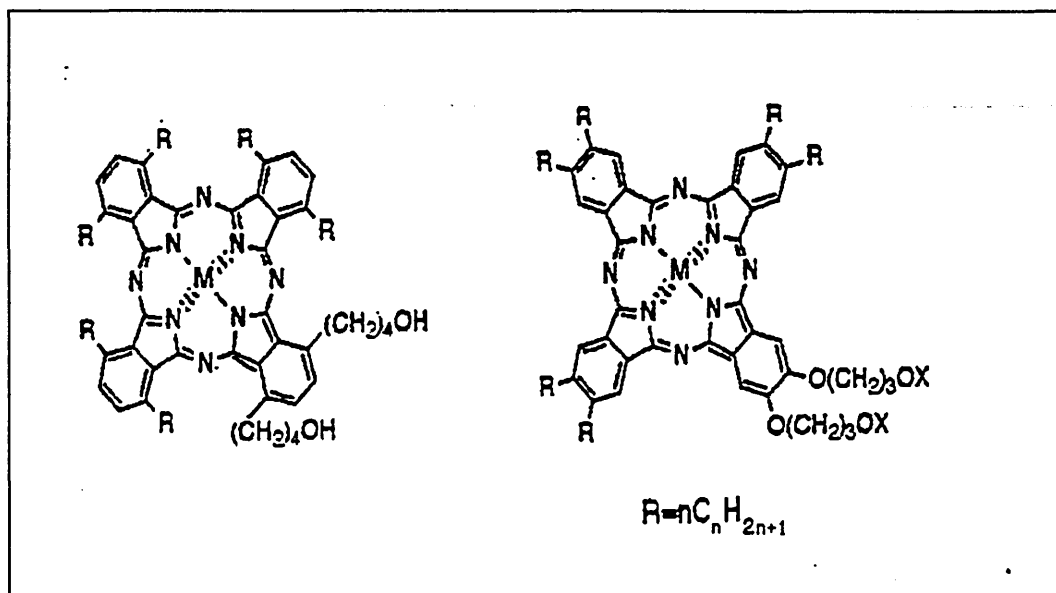
Figure 2.1   *Non-peripheral (left) and peripheral (right) phthalocyanines. The central M location is substituted by a metal or two hydrogen atoms. The material A410 H_2 is non-peripheral and $R=nC_{10}H_{21}$ (Fernandes 1995)*

Phthalocyanines are insoluble in water. Synthesis of phthalocyanine molecules with novel substitutions on the ring periphery enables them to dissolve readily in common volatile organic solvents such as chloroform and trichloroethane. By differing the length of the substituent chain, the molecular packing can be altered.

Poynter et al (1994) observed two distinct types of molecular packing depending on the length of the hydrophobic chain. The tuning of the electrical and optical properties of organic polymers by using side chains is effective and still under development (McCullough and Williams 1993)

The phthalocyanines can be molecularly engineered with good film forming and ordering properties. The influence of the ring substituent chain length was found to affect the ordering of the type of octa-substituted phthalocyanines investigated in this thesis (Cook et al 1994).

Two metal-free, non-peripheral phthalocyanines are investigated in this thesis:

i)   A410 H_2 R=n$C_{10}H_{21}$ (A410)

ii)   A40iso6 H_2 R=iC_6H_{13} (A406)
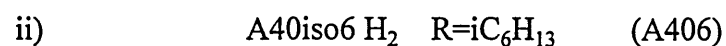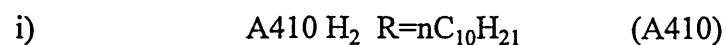
Based on the structure in figure 2.1, the aim in synthesis of these molecules was to produce novel materials suitable for Langmuir-Blodgett deposition. Mass Spectroscopy confirmed the quality of the sample synthesis. However a low success rate of synthesis was due to the extreme difficulties arising at the purification stage. This was caused by too low solubility and a high propensity for aggregation (Fernandes et al 1995). The materials selected for investigation were already expected to give good Langmuir-Blodgett film forming properties (Cook et al 1994).

2.3 Polymorphism.

Phthalocyanines are known to exist in at least three polymorphic forms alpha (α), beta (β) and gamma (γ) (Chadderton 1963). The polymorphic form significantly influences the electrical properties. (Moser and Thomas 1983). The polymorphic forms can be converted into each other by various methods. Heating alpha and gamma forms to a temperature of 673K yields the beta form. The beta form in turn transforms to alpha form after a long period of grinding in the presence of sodium chloride. The gamma form will convert to alpha form when treated in 60-70% sulphuric acid and then immersed in water. Of the three, the beta form is the most stable. Electron microscope studies confirm that the beta form is more ordered than the alpha which has disordered spacing (Stabenow 1968), implying that the high stability of the beta form is due to its higher ordering.

Metal free phthalocyanine was found to exhibit a fourth form x-polymorph that can be prepared by extended milling of alpha or beta phases (Bryne & Kurz 1967, 1971). This polymorph has potential as a photoconductive material.

2.4 Methods of Producing Thin Phthalocyanine Films.

Thin organic films are being developed for use in solar cells, optical data storage devices, gas sensors and optical switches. For fabricating devices, thin films of phthalocyanines are usually deposited by one of the following methods: sublimation, vacuum evaporation or the Langmuir-Blodgett technique.

2.4.1 Sublimation.

Sublimation of materials is by definition a direct transition from solid phase to vapour phase. Organic compounds have suitably high vapour pressures below their fusion temperatures, thus permitting sublimation. The powdered phthalocyanine is vaporised by heating. The vapour is then carried by a stream of oxygen-free nitrogen. Then the phthalocyanine condenses on cool surfaces in a cool zone. The substrate is positioned in this cool zone to collect a layer of phthalocyanine. This technique was found to produce needle like crystals of a monoclinic structure (Gutmann and Lyons 1967).

2.4.2 Vacuum Evaporation.

The vacuum evaporation process is detailed in Chapter 6, as a means of depositing metal electrodes on samples. The method is also valid for deposition of thin organic films. However the control of the substrate temperature is important to optimise the thin film structure (Vincent et al 1981).

The main problem with evaporated organic films arises from coherence and lack of uniformity. Such unordered films will have complicated properties and unrepeatability from one sample to another. The Langmuir-Blodgett deposition method was therefore used in this work for the deposition of phthalocyanine. Vacuum evaporation was used as the method for depositing metal films.

2.4.3 Langmuir-Blodgett Deposition.

Langmuir-Blodgett deposition is a room temperature, molecular transfer process using a Langmuir-Blodgett trough (figure 2.2).
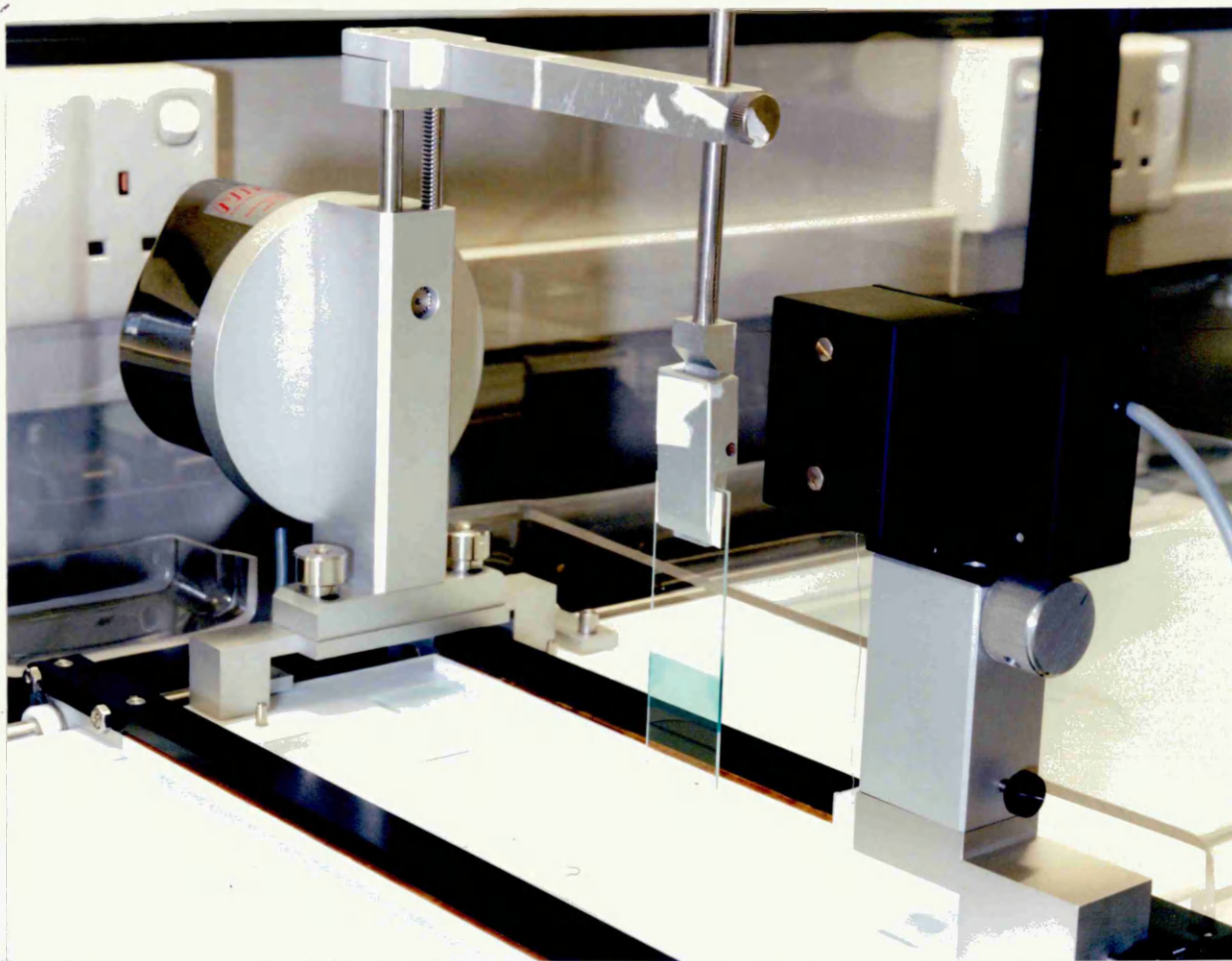
Figure 2.2   *A NIMA 622 L-B trough with dipper (left), pressure sensor (right), and barriers (on water surface). A glass slide is being used as a substrate (but the deposited L-B film is not uniform).*

The film molecules, in a volatile solvent, are spread on a pure water subphase. The molecules spread out to form a monomolecular layer in much the same way that a drop of oil will spread out when dropped on water. The monomolecular layer is then compressed to form a 2D solid that is transferred to substrates as they are passed through the air water interface (figure 2.3). This is performed at

room temperature and pressure (Peterson & Girling 1985). The main requirement

for successful Langmuir-Blodgett films is to reduce contaminants to a minimum.
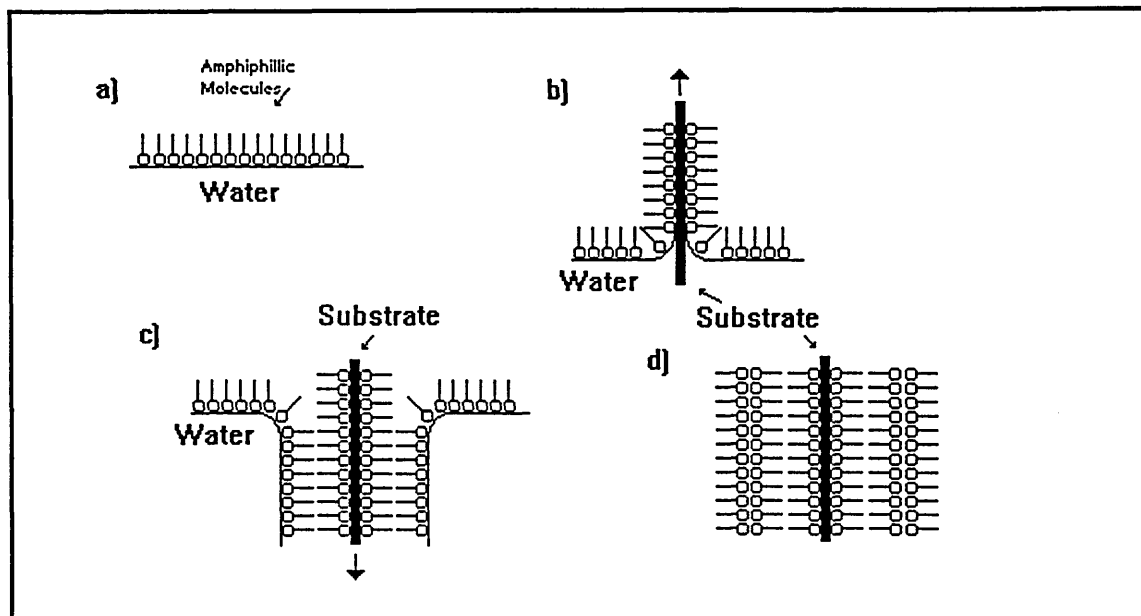
Figure 2.3   *The process of L-B deposition, molecules transferred from*

subphase (water) to substrate.

This technique is very valuable because it can be used to create highly ordered

films of precise thickness. It does not use high temperatures which would damage

the film or substrates during deposition.

Unfortunately phthalocyanines do not readily dissolve in solvents or possess the

amphiphillic properties required for ordering on a subphase. The phthalocyanine

molecules are then modified with additions on the periphery rings, improving the

film forming properties and solubility.

Another aspect of Langmuir-Blodgettry is that the substrate should theoretically

be flat. If the film is deposited on raised electrodes, there is a possibility that the

film could break at the interface. Langmuir-Blodgett deposition is detailed further in Chapter 3.

2.5 Structure of Phthalocyanine Thin Films.

Peterson and Girling (1985) state that the strength of unsupported Langmuir-Blodgett films can span much greater gaps than their thickness, and note the interest in using Langmuir-Blodgett films as biological membranes for hyperfiltration. This strength property would depend on the Van der Waals forces between molecules in the film and thus depend on the type of molecule used. Clearly some molecules would form stronger films than others. Carrara et al. (1995) conduct electrical current voltage tests on a surfactant Langmuir-Blodgett film (C16H33-BEDT-TTF). The film is deposited on a raised electrode substrate. They observe degradation in conducting films and conclude that the tunnelling barrier is due to the detachment of the single monolayer ($\approx$2nm thick) at the edges of the electrodes ($\approx$40nm high).

This demonstrates the range of strength found in Langmuir-Blodgett films, on the one hand being able to be used as stand alone micro filters, yet detaching at surface interfaces on the other. The choice of molecule has a strong influence on the strength of the film. Phthalocyanines are not particularly well documented in terms of strength, indicating the difficulty in measuring this parameter.

From analysis of the pressure area isotherm and calculating the molecular dimensions, the monolayer structure on the subphase can be surmised. Barger et al (1988) suggested a virtual aggregation whilst on the subphase as the area per molecule was too small for the phthalocyanine molecules to be laying flat on the subphase. Further structural studies of the deposited films revealed 'edge-on' configuration to the subphase (Fujiki and Tabei 1985). However there are discrepancies as to the exact ordering of the molecules on the subphase and substrate. Optical measurements are being used to further the knowledge about deposited films (Yoneyama et al 1986).

2.5.1 Optical Properties.

To obtain the molecular orientation and structure of the films, optical methods can be used.

Molecules in phthalocyanine lattices are bonded by Van-der-Waals forces as expected for organic solids. Therefore optical absorption is molecular in nature and can be simply represented by the discrete transition between the ground and the exited electronic states of the free molecule. The crystal form retains the characteristics of the free molecule. The π-π* transitions are responsible for the strong absorption observed in phthalocyanine. Since the absorbance ($A = \ln(I_0/I)$) at a given wavelength is dependent upon the sample thickness, the results are usually presented in terms of the absorbance coefficient (the ratio between A and

the film thickness). As the absorbance is directly proportional to the thickness, the absorbance can be used to confirm the Langmuir-Blodgett deposition quality. Various epitaxially deposited metal phthalocyanines were characterised optically using their optical spectra (Chau et al 1993). A proposed packing geometry (after using electron diffraction data) suggests domains of phthalocyanine lying with their face parallel to the substrate.

Copper phthalocyanine deposited by the Langmuir-Blodgett method was studied by Yoneyama et al (1986) with polarised light polarised parallel and perpendicular to the dipping direction. They observed a difference in the absorbance spectra, the ratio between the two absorbencies at a given wavelength is known as the dichroic ratio. Yoneyama et al (1986) concluded after some calculation that the molecules were oriented with the molecular flat nearly facing the dip direction. They also noted a higher ordering with further deposition, i.e. thicker films. Tokito et al (1995) also used optical spectroscopy (together with X-ray diffraction) to obtain the orientation of copper phthalocyanine molecules in Langmuir-Blodgett films on metal substrates. They observed the molecular planes lying parallel to the substrate. Thicker films revealed a change in the orientation with the planes inclined away from the substrate corresponding to a crystal structure of the alpha phase. The polarised light optical absorption method is detailed in chapter 4.

Lou et al (1993) observed an optical hysteresis effect in tetranonyl phthalocyanine copper Langmuir-Blodgett films. They noted the destruction of aggregates at high temperature (up to 523 K) and their restoration when at room

20

temperature. They note that the use of annealing can improve the order of molecules in the TNPcCu film and benefits the formation of aggregates.

2.5.2 Electron Microscope Studies.

Ordering of molecules in Langmuir-Blodgett films has been successfully studied using Electron Microscopy. Hann et al (1985) report highly ordered copper phthalocyanine films. However Fryer et al (1985) reported small and highly disordered columnar domains. Crockett et al (1990) used Transmission Electron Microscopy (T.E.M.) to analyse their silicon substituted phthalocyanine, they observed a strong substrate dependence finding higher alignment with glass substrates over amorphous carbon film substrates. They also observed inter-layer alignment.

One of the best film forming phthalocyanine molecules was found by Mckeon et al (1988) who found that asymmetrically substituted hexa-octyl-dibutanoate phthalocyanine transferred as well ordered Y-type (see Chapter 3) films. The molecules remaining perpendicular to the subphase surface even at zero subphase pressure demonstrating the ease of deposition of high quality films.

2.5.3 Electron Spin Resonance.

This technique has been used to determine the orientation of copper phthalocyanine molecules in Langmuir-Blodgett films from the Electron Spin Resonance Spectrum. Cook et al (1986) deduced that the molecules were aligned with the plane of the ring at 80 ± 10° to the silica substrate surface. Further tests revealed that films produced with a dipping direction perpendicular to the former, produced similar results, concluding the isotropic nature of the films in the plane of the substrate (Cook et al. 1987).

2.6 Electrical Properties.

Electrical conductivity of phthalocyanine is affected by defects and impurities arising from the preparation of the samples. Organic impurities form charge complexes thus enhancing the actual conductivity of the pure phthalocyanine sample. In general metal phthalocyanines have higher electrical conductivity than the metal free variety due to the introduction of the usually larger central metal atom. The delocalisation causes larger intermolecular wavefunction overlap thus increasing the mobility of the charge carriers (Mukhophadhyay 1990).

2.6.1 Conduction in Thin Films.

Phthalocyanine has been shown to have semiconductive properties (Eley 1948, Vartanyan1948). Within the temperature range 673 -873K the conductivity (σ) of phthalocyanines has been shown to vary with temperature following the equation:

$$\sigma = \sigma_0 \exp(-\frac{E}{kT}) \qquad\qquad 2.1$$

Where σ_0 is the specific energy and k is the Boltzmann constant. Vartanyan (1948) estimated σ at 5 x 10^{-10} ohm^{-1}m^{-1} for copper phthalocyanine and 10^{-8}ohm^{-1}m^{-1} for magnesium phthalocyanine. The effect of the environmental gas was also noted, hydrogen and oxygen having a marked effect.

The AC conduction of thermally evaporated copper phthalocyanine was reported as being dominated by the hopping process at low temperatures and high frequencies, yet at higher temperatures and lower frequencies, free carrier conduction with mean activation energy of 0.3eV was observed. The conductance was however lowered after heat treatment at 370K (Gould & Hassan 1993). This lowering in conduction was ascribed to the desorbtion of oxygen.

The effect of the contact material was investigated by Wilson and Collins (1987) who noticed that copper phthalocyanine in a planar structure with electrodes of Cu, Ag, Ni and Al displayed non-linear I-V response. Au and In electrodes enabled linear characteristics to be obtained. Al and Cu are known to oxidise rapidly and hence tunnelling is likely through the thin oxide layer. The type of contact used (ohmic or barrier) is an important factor when designing a device. The properties of phthalocyanine-to-silicon junctions were investigated by So and Forest (1987) who report a high density of states existing at the interface which 'pin' the surface Fermi energy in the inorganic semiconductor band gap thereby determining the junction band gap.

2.6.2 Conduction in Langmuir-Blodgett Films.

The conduction mechanism in thin films is dependent on the preparation of the sample, the impurity level and the environment. By depositing films using the Langmuir-Blodgett technique the purity of the film can be optimised together with the structure.

Planar structures of metal free phthalocyanine deposited on aluminised glass substrates produced linear Current-Voltage characteristics (Baker 1983), the current varying linearly with film thickness. The samples also displayed their original properties even after cycling between 78K (Liquid Nitrogen) and 373K.

Copper tetra-tert-butyl phthalocyanine when deposited on arachidic acid coated substrates and then a gold top electrode deposited on top, has ohmic conduction over several orders of magnitude. However traces of water and other impurities affected the conductivity (Hann et al 1985).

Evaporated copper phthalocyanine films have been investigated and their electrical properties determined as consistent with an exponential distribution of trapping states (Sussman 1967a) further tests concerned the effect of ambient gases on the Fermi level. Oxygen moved the Fermi level towards the valence band thereby increasing conductivity. Hydrogen had the opposite effect, decreasing the height of the Fermi level and reducing the conductivity. This was attributed to the addition or removal respectively of acceptor states (Sussman 1967b).

Langmuir-Blodgett films of tetra-tertiary-butyl phthalocyanine monosulphonic acid have been incorporated in a multilayer system of tricosenoic acid (insulating) and aluminium electrodes. The devices were found to approximate to organic multiple quantum wells (Donovan et al 1994).

2.6.3 Photoconduction in Thin Film Devices.

It is a well known property of phthalocyanines, that light has a positive effect on the conductivity. Thin phthalocyanine films have been incorporated in photovoltaic devices. Evaporated magnesium phthalocyanine in a sandwich

structure produced photocurrent at low applied voltage, the photocurrent varying exponentially with applied voltage. The open circuit photovoltage was directly proportional to the logarithm of the applied light intensity. This is as would be expected for a Schottky barrier or p-n junction (Ghosh et al 1974).

Sublimed alpha phase metal free phthalocyanine in a sandwich configuration with SiO as a blocking layer was investigated by Nespurek et al (1985). The blocking layers were to eliminate the possibility of carrier injection from the gold electrodes. The photocurrent was then believed to be due to transport of holes generated in the bulk phthalocyanine.

Copper phthalocyanine Langmuir-Blodgett films were incorporated in sandwich structures with Al and Ag as the base and top electrodes respectively. A maximum photocurrent of 10^{-10} Acm^{-2} was obtained with 100µV for samples of between 10-15 monolayers thickness. This relatively high value is attributed to the lack of long alkyl chains and the high ordering of the film. They also noted the influence of oxygen, producing acceptor levels within the band gap enhancing the photoelectric properties. The thickness of the film was optimised at between 10-15 monolayers. Thinner films had poor performance likened to disordered films. Higher thickness films had decreased performance, because of the reduction in efficiency of the thicker device due to the increased trap concentration. Sublimed films are observed to have shown similar properties, Nespurek (1984), Valarian and Nespurek (1993) and Nespurek et al (1994) present models for device conduction based on trap concentration levels.

The efficiency of Schottky barrier photodiodes can be much improved using a monolayer of a suitable amphiphillic substance. However Tredgold and Smith

(1982) concluded that adsorption produced better results than the Langmuir-Blodgett method for monolayers. GaAs Schottky photodiodes were improved in terms of efficiency, temperature stability (up to 473 K) and mechanically by the inclusion of a polymer Langmuir-Blodgett film (Tredgold and Badawy 1985). Clearly organic films have a role in photoelectric devices.

2.6.4 The effect of Ambients on Photoconduction.

The photoconduction of single crystals of Pb and Zn phthalocyanine under oxygen, nitrogen dioxide and triflouroborane environments were enhanced and showed clear similarity to the optical absorbance spectra of these materials (Van Ewyk et al 1981). The photoconduction spectra in vacuum were approximately the inverse of the optical absorption spectra that was consistent with the work based on metal free phthalocyanine films (Popovic and Sharp 1977). The result suggested that the charge carrier generation was not restricted to the surface but it was a bulk phenomenon. Metal and evaporated copper phthalocyanine junctions were fabricated to test their rectification and photovoltaic effects (Yamamoto et al 1981). Current Voltage characteristics produced ohmic behaviour in the absence of hydrogen. Whilst in the presence of hydrogen, a rectification effect was observed which increased with the concentration of hydrogen. The increase in hydrogen concentration produced an increase in the photovoltage. The hydrogen sensitivity of the device was explained by the p-type nature of the material giving rise to a Schottky barrier which changes with the work function of the different

metal used. It was suggested, from the spectrum, that the light was absorbed only in the space charge layer of copper phthalocyanine near the interface, which effectively contributed to the carrier generation. Thus copper phthalocyanine films were suggested as good gas sensing elements.

2.6.5 Phthalocyanine Langmuir-Blodgett films as Gas Sensors.

Sensitivity of phthalocyanine Langmuir-Blodgett films to electron accepting or electron donating gases has been investigated for fabrication of gas sensors. Unsubstituted metal free phthalocyanine together with symmetrically and asymmetrically substituted phthalocyanines were exposed to NO_2 in order to obtain the response and recovery times for each of these materials (Baker et al 1983, 1985). A large increase in the conductivity values was observed due to the result of electrophillic attack on the extensive π - orbital system of the phthalocyanine molecule, by the gas. The asymmetrical copper phthalocyanine compound proved to be by far the best detector amongst all the other derivatives investigated. An eight layered structure responded almost immediately when exposed to NO_2 in nitrogen carrier gas. The recovery rate was rapid in the initial 50 seconds slowing as time progressed. The thinness and ordered structure were responsible for the response and recovery times observed, which were faster than those reported for vacuum evaporated films. The gas absorption effect was

believed to be a surface phenomenon. It was suggested that the more ordered structure fabricated by the Langmuir-Blodgett technique enabled the gas molecules to absorb and desorb from the molecular sites more readily. Travis et al (1995) and Hassan et al (1995) reported that Langmuir-Blodgett films of copper phthalocyanines would be effective as disposable NO_2 sensors. This was due to their poor recovery when withdrawn from the gaseous environment. Although as Gould & Hassan (1993) noted (the desorption of gas from the film when annealed), it is a possibility that the gas sensor could have better recovery if used at an elevated temperature.

Langmuir-Blodgett films of metal free, copper, nickel and lead constituting of tetra-butyl, isopropyl and cyano groups were exposed to active gases such as iodine, triethylamine and n-butanethiol vapours (Fujiki and Tabei 1988). A substantial amount of change in the conduction values of the films was observed with low recovery times. When Langmuir-Blodgett films were exposed to the electron-accepting gas such as iodine vapour (with a vapour pressure of 0.5mm Hg) the conductivity increased steeply by 3-5 orders of magnitude in a few seconds. Metal free phthalocyanines exhibit rapid changes in film conductivity as well. When exposed to triethylene vapour there was an increase from 2-400 times within 1 minute, and an increase of 600-3000 times was observed with n-butanethiol gas. The change in conductivity with electron accepting gas correlates with the generation of hole carriers as functions of active site density of the surface, gas concentrations, ionisation potential of the film and electron affinity with the gas. It appeared that the conduction phenomenon depended not only on the central metal atom as in evaporated thin films (Sadaoka et al 1980, Jones and

Bott 1985) but on the type of substitution as well. Evidently the gas sensing properties of thin films of phthalocyanine derivatives can improve with techniques such as the Langmuir-Blodgett method since improved homogeneity and optimal thickness can be controlled. Films deposited by the evaporation technique often give rise to heterogeneous film surfaces. These have a range of different types of active sites that may complicate the gas absorption phenomenon.

2.6.6 Phthalocyanine in Electronic Devices.

The final goal for investigating the various properties of the phthalocyanine derivatives obviously lies in the development of practical electronic devices. A number of researchers have produced evidence of the potential of photovoltaic cells as discussed earlier. The first investigation of the surface acoustic wave sensor, using conductivity changes of the lead phthalocyanine thin film on acoustic propagation path of a LiNbo$_3$ SAW delay line was performed by Ricco et al (1985). The sensor was found to be 1000 times more sensitive to NO$_2$ molecules than an identical SAW detector. Chamberlain (1971) investigated the mechanism of the increased photoresponse of indium phthalocyanine photocells on exposure to iodine vapour. The iodine formed charge transfer complexes with the phthalocyanine molecules, which are excited under illumination, and dissociate in the built-in field. The electrons and holes generated constitute a

negative and positive space charge respectively. The drift of the space charge by electron hopping to the electrodes under the influence of the built in field limits the photocurrent. Organic solar cells incorporating polycrystalline particles of metal free phthalocyanine sandwiched between tin oxide and indium electrodes, provide a viable approach to construct photovoltaic cells. They were believed to perform more efficiently than evaporated films (Loufty et al 1981). However it was suggested that although the potential power conversion was high the engineering efficiency was low due to low transmission of light through the indium electrode and therefore highly transparent electrodes were preferable. The limiting factor reported in this communication was the series resistance of the cell that could be resolved by construction of thinner layers. The Langmuir-Blodgett method of deposition of thin highly ordered film is ideal for such a construction. Langmuir-Blodgett films of phthalocyanine were investigated with a similar aim of creating active or passive devices. Roberts et al (1985) discussed the possibilities of electronic devices with Langmuir-Blodgett films of asymmetric copper phthalocyanine. Electroluminescent diodes (Fowler et al 1985), Metal-Insulator-Semiconductor (MIS) diodes and bistable switching devices were fabricated. Low level minority carrier injection can be achieved by fabricating Schottky barriers (Metal-Semiconductor). However, the levels of injection become considerably higher with a thin insulating layer incorporated between the metal and the semiconductor (forming an MIS device). Langmuir-Blodgett films of phthalocyanines are considered suitable for forming thin insulating layers since they are also required to be sufficiently stable to survive high current levels. A typical (Au/LB film/ZnSeS) MIS diode produced a maximum power efficiency

of about 2×10^{-4} %. Four Langmuir-Blodgett layers in an MIS structure, prepared on GaAs substrate, were used to explore the possibilities of its bistable switching characteristics. MIS diodes using various thicknesses of Langmuir-Blodgett films were exposed to different concentrations of NO_2. The change in the conductivity reflected the additional charge introduced by the gas at the oxide-phthalocyanine interface.

All these potential device applications will benefit once the film morphology and the transport mechanism occurring in the Langmuir-Blodgett layers are understood in greater detail. Evidently there are several well-documented investigations on the interesting properties of phthalocyanine derivatives. Organic materials are already being utilised in high technology applications where they are believed to be superior to their inorganic counterparts. Langmuir-Blodgett films can certainly enhance the efficiency of a range of inorganic devices including electronic displays, surface acoustic wave oscillators and field effect transistors. However in spite of the recent upsurge of Langmuir-Blodgett film deposition using various phthalocyanine compounds, there is still a need to understand the transport mechanism, and the structure of the film on a molecular level. These investigations are essential to exploit the potential of Langmuir-Blodgett phthalocyanine films in electronic devices.

Chapter 3

LANGMUIR-BLODGETT FILM DEPOSITION TECHNIQUE.

3.1 Introduction.

It is a well-known fact that oil spreads out to form a thin film, when dropped on water. In the late 19th and early 20th centuries, scientists performed experiments to confirm that the thickness of the film is one molecule thick. Langmuir (1917) established the use of the pressure-area isotherms to study fatty-acid mono-molecular films. Later, Langmuir and Blodgett (1934) collaborated to investigate the monolayer properties of stearic acid.

In the late sixties, Langmuir Blodgett (LB) deposition was reviewed as a method of incorporating organic films in electronic devices. It was seen that the LB technique could be used in a wide range of applications. These consist of devices ranging from biological membranes through electronic gas detectors to solar cells

(Roberts 1985). The key factors are that Langmuir-Blodgett films are highly ordered, they are of a precise thickness (to the order of molecules) which can be precisely controlled by the manufacturer, and they can be made under normal, clean laboratory conditions. In addition sandwich style structures can be made by simply changing the deposited film material at the required points.

3.1.1 The Field of Work.

The Langmuir-Blodgett technique has been increasingly utilised over the last 20 years to produce thin organic films. The ability to produce highly ordered films of a precise thickness only a few molecules thick has many applications in the electronics industry. Phthalocyanines have been widely used as commercial dyes in the clothing, plastics and paints industries (Cook 1994). Their photo conductive properties have been utilised for solar cells (Yanagi et al. 1994) Their gas sensitivity has been used to make gas sensors (Cole et al. 1993). Cook has been looking at increasing the variety of phthalocyanines available by introducing substituents on the ring system. These new compounds may have novel and interesting properties that may be used in commercial applications. They are designed for Langmuir-Blodgett deposition and display good film forming properties (Cook et al. 1987). Alternative deposition methods include: evaporation and adsorption.

The Langmuir-Blodgett technique is limited in that it can only deposit certain types of materials. These materials are called amphiphiles. They have a hydrophobic end and a hydrophilic end. Molecular engineers can manufacture materials that have the required device properties and may also be deposited with the Langmuir-Blodgett technique. Some of the most popular materials with device engineers are the various forms of phthalocyanine. Copper substituted phthalocyanine has had a concentrated work effort due to its ease of use (deposition by LB, or evaporation) and its wide range of applications. Other popular films include charge transfer complexes (Xiao et al. 1993) (deposited by LB) and polyanaline/polypyrolle (Cheung et al. 1994) (Adsorbed). The charge transfer complexes have been successfully deposited by the Langmuir-Blodgett technique and show good conductivity, 10^{-2} Scm^{-1} in the direction parallel to the dipping direction (Xiao et al. 1993). The film material used was tetrabenzylthiotetrathiafulvalene-tetracyanoquinodimethane (TBTTTF-TCNQ) mixed with stearic acid in a 1:1 ratio.

Molecular engineering, such as two or more film materials deposited alternatively (or as desired) by the adsorption technique, is possible (Cheung et al. 1994). This opens up new possibilities in that the conducting properties of the film can be adjusted by altering the molecular make-up of the film. Cheung et al. (1994) was able to produce high conductivities of 40 Scm^{-1} with thin films (as few as four layers) made up of polypyrrole, polyaniline and poly(3-hexylthiophene). These thin films were transparent and Cheung et al. (1994) suggested their use as anti static coatings of plastics. The alternate deposition process realises the possibilities for thin film processing of conducting polymers and their use in

electronic devices. In particular the need for non-linear optical devices can be approached with the use of alternate deposition. The ability to retain the polar orientation of the individual molecule with the use of 'inert' in-between layers, overcomes the typical orientation problem with Langmuir-Blodgett films (in that the molecules are deposited head to head, tail to tail). This would normally lead to a cancelling-out of the polar orientation when in the film structure. By using an inert film in an alternate structure, all the active molecules have the same orientation so the bulk properties can be predicted from the properties of the individual molecule.

3.1.2 Langmuir-Blodgett Issues.

The Langmuir-Blodgett process is not a straight-forward technique. Before new films can be produced the various parameters required for successful deposition need to be investigated. This involves testing the film material under various conditions to obtain the ideal conditions for Langmuir-Blodgett deposition. This process is largely trial and error and can take some time. The following table indicates a sample of the range of materials that can be deposited by the Langmuir-Blodgett technique and the most important parameters for deposition. These parameters are: the pressure of the film during deposition, the properties of the substrate that is to be coated, any additives in the water to assist in the film spreading process, and the temperature of the subphase during deposition.

Film material	Deposition pressure	Substrate properties	Additive in water	Temperature C	Reference
Stearic acid	33 mN/m	Hydrophilic gallium phosphide	CdCl2	14	Tredgold & Jones 1981
Metal free Phthalocyanine	20 mN/m	Hydrophobic glass	None	18	Author's experience
Copper Phthalocyanine	25 mN/m	Aluminium on glass	CdCl2	20	Yoneyama et al 1986
Copper Phthalocyanine	25 mN/m	Hydrophobic glass	None	17	Brynda et al 1991
Copper Phthalocyanine	30 Pa *	CaF2, 2mm thick	None	Not stated	Yan et al 1992
Copper Phthalocyanine	25-30 mN/m	Quartz	None	Not stated	Ray et al 1993
Dioctadecylamine picrate	20 mN/m	Hydrophobic glass	Various (6)	20	Brynda et al 1989
Acryloyloxy + alkyl group	20 mN/m	Quartz	BaCl2 $(10^{-4}mol-1)$	17	Isomura et al 1994
Ru(II)-bipyridine complex	20 mN/m	Glass	"Dextran sulfate"	25	Sakaguchi et al 1994
Anthracene	30 mN/m	Aluminium on glass	None	20	Williams et al 1994
Poly(styrene/maleic anhydride)	~30 mM/m	Hydrophilic gallium phosphide	None	28-30	Winter & Tredgold 1983
Charge transfer complex (TCNQ)	25 mN/m	Hydrophilic glass	None	20	Author's experience
Charge transfer complex (TCNQ)	38 mN/m	Gold coated glass + silicon dioxide	None	20	Pearson et al 1994
Charge transfer complex + Stearic acid	~10 mN/m	Hydrophilic glass	pH adjusted	not stated	Xiao et al 1993

N.B. Where "None" is stated, no additive is mentioned in the reference, but pH adjustment may have been used. * Pa assumed to be equivalent to mN/m.

Table 3.1 The range of L-B deposition parameters used by workers in the field.

From table 3.1 it can be seen that the parameters vary over considerable ranges. The effective pressure and temperature can vary over 4 times their average window range for effective deposition. The pressures that workers have found to be effective for their materials range from 10 mN/m (Xiao et al. 1993) to 38mN/m (Pearson et al. 1994). The effective deposition window for a material is typically 3 to 4 mN/m wide. The temperatures range from 14 C (Tredgold & Jones 1981) to 30 C (Winter & Tredgold 1983) and again the effective temperature window can be as small as a few degrees. The additives in the water (subphase) commonly adjust the pH. Adding $CdCl_2$ (metallic ions) when depositing long chain fatty acids such as arachidic acid, assists in deposition and stabilises the film molecules on the air-water interface (Petty 1987). There are a large variety of substrates that have been used for deposition. All substrates have in common their high degree of cleanliness and smoothness. These are the most important parameters. The other parameters such as barrier speed, deposition speed, drying times between dips, all need to be optimised for each material and Langmuir trough for effective film deposition. It was noted that there is a great temptation to use the Langmuir-Blodgett technique to make devices, without fully investigating the film forming properties. This can lead to difficulties in repeating the deposition at a later date. One environmental parameter may have changed leading to poor or zero deposition. For similar reasons, it is also essential to investigate the electrical junction properties between the Langmuir Blodgett film and electrodes before utilising Langmuir Blodgett films in electronics (Iwamoto et al. 1994).

The first step after depositing a film is to check that the film is of good quality. As the first monolayer is typically a few nanometers thick, it is not practical to perform a valid inspection of this monolayer by eye. However a visual check of thicker, visible films can often reveal inconsistencies such as blotchiness or streaking of the film which are clearly not desirable qualities. The first indicator of the Langmuir-Blodgett monolayer film quality is the transfer ratio. This is calculated from the ratio between the area of the substrate, to the reduction of area of the film, when the substrate completes a deposition traverse. This should always be unity, but experimental values vary. Values of 1.05 for the up-stroke and 0.93 for the down-stroke were obtained by Xiao et al. (1993). These transfer ratios are typical of good films. The variation can be explained by the inaccuracies in the area calculation caused by the change in the polarity of the meniscus that occurs at the transition of dip direction, at the end of each deposition stroke. It is unavoidable due to the physics behind the process (a meniscus change is essential for deposition). A correction factor in the NIMA Langmuir-Blodgett trough control software could be introduced. However as the variations in substrate properties, film stiffness and deposition pressure would be time consuming to model, the time involved in developing this correction would not be justified by the benefits. Another reason for inaccuracies in the transfer ratio calculation is film leakage. Leakage is avoidable as it occurs at a break (or breaks), in the film barrier. If the symptoms of large transfer ratios and poor isotherms are present, then the Langmuir-Blodgett trough operator should check for gaps (however small) in the film barrier. Gaps are easy to cure as they are usually due to the trough being assembled incorrectly after cleaning. If the film is

visibly poor with blotches or streaking apparent on the substrate, this is usually attributed to either too high, or too low (respectively) process temperature (Roberts 1985). If the mentioned parameters have been investigated, the next step is to ensure the preparation of the sample film and the substrate are optimised in terms of purity and cleanliness. It is sensible to check the basic (easy to put right) parameters before assuming that there is something wrong with the film or substrate (which can take much time and effort to correct).

Many workers have been concentrating solely on the Langmuir-Blodgett technique and the characterisation of the films themselves. This is an important role, as there are many properties of Langmuir-Blodgett films that are not fully understood. Further development of useful devices depends on high quality research into the fundamental properties of monomolecular films and the physics of Langmuir-Blodgett.

3.2 Theoretical consideration of techniques.

A monolayer is formed on the surface of the subphase in much the same way as a droplet of oil spreads out on water to form a monomolecular film.
The reason that this spreading of the film molecules occurs is that the molecules have a water repellent (hydrophobic) component and a water attractive component (hydrophillic). Molecules that have this structure are called

"amphiphillic" molecules. This type of molecule, when in solution with a solvent of low water miscibility, will spread over the water surface to form a single molecular layer. The hydrophillic component of the molecules will force the spreading of the molecules, as they all try to gain a space on the water surface. Whereas the hydrophobic component will ensure the molecules are all aligned in the same direction, as it tries to move away from the water surface.

The film material (usually a solid) is dissolved in an organic solvent. The solvent must not be miscible in water. The solvent is then dripped, using a microsyringe, on to the subphase from a height of a few millimetres. The solvent spreads out over the subphase (like oil) carrying the film molecules with it. When the solution has spread to its maximum extent the solution is one molecule thick. The solvent choice (made on evaporation rate and solubility with film) and the concentration decide the spreading and evaporation process. Clearly the solvent has to spread the film molecules out to a monomolecular layer before evaporating. The film material concentration in the solution must be small enough and the solvent should not be too volatile. As the amphiphillic properties of the phthalocyanines tested is not as strong as the more traditional film materials (fatty acids, eg. stearic acid), the proportion of solvent to film material is increased. A concentration of 1mg/ml is common for stearic acid but phthalocyanines need concentrations closer to 0.1mg/ml. The larger quantity of solvent allows more time for the film to disperse over the water surface before the solvent evaporates. The film molecules are left behind as a two-dimensional "gas" on the air water interface. The film is then compressed with a barrier. A surface

tension meter is used to monitor the surface tension. The film undergoes a two-dimensional gaseous compression involving gas phase, liquid phase and a solidous phase. A plot of area per molecule versus surface pressure is called an isotherm. As the film is further compressed from the solidous phase, it collapses (the film buckles and then rides on top of itself) the film is then unusable. Care should be taken to ensure that the film does not exceed its collapse pressure. Films are characterised with their isotherm and with an area-time plot. The area-time plot displays the change in area, over time, at a given pressure (usually the intended dipping pressure). If any collapse in the film is evident, it indicates that the pressure is too high for the film. If collapse occurs at a lower pressure than expected, it is usually due to impurities in the film or ineffective spreading.

Films are transferred onto solid substrates at, ideally, a midpoint pressure in the solid phase. In practice, the phases are rarely apparent from the isotherm and the deposition pressure is usually obtained by trial and error. The pressure being increased or decreased depending on whether there is no deposition or film collapse, respectively. The substrate is passed through the air water interface dragging the film from the subphase, onto the substrate. This transfer takes place on both the up and down strokes, figure 3.1.
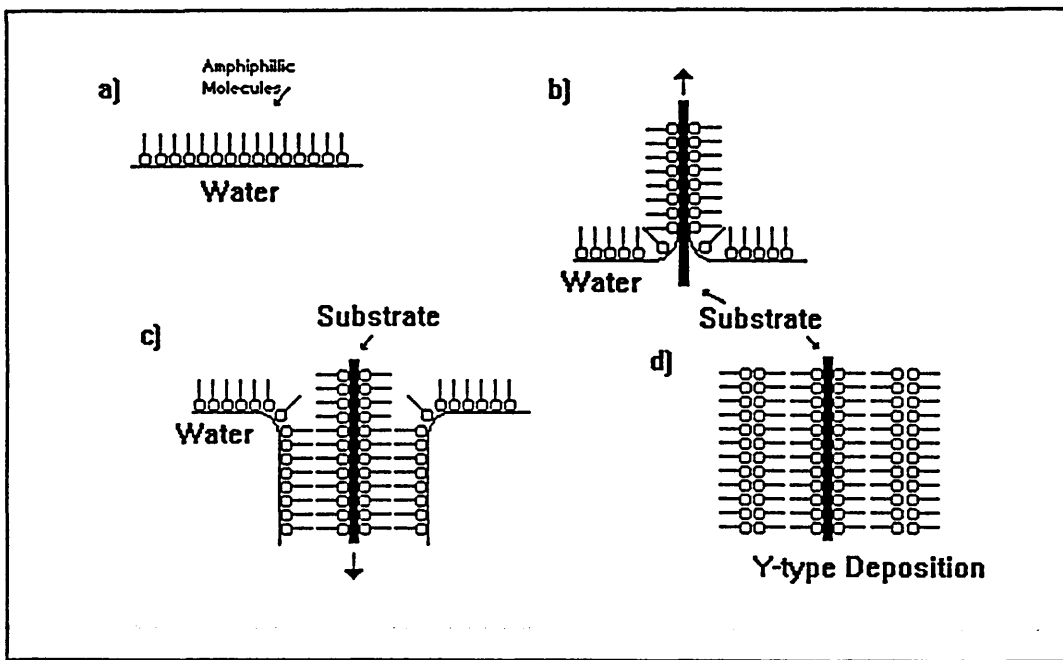
Figure 3.1   The Langmuir-Blodgett transfer process -Y type deposition.

This deposition leads to a head-tail-tail-head-head-tail configuration of the molecules normally referred to as Y-type deposition. If the film does not transfer on up or down strokes, repeatedly the molecules stack head-tail-head-tail and are called X or Z-type depending on whether down or up transfer is dominant, respectively, figure 3.2.
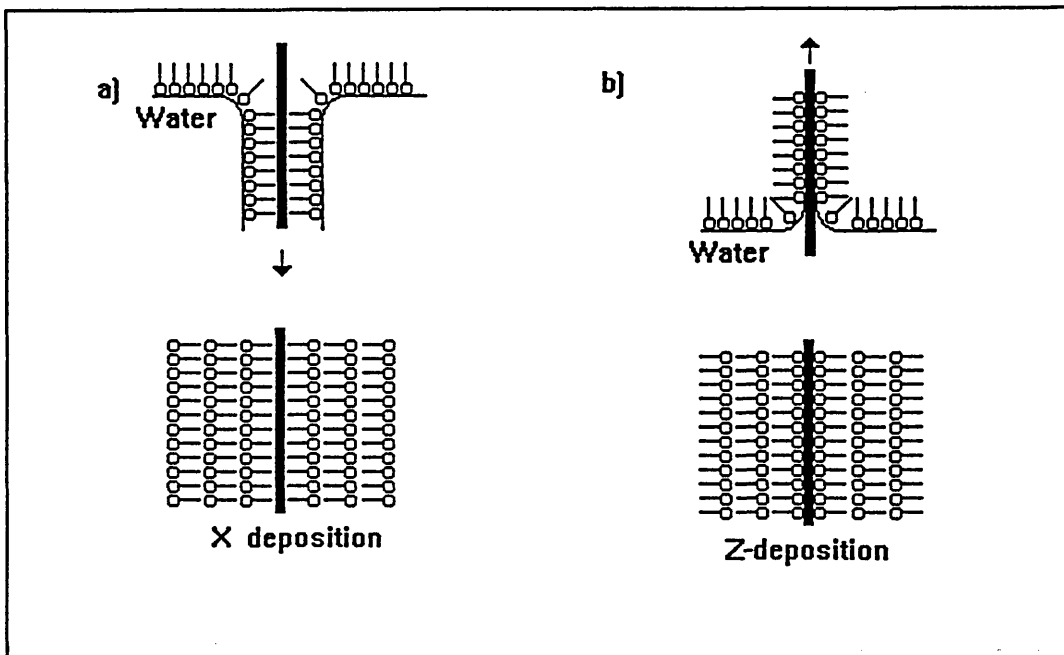
Figure 3.2 The Langmuir-Blodgett deposition variations X and Z type.

If a variation of thickness is required, the height of traverse can be adjusted between dips to produce the step structure as in figure 3.3.
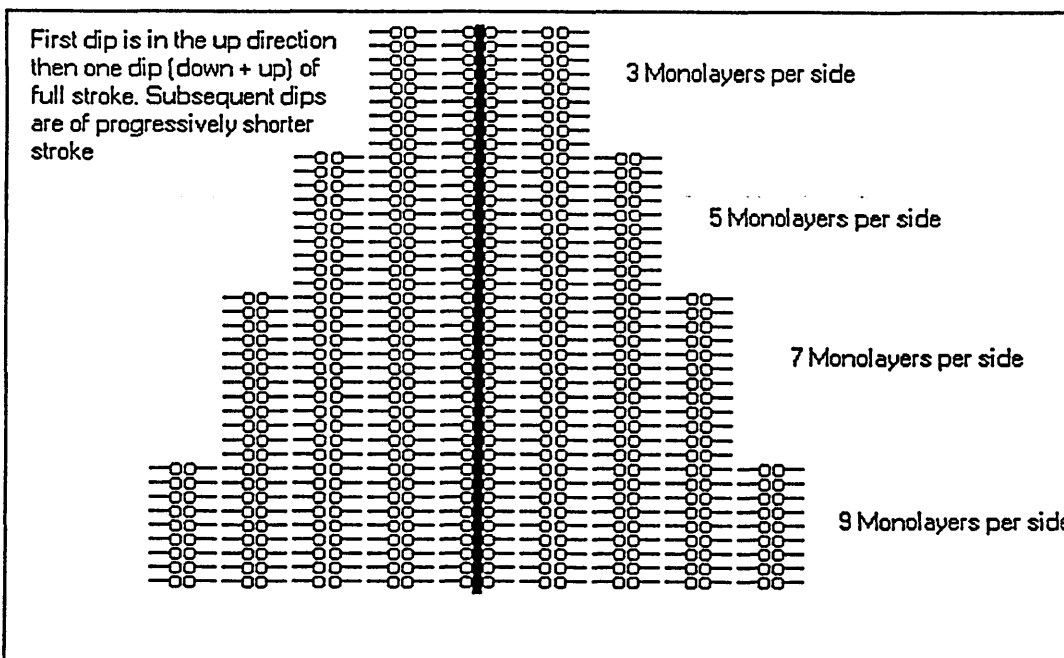
Figure 3.3 The Langmuir-Blodgett deposition in a stepped thickness structure.

44

If a contaminant (LB film) is placed on the water surface then the surface tension will decrease in order to reduce the free energy of the surface. The surface pressure is the difference between the surface tension of pure water and the surface tension of water with a contaminant. The surface pressure (SP) of the film is measured using a Wilhelmy plate (a strip of chromatography paper) suspended from a microbalance, in the subphase. The force measured on the plate is proportional to the surface tension of the water. The relationship between the force acting on the plate and the surface tension (ST) can be derived as:

$$ST_{plate} = Force / perimeter \qquad\qquad 3.1$$

Where Force is the measured force acting on the plate (mN) and perimeter is the perimeter of the plate at the contact with water (m). The surface tension and surface pressure have the same units (mN/m). The weight of the plate and the upthrust due to part of the plate being submerged can be ignored as they are constant and the measurement microbalance is zeroed in pure water. The variation in the force on the plate due to the changes in the surface tension caused by variations in the water contact angle to the plate are eliminated by using a filter-paper plate. This ensures a zero contact angle as the paper is saturated with water. Although the name surface pressure implies force per unit area, in this case it is force per unit length, as SP is purely the reduction in ST due to a contaminant. For water: (Tennent 1971)

$$ST + SP = 72.7mN/m. \qquad\qquad 3.2$$

Fernandes et al (1995) suggest that the ordering of Pc films would be improved by increasing the deposition pressure of the Langmuir-Blodgett process. However, as the effective deposition pressure range is small, a study to investigate this suggestion would need to be done under very controlled environmental conditions.

3.3 Experimental Procedures

Due to the Langmuir-Blodgett process being very detailed and precise, the experimental procedures are divided into sections: the experimental requirements, the preparation of materials, the spreading of a monolayer on the subphase and obtaining an isotherm, film transfer and an outline of the methods used to check the quality of the film.

3.3.1 Experimental Requirements

Two NIMA Langmuir-Blodgett troughs are used for this work. One is an early (mid eighties) generation NIMA circular perimeter model. The other trough is an

alternate layer NIMA trough (figure 3.4) that is designed to deposit films of two materials onto one substrate (Grunfeld et al 1993).
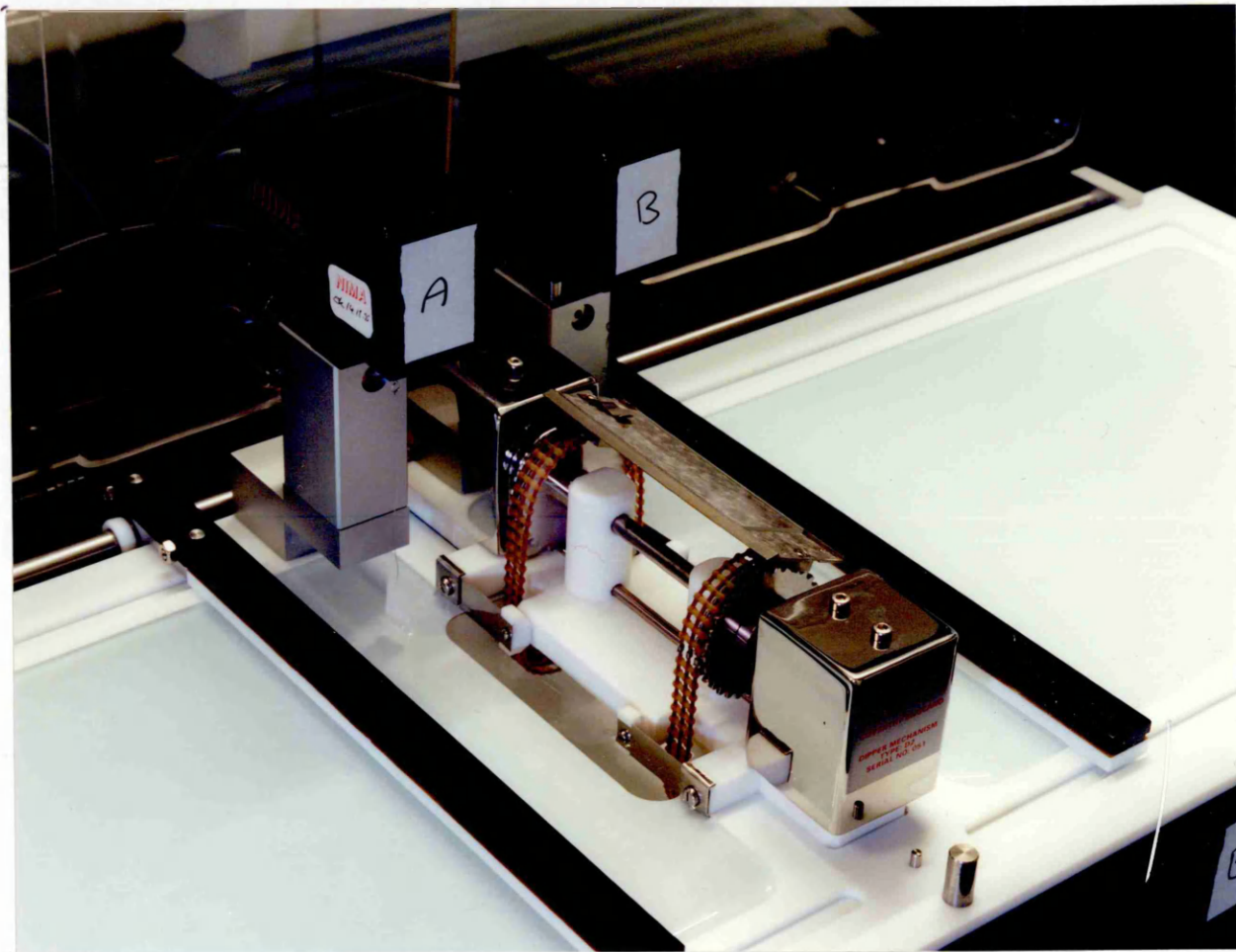
Figure 3.4   *A NIMA 622D2 L-B trough with alternate dipper (centre),*

pressure sensors (top) and barriers (left and right). A glass

slide is being used as a substrate.

Langmuir-Blodgett troughs generally consist of a water container with a moveable barrier that encloses area on the water surface. In addition a surface pressure gauge, usually a microbalance, and a mechanism for traversing a substrate through the air-water interface is used as shown in figure 3.5.
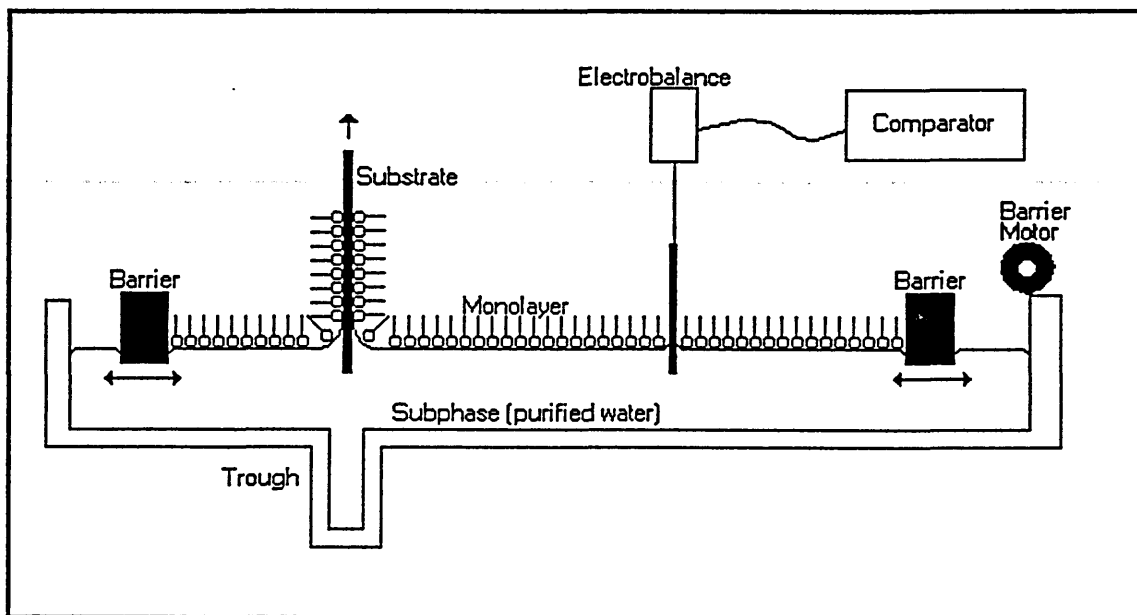
Figure 3.5 The Langmuir-Blodgett trough.

The experimental requirements detailed below are:

* High purity water

* Cleanliness of equipment, materials and environment

* Film purity

* Vibration free

3.3.1.1 High Purity Water

Very high purity water is required, the subphase water is distilled, and filtered using the Millipore water purification system that involves high grade filters. A satisfactory water purity obtains an electrical resistivity of 18 MOhms/cm when measured by the Millipore system. This process reduces the number of contaminants to a minimum. It is essential for Langmuir-Blodgett deposition. Some form of cleaning system is required for the water surface. This is to remove dust and waste film from the surface prior to, and after, deposition. Various techniques are employed, the most common is a suction device consisting of a pump (water driven, or electrical) and a narrow nose pipette. This pump is used to suck air and water at the same time from the air water interface. By moving the suction pipette across the whole subphase surface and by visual inspection, the surface is rendered clean.

3.3.1.2 Cleanliness of Equipment, Materials and Environment

Cleanliness is extremely important. As Langmuir-Blodgett is a molecular process, all implements, instruments, samples and substrates are cleaned to a molecular level. This involves first rinsing the items with a readily available solvent, such

as acetone. Finally the items are ultrasonically cleaned in a series of organic solvents, of increasing purity.

Solvent	Ultra-sonic bath duration
1) Acetone	N/A, rinse.
2) Analar grade Chloroform	5 mins.
3) Analar grade Iso-pro-Alcohol	5 mins.
4) Aristar grade Chloroform	5 mins.
5) Aristar grade Iso-pro-Alcohol	5 mins.
6) High purity water, Distilled and Millipore filtered	N/A, rinse.

Table 3.2 The solvent sequence used for substrate cleaning.

This solvent sequence (Thorpe 1993), as detailed in table 3.2, is effective for most substrates, containers and cleaning implements. The use of the lower grade "Analar" solvents is to reduce solvent costs, but as fume cupboard space is limited the Analar grades are replaced by the higher grade Aristar solvent, reducing the number of organic solvent containers from five to three. Longer sonification times are found to be more effective for cleaning difficult-to-deposit-on sample substrates.
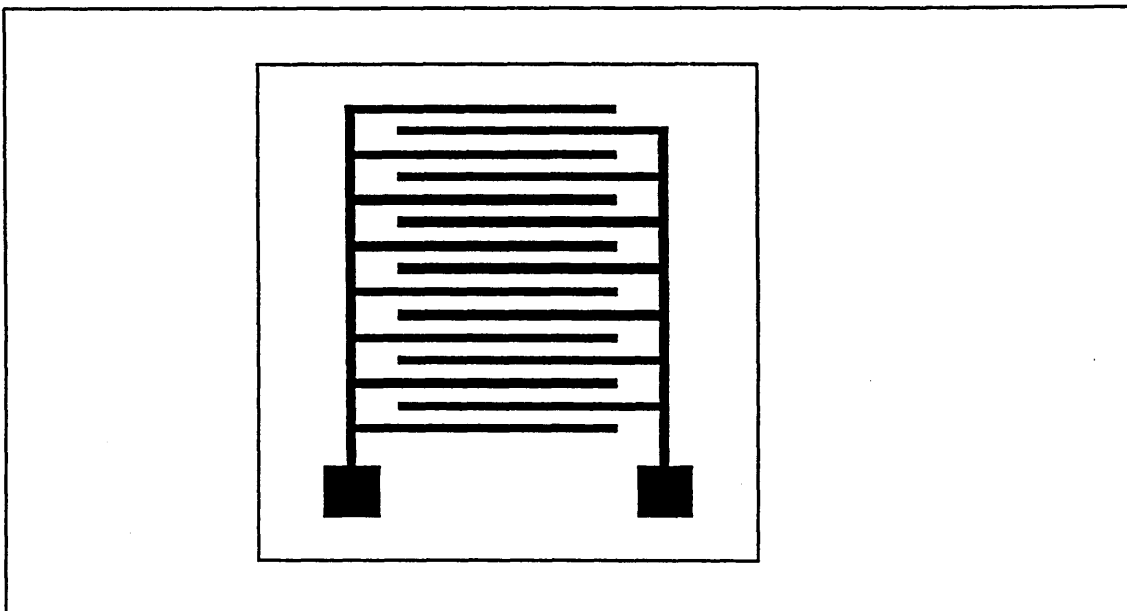
Figure 3.6   *The Yoshi platinum electrode pattern (not to scale) each*

electrode grid is approximately 5mm square. with at least six

grids per substrate.

The Yoshi substrates (figure 3.6) are especially difficult to clean, the electrode

pattern may be responsible as the edges and corners will allow dirt to collect. The

heating that takes place when cleaning in the ultrasonic bath for periods over five

minutes will increase the effectiveness of the solvent.

The appropriate safety precautions are required when using the solvents, i.e.:

sensible clothing, fume mask and fume-cupboard, solvent proof gloves, safety

glasses, and good ventilation.

3.3.1.3 Film Purity

Purity of the film material is very important as a mono-molecular layer of the film will be deposited. The solvent that the film is dissolved in is of high purity, and the container is scrupulously cleaned.

Dust and atmospheric contaminants must be reduced to a minimum. Dust particles can be deposited with the film and cause dirt islands and even disrupt subsequent films. A cupboard enclosure (see figure 3.7) is used to reduce dust contamination. The cupboard is designed for the trough table. It has a steel frame for rigidity and clear polycarbonate panels to allow natural light illumination of the subphase surface that allows the sighting of dust particles on the surface. This enclosure is "sealed" when closed. This is to reduce airflow over the subphase that can cause ripples in the water and increase the amount of contaminating dust.

Figure 3.7   The L-B trough showing the cupboard and the PC.

3.3.1.4 Vibration Free Environment

Excessive vibrations in the water subphase can disrupt the film on the water surface. It has been noticed however, that high quality films can be produced despite the presence of visible minor ripples on the water surface. The NIMA Langmuir-Blodgett trough is mounted on a heavy optical bench. This increases the mass of the trough "unit" thus the vibrational inertia is increased and there is a reduction in the natural harmonic frequency of the trough unit. All these factors decrease the possibility of violent waves occurring on the subphase. The manufacturer of the trough (NIMA) has suggested that minor vibrations mobilise the film resulting in better film transfer. This suggestion together with the quality of the results obtained, have meant that at present, no further measures have been taken to eliminate vibrations. Foam vibration damping material could be introduced at a future stage if vibrations become too great to allow film stability.

3.3.2 Preparation of Materials

The synthesis of the metal free phthalocyanine molecules was undertaken at the University of East Anglia. The preparation of the sample for deposition involves dissolving it in a solvent. The choice of solvent depends on the film material.

The choice is made depending on how quickly and completely the sample dissolves in the solvent and the evaporation rate of the solvent when placed on the subphase. Commonly used solvents are chloroform and trichloroethane. A mixture of solvents is used for materials that are very difficult to dissolve. The appropriate safety precautions are taken. Concentrations of 1 milligram per millilitre are common but the varieties of metal free phthalocyanine require a much more dilute solution. 0.1 mg/ml is found to be effective.

The quality of the substrates (glass slides or silicon wafers) is very important. The substrate must be clean and as smooth as possible. Scratches are avoided by careful handling and by inspecting each slide individually. Depending on the film material, the slide is made hydrophobic or hydrophilic. Hydrophobic slides deposit first on the down stroke and hydrophilic slides deposit first on the upstroke. Again, depending on the film properties, the film continues to deposit on both up and down strokes (Y type). Some films deposit on only one direction, these are called: X type (down only) and Z type (up only). However X and Z deposition can be caused by poor substrate treatment (an excessively hydrophobic or hydrophillic surface). To make a glass substrate hydrophilic, it is cleaned first and then placed in a sodium hydroxide solution (water) for one hour and then rinsed in water. Slides are made hydrophobic by placing the slides in a dichloromethane-silane solution 2 % (Repelsilane) for one hour. They are then allowed to dry, and finally rinsed with water. A good indicator of the cleanliness of a hydrophobic substrate is whether small droplets of water remain on the substrate after rinsing. If droplets appear, they are due to the hydrophillic properties of dirt. Further cleaning should then be performed. It follows that

hydrophillic substrates are more difficult to asses for cleanliness. However as all substrates should be dried after rinsing (using a jet of air), if the water has a tendency to 'stick' to certain parts of the substrate, then it is apparent that the substrate surface is not uniform and further cleaning and treatment is required. These methods are found to produce substrates with surface properties suitable for deposition. It was noted that leaving the substrate in the treatment solution for longer than the stated times, is detrimental to effective deposition.

The trough is drained after each work day and left drained for at least 12 hours. The trough is then cleaned with solvents and rinsed before filling and deposition. The trough is also thoroughly cleaned between differing sample films deposited on the same day.

The 100 μl syringes used to deposit the film and solvent on the subphase are treated with great care. They can easily become blocked with the film material if the solvent evaporates. They must be cleaned after each use, by rinsing in the same solvent that is used to carry the film.

Prior to spreading a film on the subphase, the subphase must be checked for cleanliness. This is done by closing the barriers from a fully open position to a fully closed position. If there is no change in the surface pressure, then the area compressed is clean. The area remaining after compression, must be cleaned to ensure that it is clean as well.

3.3.3 Spreading a Monolayer and Obtaining an Isotherm.

The film is spread on the subphase using the syringe to deposit one drop at a time. Allowing time for evaporation between each drop, the required amount is obtained when the surface pressure increases, and remains slightly elevated. An increase of about 1 to 2 mN/m is ideal. If the pressure is allowed to increase to much above this then the film would not spread properly. A waiting time of at least thirty minutes is introduced to ensure complete evaporation of the solvent. The first time a material is used, an isotherm should be produced. This is used to check the pressure at which the film collapses. The ideal deposition pressure is typically 20-30 % below this collapse point. Although, different materials may favour a lower or higher pressure. In general if no transfer occurs the deposition pressure should be increased. If the film gradually collapses then the deposition pressure should be reduced. An Area versus Time graph is used to test the long term stability of the film and suitability of the deposition pressure.

3.3.4 Deposition of Films

Each film material requires its own, often unique, combination of parameters for good transfer. These parameters can differ slightly when used in a different environment (different trough). Thus when using each new film material, the

correct deposition parameters must be discovered. These parameters, as detailed in table 3.1, are obtained by experimental trial and error.

Dipping is performed vertically through the air-water interface. The speed of dip is in the range 8 to 25 mm/min. The speed is not a critical parameter, as it depends on the film qualities. A mobile film can be dipped at a higher speed than a rigid film. The substrate is started in the subphase (first dip direction is up) if the substrate is hydrophilic. Hydrophobic substrates are started from the top. This is because of the subphase angle of contact with the substrate. The film will only deposit on a smooth transition (not a sharp angle) at the contact between subphase and the substrate.

A waiting time is introduced after the first withdrawal from the subphase. This time (half an hour) is to ensure that the first, and most critical, mono-molecular layer is dry and so likely to form a good bond with the substrate. The subsequent layers are allowed a smaller waiting time (four minutes) between dips. The film thickness is built up in this way, the number of transitions through the air-subphase interface, gives the number of monolayers per side of the substrate.

A graded or stepped structure can be produced by decreasing the dip distance after a specified number of dips. This structure is used for experiments monitoring the effect of varying the thickness.

3.3.5 Film Quality Testing

The quality of the resulting film can be checked visually. The film is good if it appears to be homogeneous. The presence of blotches or streaks indicates the temperature of the subphase is either too hot or too cold and should be adjusted by a few degrees (decrease the heat to eliminate blotches and increase to reduce streaks), (Roberts 1985). The quality of the film depends mostly on the cleanliness of the slide, the sample and the subphase. The isotherm should give an indication of the purity of the film sample and of the cleanliness of the subphase. The transfer ratio is calculated by the software and can be monitored during dipping. This ratio is calculated using the area of the substrate that passes through the subphase and comparing it to the change in film area per dip. The ratio should be close to 100 % for every dip. If it is too low the deposition pressure could be increased (assuming that the substrate has the correct water contact properties and is clean). If the transfer ratio is >110 % then an area versus time study should be performed to check that the film is not collapsing due to a too high deposition pressure. A final check of the substrate transition area and of the dipper and barrier calibration should be done if the transfer ratio is out of limits.

3.4 Results of the Langmuir-Blodgett Technique Development Phase and Discussion of the Information Obtained.

Results are presented for the two materials introduced in Chapter 2: A410 metal free phthalocyanine and A406 metal free phthalocyanine.

3.4.1 A410 Metal Free Phthalocyanine

Parameter	Value
Surface treatment of Substrate	Hydrophobic
Deposition surface pressure	20mN/m
Temperature of subphase	(Room) 20C
Concentration of sample in solvent	0.1mg/ml

Table 3.3 The effective deposition parameters for the A410 material.

For depositing on Yoshi (interdigitated platinum electrode) substrates, the deposition pressure was increased to 25mN/m.

Deposition: Many isotherms are produced to ensure good film reproducibility. A typical isotherm is shown in figure 3.8. The curve demonstrates the good film forming properties of this material. They are: a near vertical solid phase compression and collapse above 35mN/m. The curve reveals an area per molecule of 128 $\overset{\bullet}{A}^2$. This value is of the order expected; Fernandes et al. (1995) obtained 153 $\overset{\bullet}{A}^2$ The discrepancy can be attributed to inaccuracies in the calculation of the trough area and sample concentration. The deposited films appear homogeneous. The transfer ratios were obtained and varied from 0.9 to 1.1.
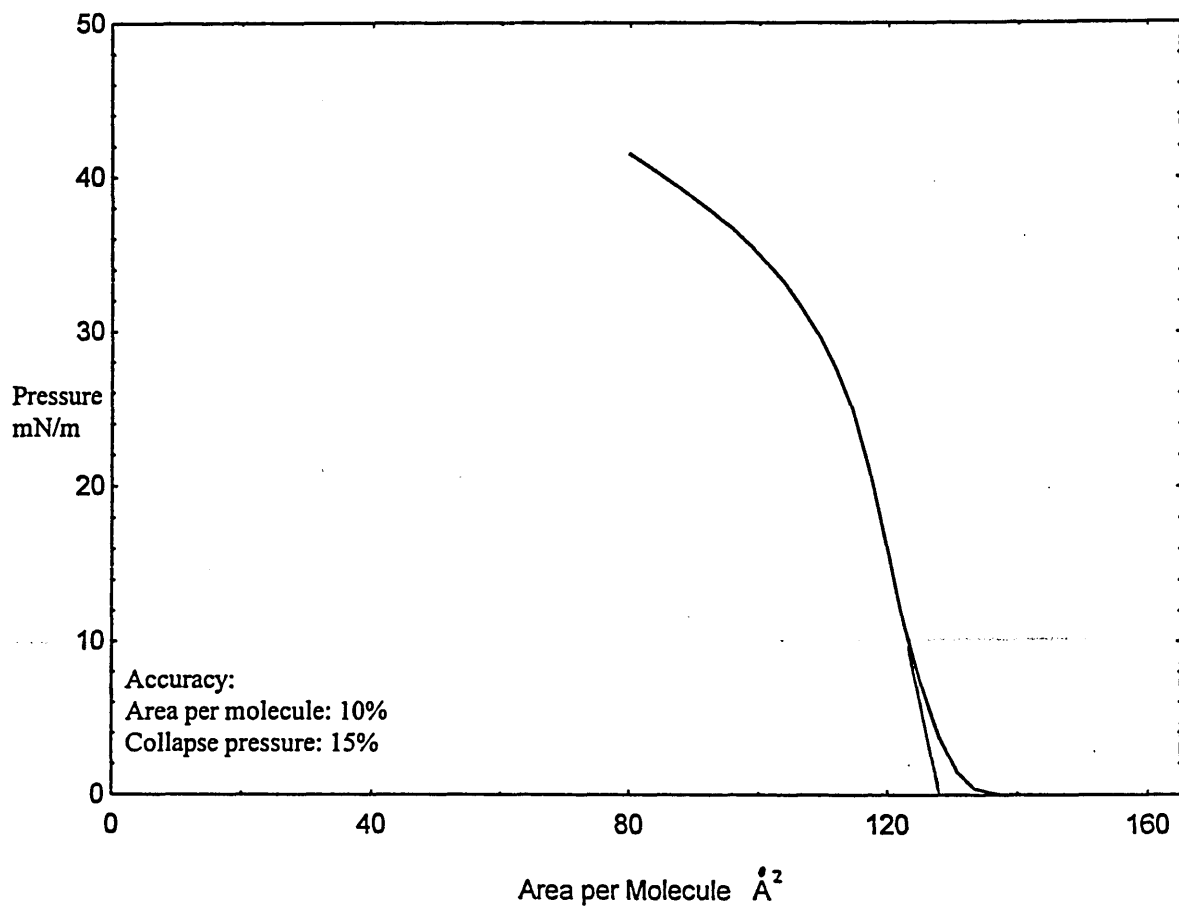
Figure 3.8 *A typical isotherm for A410, demonstrating collapse above*

35mN/m and an area per molecule of 128$\overset{\bullet}{A}^2$. The Area per molecule

is obtained by extending the linear portion of the curve to where it

intercepts the x-axis.

The use of the linear relation between optical absorbance and thickness is useful in confirming the deposition qualities of the film. In chapter 4, figure. 4.9 presents the results of the absorbance with thickness study. The curve shows good linear relation up to films of 24 layers thickness (12 per side. of the substrate). Thicker films have a reduced absorption indicating a reduction in quality of the thicker films.

3.4.2 A406 Metal Free Phthalocyanine

Parameter	Value
Surface treatment of Substrate	Hydrophobic
Deposition surface pressure	20mN/m
Temperature of subphase	(Room) 20C
Concentration of sample in solvent	0.1mg/ml

Table 3.3 The effective deposition parameters for the A406 material.

For depositing on Yoshi (interdigitated platinum electrode) substrates, the deposition pressure was increased to 25mN/m.

Deposition: Many isotherms are produced to ensure good film reproducibility. A typical isotherm for A406 is shown in figure 3.9. The curve demonstrates the good film forming properties of this material. They are: a near vertical solid phase compression and collapse above 28mN/m. The curve reveals an area per molecule of 223 $Å^2$, this value is of the order expected, but larger than that obtained, 123$Å^2$, by Nabok et al (1995). The deposited films appear homogeneous. The transfer ratios were obtained and varied from 0.9 to 1.1.

Pressure
mN/m

50

40

30

20

10

0

Accuracy:
Area per molecule: 10%
Collapse pressure: 15%

0   50   100   150   200   250

Area Per molecule $\overset{\circ}{A}{}^{2}$
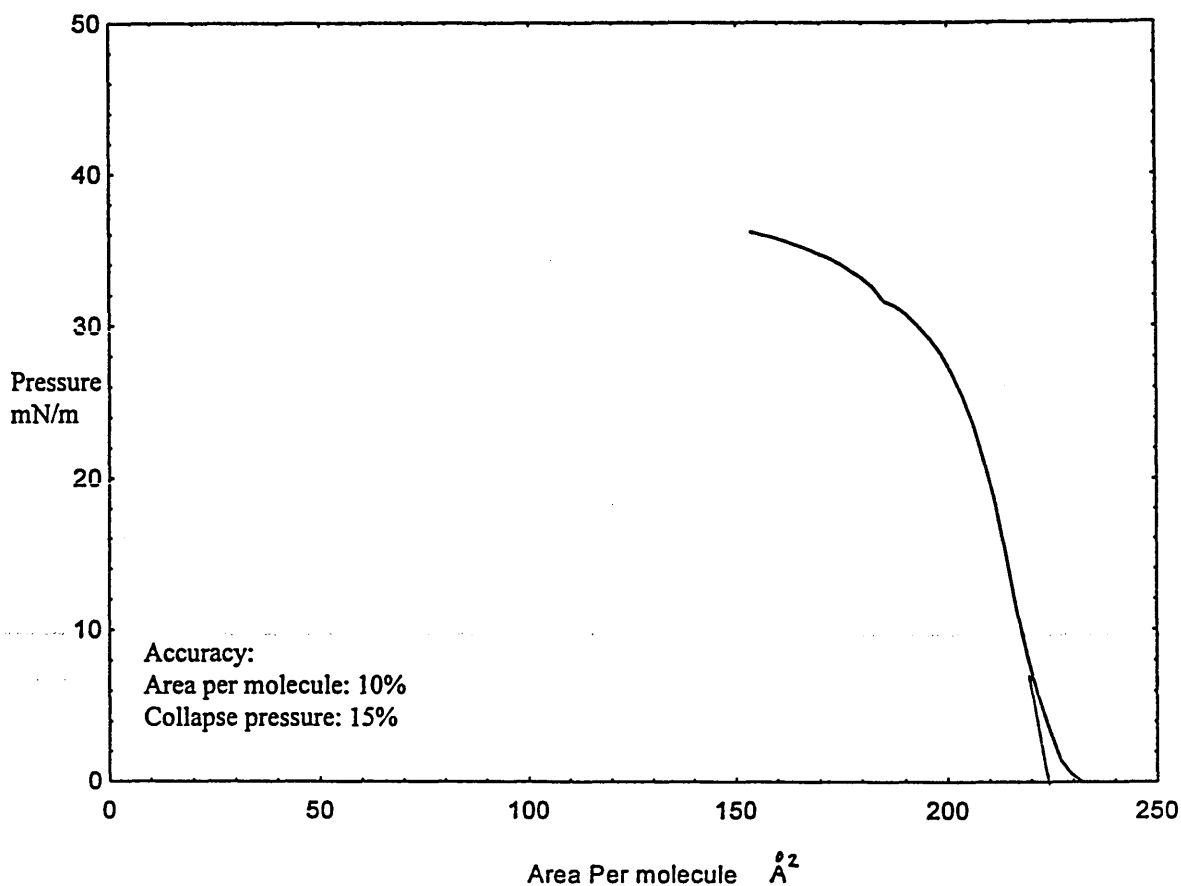
Figure 3.9 The typical isotherm of A406. Demonstrating collapse above

28mN/m and an area per molecule of $223\mathring{A}^{2}$. The Area per molecule

is obtained by extending the linear portion of the curve to where it

intercepts the x-axis.

In chapter 4, figure. 4.7 presents the results of the absorbance with thickness

study. The curve shows a good linear relation for all the thicknesses up to 18

monolayers thick (9 per side of the substrate). These were confirmed as good

depositions. Thicker layers were not tested as the optimum thickness for organic

films in opto-electronic devices is ideally low (Nespurek et al 1994)

In summary, the areas per molecule obtained for these samples of metal free phthalocyanine are:

Source	Area per molecule, A (Angstroms^2)	
	A406	A410
Present Investigation	223	128
Fernandes at al 1995	N/A	153
Nabok et al 1995	123	N/A

Table 3.4. Summary of the results obtained for the area per molecule.

As mentioned before, the values obtained in this work do not agree with those obtained by other workers on these materials. The reasons for the difference include inaccuracies when measuring out the quantities for the sample solution prior to deposition, and inaccurate calculation of the trough area. As the calculation of the trough area is relatively easy, the error is most likely due to poorly measured sample quantities (see Appendix B) which could account for the difference.

Using these results and the geometrical dimensions of the molecules, the average

tilting angle, θ, of the molecular rings can be calculated by using trigonometry.

	A406	A410
l_1 (Angstroms)	23	25
l_2 (Angstroms)	25	28
h (Angstroms)	4.5	5

Table 3.5. The molecular dimensions for the metal free phthalocyanines (Cook 1995)

Assuming the molecule takes the shape of a rectangular box of dimensions: $l_1.l_2.h$
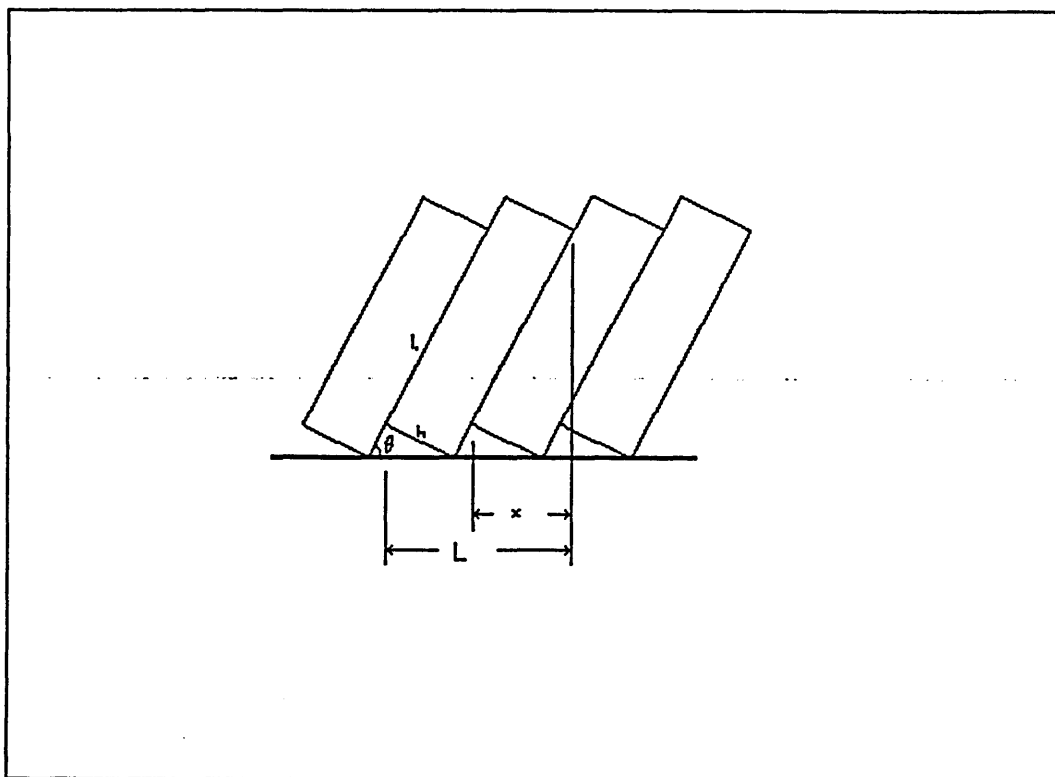
Figure 3.10. The phthalocyanine molecules represented as rectangles, aligned on the substrate at an angle of lean, θ.

65

According to the simple two dimensional geometrical model shown in figure 3.10, the area per molecule can be represented as: (Nabok et al 1995)

$$A = l_2 (L-x) \qquad\qquad 3.3$$

Where:

$$L = l_1 \cos\theta + h \sin\theta \qquad \text{and} \qquad x = (l_1 - h \cot\theta) \cos\theta$$

so,

$$A = l_2 (l_1 \cos\theta + h \sin\theta - (l_1 - h \cot\theta) \cos\theta)$$

$$A = l_2 (l_1 \cos\theta + h \sin\theta - l_1 \cos\theta + h \cot\theta \cos\theta)$$

$$A = l_2 (h \sin\theta + h \cot\theta \cos\theta)$$

$$A = l_2 (h ((\sin^2\theta + \cos^2\theta)/ \sin\theta))$$

$$A = l_2 h / \sin\theta \qquad\qquad 3.4$$

If θ approaches $90°$, $A = l_2 h$

If θ approaches zero and becomes less than the critical angle:

$\theta^* = \text{ArcTan } h/l_1$, $A = l_2 l_1$

So the tilting angle is:

$$\theta = \text{ArcSin } (l_2 h / A) \qquad\qquad 3.5$$

Results of this estimation are presented in table 3.6.

	A406	A410
Present Investigation	30 °	(A too small to calculate θ)
Fernandes et al 1995	N/A	66 °
Hassan et al 1995	59 °	N/A
Nabok et al 1995	66 °	N/A

Table 3.6. Summary of the results obtained for the molecular tilt, θ, and comparison with the results obtained using the Area per molecule obtained by other workers.

Clearly this work is dependant on the accuracy of the measurement of the area per molecule. As the calculation of the tilt for A410 was not possible (due to the area per molecule being less than that of the molecule standing upright), the Langmuir-Blodgett work would need to be repeated with a higher degree of care to ensure the area per molecule results are valid.

The results obtained for the molecular tilt using the area per molecule obtained by other workers give a very similar result for the two materials, at around 66°.

This angle is in the same range as the results of the optical interrogations presented in the chapter 4 (section 4.4.2).

3.5 Summary

The metal free phthalocyanines (A410 and A406) can be successfully deposited on glass and gold coated glass slides. Both materials preferred hydrophobic substrates indicating a strong polar bias of the molecules. The slightly better isotherm of the A410 material mirrored the slightly easier film forming properties of this material over A406.

A410 showed gradual collapse above 35mN/m and A406 showed collapse above 28mN/m the collapse pressure, for each material, varied over 15% due to variations in the quality of the film. Both pressures are acceptable for film forming materials.

A geometrical analysis revealed a tilt angle for both materials using the area per molecule method. The values obtained for the tilt angle using the areas per molecule calculated in this work do not agree with other workers on these materials. Performing the calculation using the areas per molecule of other workers gives a tilt angle of around 66°, which agrees with the result obtained in chapter 4 (section 4.4.2) . This method also revealed the inaccuracy in the area per molecule calculated in this work. This inaccuracy is attributed to the calculation of the concentration of the sample when performing Langmuir Blodgett deposition, and to a lesser extent, the calculation of the subphase area.

Both films were successfully deposited on Yoshi slides (platinum interdigitated electrodes) using the same deposition parameters presented. These samples were used for the electrical tests performed in Chapter 6.

Chapter 4

OPTICAL ABSORPTION IN THIN FILMS

OF PHTHALOCYANINES.

4.1 Introduction

When light of a given wavelength (λ) is incident upon a film, the absorbance (A)

is determined as a function of λ by measuring the intensities of the incident and

transmitted beams ($A = \ln(I_0/I)$). The absorption coefficient α is defined as the as

the ratio of A to film thickness x. The absorbance spectrum is the variation in A

for the sample, over a wavelength range. Absorbance measurements are a useful

tool, because the spectrum provides information about the electronic structure and

the orientation of the molecules in the film. This measurement is also used to

monitor the change in optical absorbance with thickness of the Langmuir-

Blodgett film. The number of monolayers can be compared with the absorbance,

at a given wavelength, to give a measure of the quality of the film deposition. A linear relation is expected to exist between the absorbance and the number of monolayers, if the quantity of molecules transferred per dip is assumed to be constant. The film thickness is directly proportional to the number of monolayers, and the absorbance is directly proportional to thickness. Polarised light absorption spectra give quantitative information about the molecular dipole orientation, in relation to the substrate.

Langmuir-Blodgett films tend to be the same colour as the pre-deposited solid material. Variations in the colour from pre-diluted solid to film, can occur for highly ordered films. Metal free phthalocyanine thin films are typically a green colour, thin films of less then 6 monolayers are virtually transparent. Thick films of 20 to 40 monolayers are ideal for optical investigation. They are well coloured, but are not too thick to be undesirably opaque.

The orientation of the dipoles (molecules) in the film in relation to the slide normal, can be measured optically. Yoneyama et al (1986), Yan et al (1992) and Brynda et al (1991) used polarised light absorbance measurements to obtain the orientation of copper phthalocyanine molecules. They all noticed that the disc shaped molecules were oriented with their flat face towards the dipping direction.

4.2 Practical Issues

Experiments are performed using both unpolarised and polarised light within the visible light range of wavelengths.

This section is split into two parts, 4.2.1 Optical Absorption, and 4.2.2 Polarised-Light Optical Absorption to obtain the molecular orientation of the film molecules.

4.2.1 Optical Absorption

Absorption in organic materials is represented by discrete electron transitions from ground to excited state of a free molecule. This is valid for Langmuir-Blodgett films as organic film molecules are bonded by weak Van-der-Waals' forces and thus they do not have a profound effect on the bulk properties.

Altering the phthalocyanine substituent metal causes differing optical effects, structure effects and molecule-molecule interactions. (Luo et al 1993)

Van-der-Waals forces are typically found in polymer chains and are relatively weak. They are due to the synchronisation of motions of electrons as they approach one another. The attractive force is rapidly overcome by repulsive forces when the inter-nuclear distance becomes too small.

In Van-der-Waals' solids the oscillations of one molecule weakly couple with the adjacent molecules. This has the effect of broadening the absorption peaks as the resonant frequencies of the molecules are affected by the adjacent film. This is due to part of the energy being transmitted through the lattice.

To analyse the absorption spectra, five principle bands are recognised, referred to as Q, B(soret), N, L, and C. Of these the Q band is of the lowest energy. It is well separated from the others and occurs in the far red region of the spectra, accounting for the characteristic blue-green colours of the phthalocyanines. The remainder absorb in the UV region when the B band is normally the most intense and is observed as a broad absorption between 320-370nm. The N, L, and C are of higher energy at around 280, 245 and 210nm respectively. Metal free phthalocyanine is of lower symmetry than the metal-substituted derivatives, and the B and Q bands are split due to axial ligation (Cook 1993).

Absorption of visible and UV light produces changes in the electronic energy of molecules associated with excitation of an electron from a stable to an unstable orbital as shown in Figure 4.1. This transition is accompanied by vibrational and rotational changes in the molecule. It is not usually possible to resolve the resulting absorption bands well enough to see the fine structure; this is due to the vibrational-rotational transitions broadening the absorption peaks.
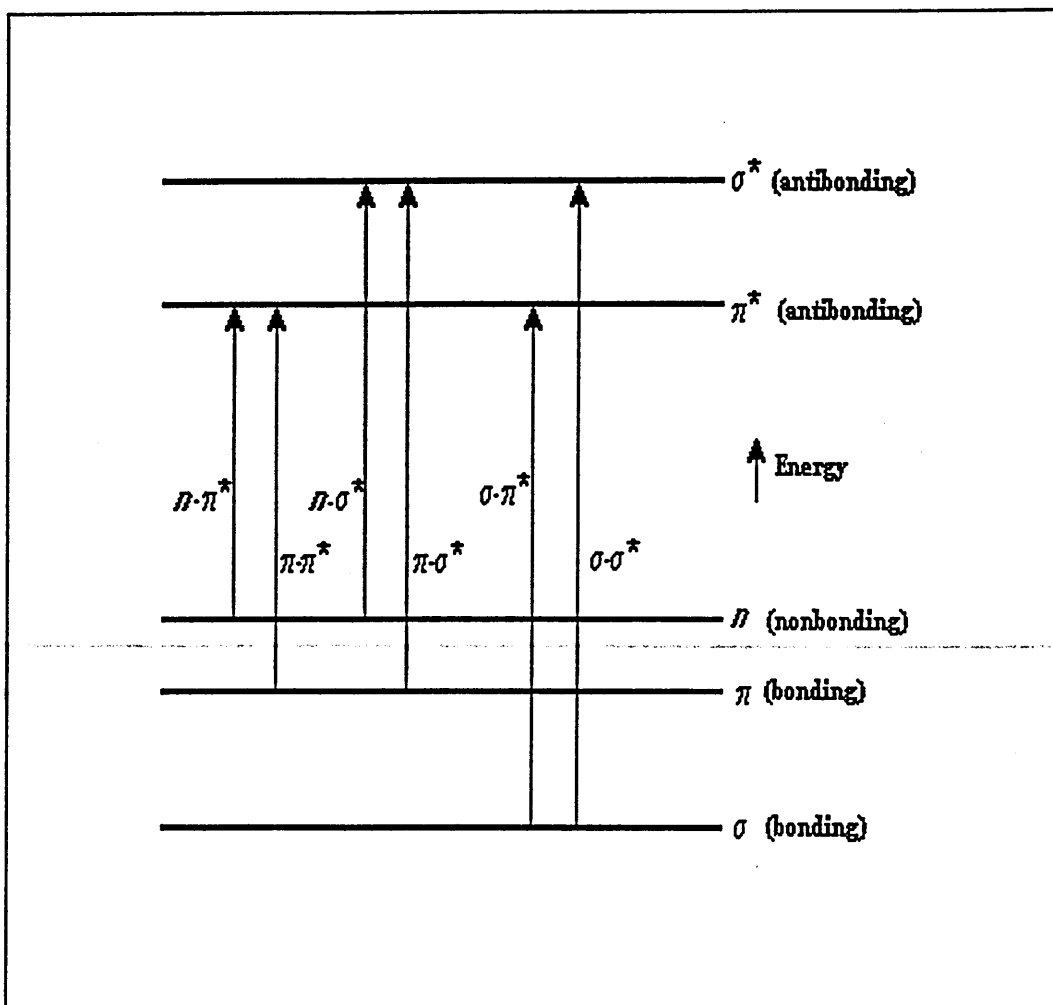
Figure 4.1. Sequence of electronic orbital energies, showing the different transitions in approximate order of increasing energy left to right. (Roberts & Caserio 1965).

π-π* transitions occur in substances with double bonds. Phthalocyanine typically has this structure and the Q-band absorption is generally accepted to arise from the π-π* transitions. The wavelength of the peak relates to the energy of the transition. The lower the energy transition, the longer the wavelength (Roberts & Caserio 1965).

The spectra of aggregated phthalocyanines shows a blue shift of the Q-band. This shift is attributed to near or full co-facial alignment of two or more phthalocyanine molecules. It is explained using the molecular exciton theory which owes much to Davydov (Hush and Woolsey 1971). The close proximity of two or more phthalocyanine rings can lead to coupling between their electronic states. This leads to new energy levels in the excited state, and hence the multiple peaks within the Q-band envelope (Cook 1993).

4.2.2   Polarised-Light Molecular Orientation Measurement

P-polarised light can be explained as the vector sum of two beams of opposing rotation of circularly polarised light (figure 4.2).

An asymmetric molecule will affect the two circularly polarised light beams to different degrees. This means that the resultant beam will be rotated in the direction of the least slowed component. This is called Specific Rotation (Roberts & Caserio 1965). By using p-polarised light incident on an asymmetric molecule, at differing angles of polarisation and incidence, the variation in light absorbed together with the light direction can be used to determine the orientation of the molecule. It is to be noted that the angle of rotation is not measured, but rather the resultant change in absorption.
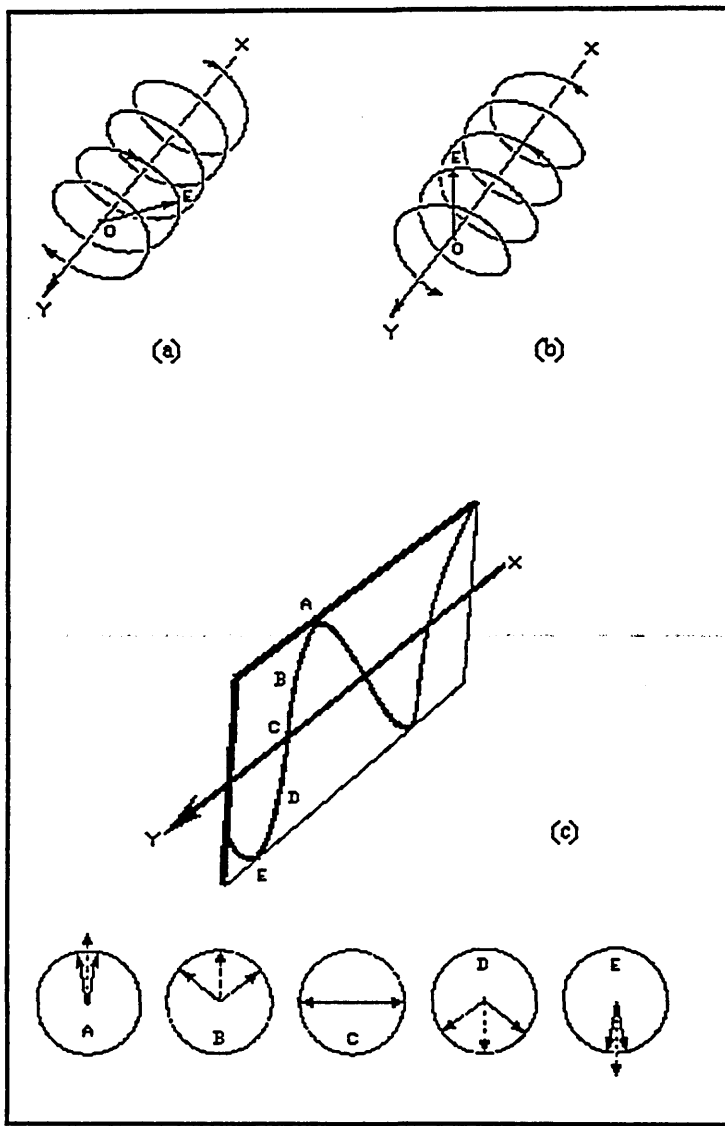
Figure 4.2   *Circularly polarised light (a,b). The spiral represents the path*

followed by the component electric field of a light beam XY,

and may rotate clockwise (a) or counter clockwise (b).

Plane polarised light (c) as the vector sum of two oppositely

rotating beams of circularly polarised light. The two electric

vectors and their resultant are shown separately for the points

A, B, C, D, and E in order to clarify that the resultant vector

oscillates in the form of a sine wave.

(Roberts & Caserio 1965).

Dichroism ratios (D) are the relation between absorption with light polarised parallel to the dipping direction (A//) and absorption with light polarised perpendicular to the dipping direction (A⊥), at a refracted internal angle of incidence (β) and at a given wavelength.

A dichroism ratio of unity indicates an amorphous structure. The greatest deviation from unity of the dichroism is observed in films of high molecular ordering. This is explained by the reasoning that if the film were unordered, (with the molecular dipoles distributed in random directions) the polarised light interrogation from different angles would not differ, i.e. the ratio would tend to unity.

The polarised light is directed at different angles of incidence and polarisation, The molecular dipoles (direction of electronic imbalance) are excited by the p-polarised light when it is oriented in the direction of oscillation of the electro-magnetic field in the incident light. The absorption of light occurs due to this excitation. If all the molecules have the same or a similar orientation, there will be an angle of incidence (and direction of polarisation) that causes the most absorption. This variation of absorption with polarisation of the incident light gives rise to the dichroism. The dichroism can be used to obtain the molecular orientation (Yoneyama et al 1986).

The following method for measuring the molecular orientation, has been adopted

for the present investigation. This is based on the method used by Yoneyama et al

(1986).

Cartesian co-ordinates (X, Y, Z) are introduced, Y is parallel to the dipping

direction and Z is perpendicular to the substrate. To simplify the situation, the

phthalocyanine ring is approximated as a flat circular plate, on which the π - π^*

transition dipole is uniformly distributed. The centre axis of the plate, Z', is

oriented at an angle θ to the Z-axis, with an azimuth of ϕ in the X-Y plane.
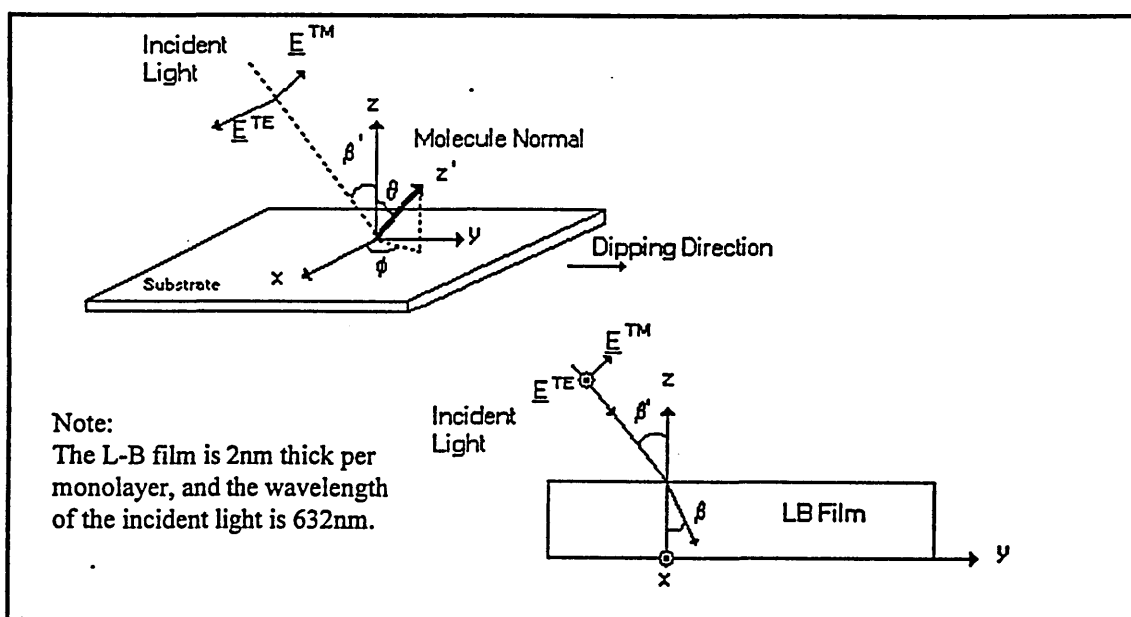
Figure 4.3   *The co-ordinate system and notation used in the calculations*

of the molecular orientation.

The dichroic ratio, $D_\beta = A_{//}/A_\perp$ ($A_{//}$ and $A_\perp$ are the absorbance of the film for polarised light parallel (//) and perpendicular ($\perp$) to the dipping direction, respectively) can be expressed as:

$$D_\beta = \frac{[\langle \cos^2 \phi \rangle + \langle \cos^2 \theta \sin^2 \phi \rangle]}{[\{\langle \sin^2 \phi \rangle + \langle \cos^2 \theta \cos^2 \phi \rangle\} \times \cos^2 \beta + \langle \sin^2 \theta \rangle \sin^2 \beta]} \qquad 4.1$$

Where $\langle\rangle$ denotes a statistical average over the absorption peak of interest.

The orientation of the Z' axis can then be estimated from the dependence of D_β on β. This is done by measuring D_β at two angles $0°$ and β ($\neq 0°$), and to calculate $\langle \cos^2 \theta \rangle$ and $\langle \sin^2 \theta \cos^2 \phi \rangle$, by the following equations:

$$\langle \cos^2 \theta \rangle = \frac{D_0 - (1 + D_0 \sin^2 \beta) D_\beta}{(1 - 2\sin^2 \beta) D_\beta - (1 + D_\beta \sin^2 \beta) D_0} \qquad 4.2$$

$$\langle \sin^2 \theta \cos^2 \phi \rangle = \frac{D_0 - \langle \cos^2 \theta \rangle}{1 + D_0} \qquad 4.3$$

The angles ϕ and θ, indicate the orientation of the molecules in the film, as shown in figure 4.3.

Calculating D_0 and D_β over a range of light wavelengths and angles β, will give enough information to obtain $\cos^2 \theta$ and $\sin^2 \theta \cos^2 \phi$, θ and ϕ can then be obtained. The angles θ and ϕ are an average over the area studied by the instrument. They represent the average molecular dipole orientation with respect to the substrate.

4.3 Experimental Details

Experimental details are given for two similar measurements, Optical Absorption and Molecular Orientation measurement. The basis for both measurements is the measurement of the reduction in light intensity of an incident light source due to absorption of light in the thin film. The difference between the two measurements is that the absorption measurement uses un-polarised light incident at the normal to the sample plane and the orientation measurement uses polarised light and a range of incident light angles. These extra parameters and the corresponding variation in light absorbed by the sample, are used to calculate the average orientation of the molecular dipoles in the thin film.

4.3.1 The Optical Absorption Measurement Technique

Using an ATI Unicam UV-Vis Spectrometer with Vision Software, the light absorption is measured over the visible light range. The spectrometer works on the basis of comparing the absorbance of a reference slide with the slide (with the sample deposited on it), in two separate light beams as shown in figure 4.4. The reference slide is of the same material as the substrate of the sample, this means that the absorbance due to the substrate are compensated. Film samples were prepared on glass substrates using the Langmuir-Blodgett deposition technique.

range. Taking the baseline into account, a plot of absorbance versus wavelength can be obtained. The light is scanned through a wavelength range of 350 to 900 nm. This range is limited by the instrumentation light source. The results are plotted on a graph of absorption versus wavelength. The location of the peaks produced on the graph indicate the wavelengths absorbed by the sample.

4.3.2 Molecular Orientation Measurements

The orientation of the molecules in the Langmuir-Blodgett films is examined by comparing the optical absorption results from tests performed with polarised light, parallel and perpendicular to the dipping direction (Yan et al 1992). The slide is positioned firstly perpendicular, then at various angles (β) from the incident beam in the y plane (the dipping direction) as shown in figure 4.5.
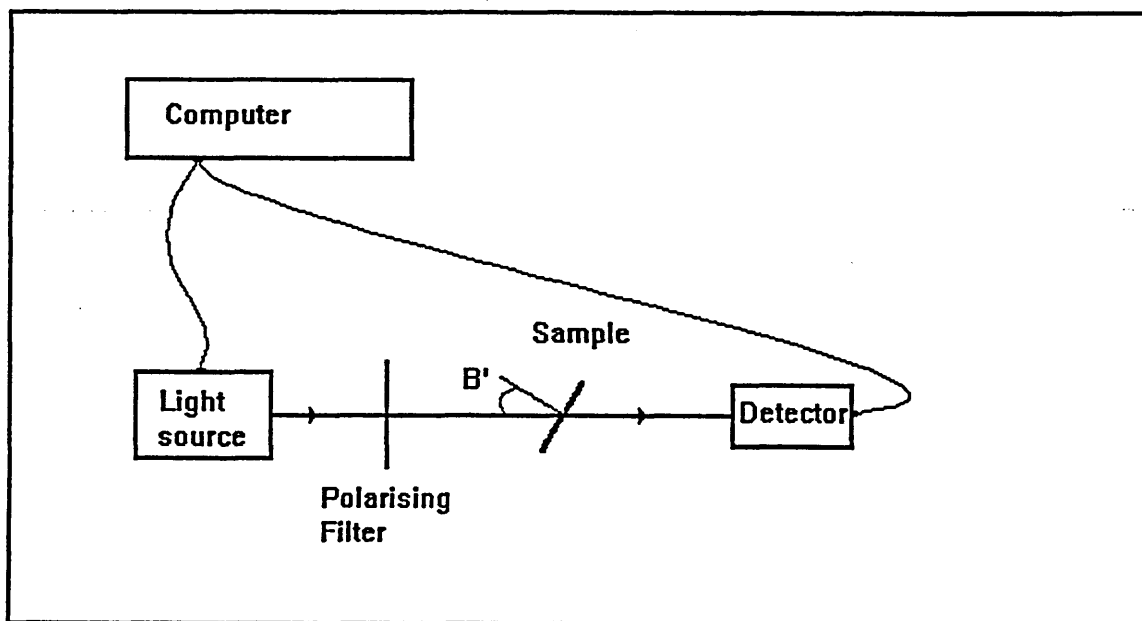
Figure 4.5   *A schematic diagram of the basic components for optical*

molecular orientation measurements.

The relation among these absorption results is used to give an indication of the dichroism of the molecules on the slide substrate. Dichroism is usually defined as the property of some materials, of selectively absorbing light vibrations in one plane yet passing them in another. Dichroism in this case, is the ratio in absorption of light polarised parallel to light polarised perpendicular (to the dipping direction in the case of LB films). Dichroism other than unity, is apparent for films that have a preferential orientation. As most of the molecules align in one direction (and it follows that their dipoles also align), the absorbance due to the film is dependent upon the angle of polarisation and also the angle of incidence. This is due to the light encountering the film at some specific angles that coincide with a group-dipole alignment and others that have minimal coincidence with dipole alignment.

4.4 Results and Discussion of the Optical Analysis

The results are presented for the two measurements, optical absorption (4.4.1) and molecular orientation (4.4.2). Two materials were tested, A406 and A410 metal free phthalocyanines as detailed in Chapter 2. An investigation into the relation between electronic transitions and the type of molecular aggregates was undertaken. This is presented in 4.4.3.

4.4.1 Optical Absorption Results
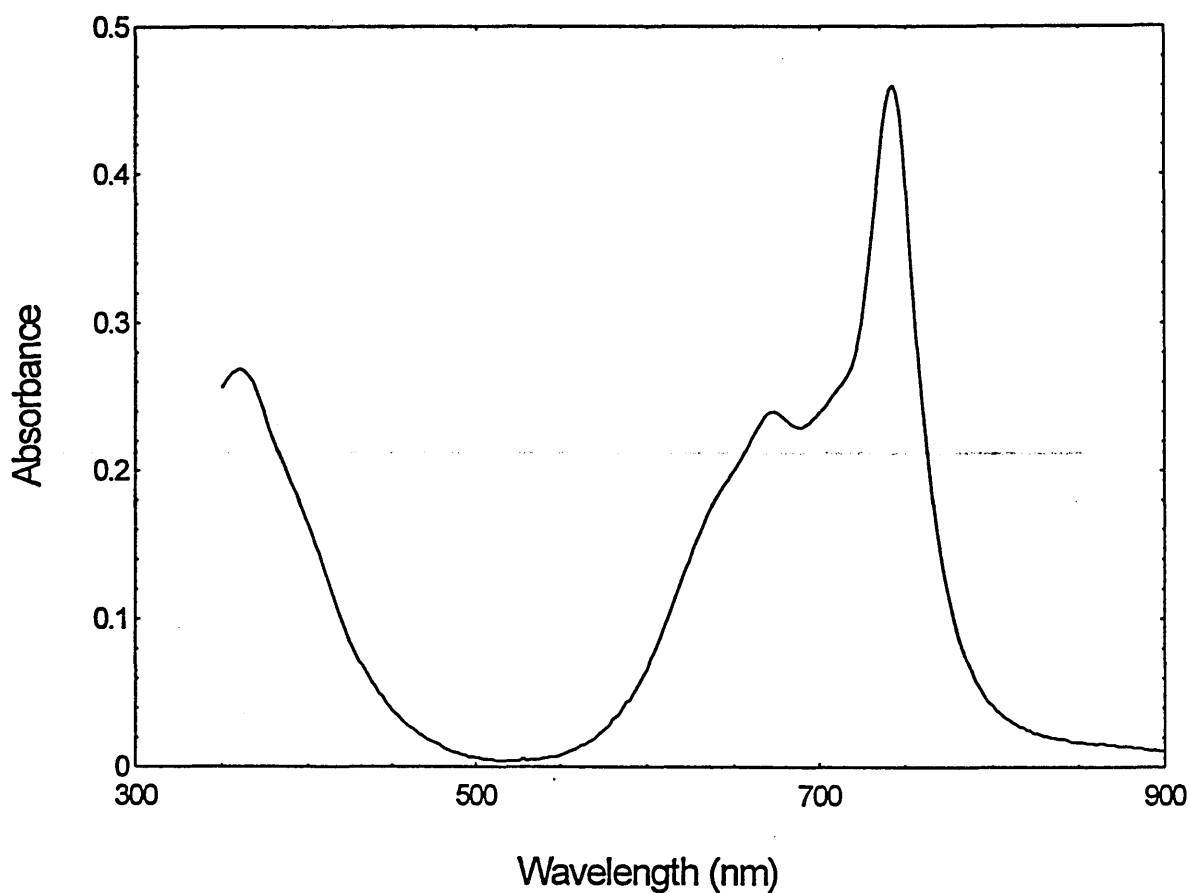
Figure 4.6 The optical absorption spectra of A406, 18 monolayers thick.

From figure 4.6 (A406), The Q-band (550-800nm) and B-band (<500nm) are apparent. Davydov splitting is apparent from the peak shape incorporating two main peaks under the absorption envelope. The longer wavelength peak at 730 nm is attributed to the aggregates in the film. The peak at 650 nm is attributed to the dimer with parallel planes. The weak sideband at 700 nm is attributed to the monomer
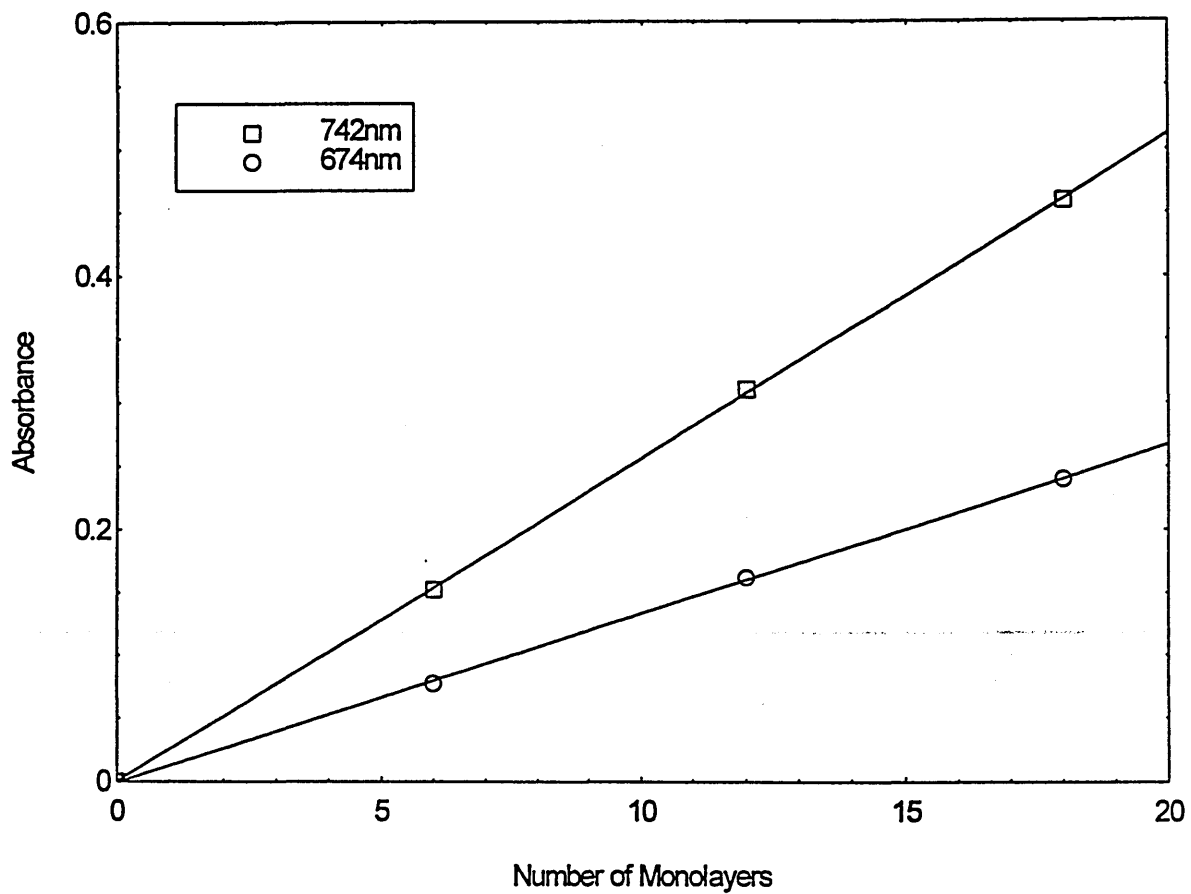
Figure 4.7 The linear variation of absorption with thickness for the two

absorption peaks of A406.

Figure 4.7 is used to confirm the Langmuir-Blodgett deposition qualities. This
figure is incorporated in the analysis in Chapter 3 (Langmuir-Blodgett
deposition).
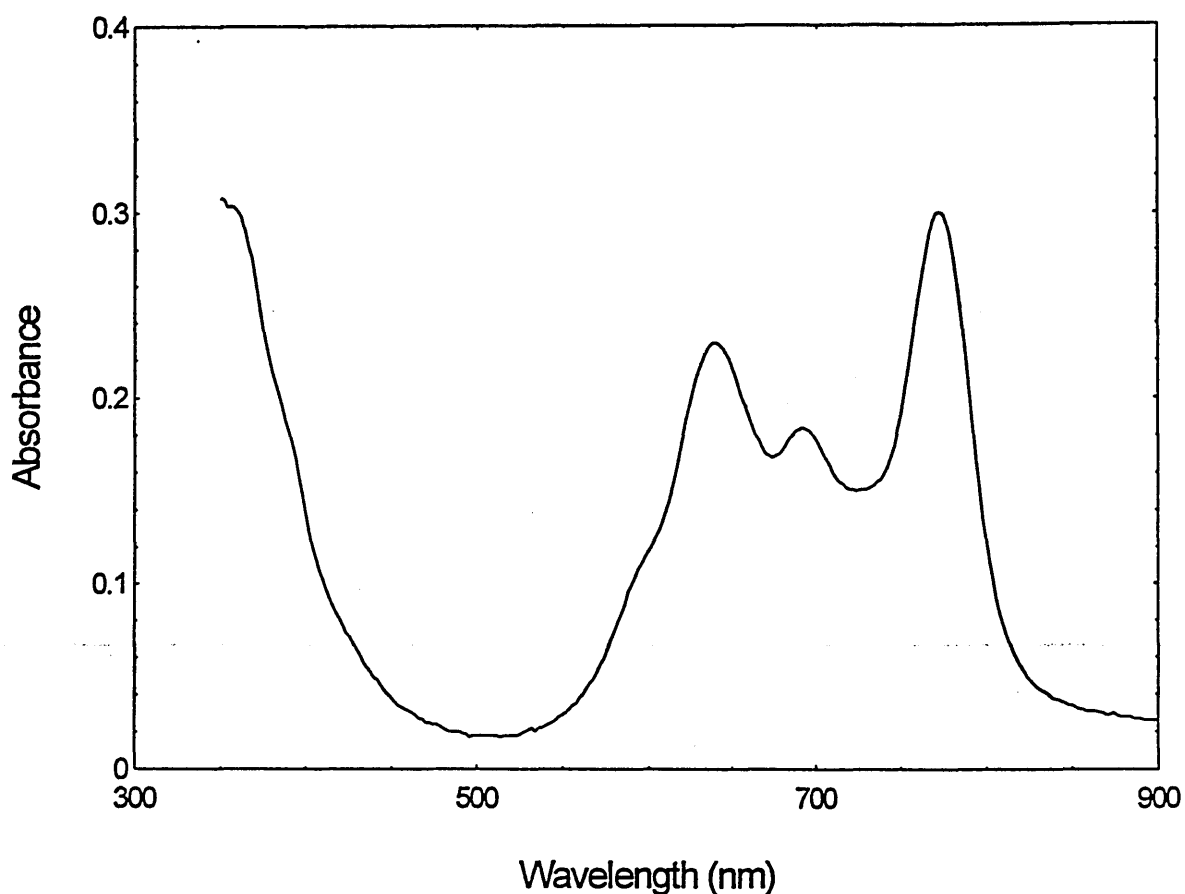
Figure 4.8 The optical absorption spectra of A410, 32 monolayers thick.

For 410, the Q-band (550-800nm) and B-band (<500nm) are also apparent. Davydov splitting is visible from the peak shape incorporating two main peaks under the absorption envelope. The longer wavelength peak at 770 nm is attributed to the aggregates in the film. The peak at 630 nm is attributed to the dimer with parallel planes. The weak sideband at 680 is attributed to the monomer.
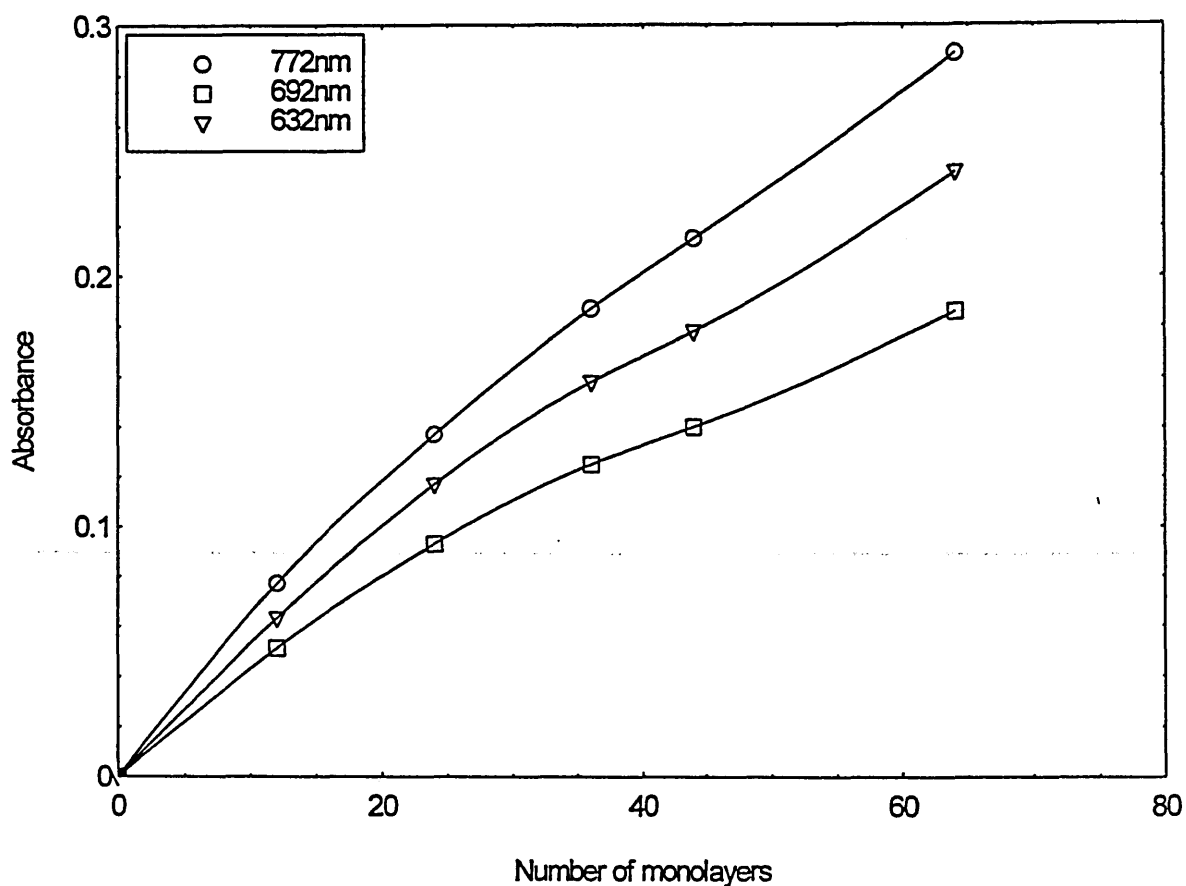
Figure 4.9   *The linear variation of absorption with thickness for the three*

absorption peaks of A410.

Figure 4.9 is used to confirm the Langmuir-Blodgett deposition qualities. This figure is incorporated in the analysis in Chapter 3 (Langmuir-Blodgett deposition). It is apparent that for this sample, the deposition is not uniform. However, the thickness of this film is greater than the film represented in figure 4.7. The decrease of film transfer quality with thick films is a common phenomenon with Langmuir-Blodgett films. It can be attributed to aberrations in

86

the first layers causing a propagation of defects, leading to poor transfer at greater thicknesses.

The two materials (A406 and A410) both display similar spectra confirming the same building blocks of this variety of material (i.e. they are both metal free phthalocyanines) as expected (Fernandes et al 1995). They both have the characteristic Q-band peaks with Davydov splitting apparent. The differences in peak size display the effect of the differing 'tail' groups of these metal free phthalocyanines. However, there was no apparent difference in the colour of the samples to the untrained eye.

The term "aggregations" describes the form of packing the molecules display. It is believed (Cook 1995) that the molecules pack face to face, in columns, lying along the surface of the substrate. This would then introduce an optical absorption due to the way that the molecules interact together on a molecular level, to give the impression of a different atomic structure than a 'stand alone' molecule. The result is a blue shift in the Q-band, and splitting of the peaks.

The results confirm the good quality of the Langmuir-Blodgett deposition; the optical absorption was proportional to the number of monolayers (thickness).

4.4.2 Molecular Orientation using Polarised Light

Analysis

Some initial dichroism tests were carried out with the Unicam spectrometer modified with the addition of a polarising filter. The baseline calibration was performed to ensure the instrument was corrected for the filter. The sample, consisting of A410 deposited on both sides of a glass slide, was positioned at normal incidence and at $23°$ to the incident beam. Again, baseline calibration was performed to compensate for the change in absorbance due to the substrate. The analysis was initially done at the absorption peak wavelengths for the material, and at two angles of incidence, $\beta' = 23°$ and $0°$.

Parameter	Value
$\langle D_0 \rangle$	1.081
$\langle D_\beta \rangle$	0.993
$\langle \cos^2\theta \rangle$	0.153
$\langle \cos^2\phi \rangle$	0.515
$\langle \theta \rangle$	67°
$\langle \phi \rangle$	44°

Table 4.1 Extracted results from the initial calculation of the molecular

orientation for A410 averaged over the Q-band.

A406 metal free phthalocyanine was tested using the Yoneyama et al (1986) method. For maximum resolution, the angle β' was 0° and 70°. Dichroism ratios were calculated at the key absorption peak wavelengths, 730nm, 650nm and 700nm. The dichroism values were used to obtain the preferred orientation angles, using the method previously outlined. The following table summarises the calculations.

Peak wavelength	β'	TM	TE	D	β		θ	φ
730nm	0°	0.37	0.67	0.56	0°		48°	67°
	70°	0.27	1.18	0.23	55°			
650nm	0°	0.22	0.30	0.73	0°		82°	49°
	70°	0.26	0.52	0.50	54°			
700nm	0°	0.23	0.35	0.66	0°		62°	54°
	70°	0.23	0.60	0.38	54°			

Table 4.2 Extracted results from the molecular orientation measurement for

A406. Note: cosβ=A(β')/A(0) and β average = 54°

For A406, the dimer is almost aligned perpendicularly to the substrate face at 82°. This value is close to the result obtained by Cook et al (1988) at 80° for CuPc. However the aggregate dipole is at 49° to the substrate face, suggesting a staggered stacking formation. The monomer is 20° out of alignment with the dimer at 62°. However the monomer orientation is between that of the dimer and aggregates. This is reasonable as the dimer and aggregates are made up of monomers. The dipoles are oriented at an average angle of 57° from the dipping direction, this would agree with the herringbone alignment as described by Nabok et al (1995)and Cook (1993).

A410 metal free phthalocyanine was also tested using the Yoneyama et al (1986) method. Again for maximum resolution, the angle β' was $0°$ and $70°$. Dichroism ratios were calculated at the key absorption peak wavelengths, 770nm, 630nm and 680nm. The dichroism values were used to obtain the preferred orientation angles, using the method previously outlined. The following table summarises the calculations.

Peak wavelength	β'	TM	TE	D	β		θ	ϕ
770nm	0°	0.16	0.12	1.33	0°		66°	39°
	70°	0.13	1.23	0.543	58°			
630nm	0°	0.11	0.13	0.846	0°		66°	29°
	70°	0.15	0.24	0.625	57°			
680nm	0°	0.10	0.08	1.187	0°		51°	51°
	70°	0.09	0.17	0.5	62°			

Table 4.3 Extracted results from the molecular orientation measurement for A410. Note: $cos\beta = A(\beta')/A(0)$ and β average = 58°

For A410, the dimer and aggregation dipole fields are both at 66° from the substrate face indicating a strong columnar stacking of the molecules. The

monomer is only fifteen degrees out of alignment at 51°. The dichroism values correspond very well with Fernandes et al (1995) (1.38 @ 772nm and 0.8 @ 636nm). The results are within five percent agreement. The dipoles are also oriented at an average angle of 40° from the dipping direction, this is also in agreement with the herringbone alignment (Nabok et al 1995).

The orientation measurements performed on these materials reveal the ordered structure of the molecules in the film and the preferred direction of orientation. The tests conform to the predicted structure expected with Langmuir-Blodgett films. From the principle that each peak in the spectra represents electronic excitations of energy (proportional to the wavelength), it follows that each absorbance peak represents a different dipole field within the molecule. The orientation of the dipole field in the molecule is apparent from the orientation results obtained for each peak. This interpretation is new as the usual approach is to analyse the visible spectrum as a whole.

4.4.3 Investigation of the Relation Between the Electronic Transitions and the Type of Molecular Aggregations.

Decomposition of the Q-band into four Gaussian-Lorentzian single band approximations was undertaken to find a correlation between the electronic transitions and the structure of the Langmuir-Blodgett film. Parameters of the Gaussian-Lorentzian fit of the figures 4.6 and 4.8, are presented in table 4.4 and

4.5 respectively. The wavelength axis was converted to wavenumber for this approximation.

Centre (Wavelength)	Centre (Wavenumber)	Amplitude	Width	% Gaussian	Area
730nm	16113.9	0.411	1196	1.9	767
650nm	18393.7	0.208	3076	84	731
610nm	19938.6	0.020	1273	97	28
700nm	17197.5	0.022	559	96	13

Table 4.4 Extracted results from the Gaussian-Lorentzian approximation of the absorbance spectra for A406 (figure 4.10).
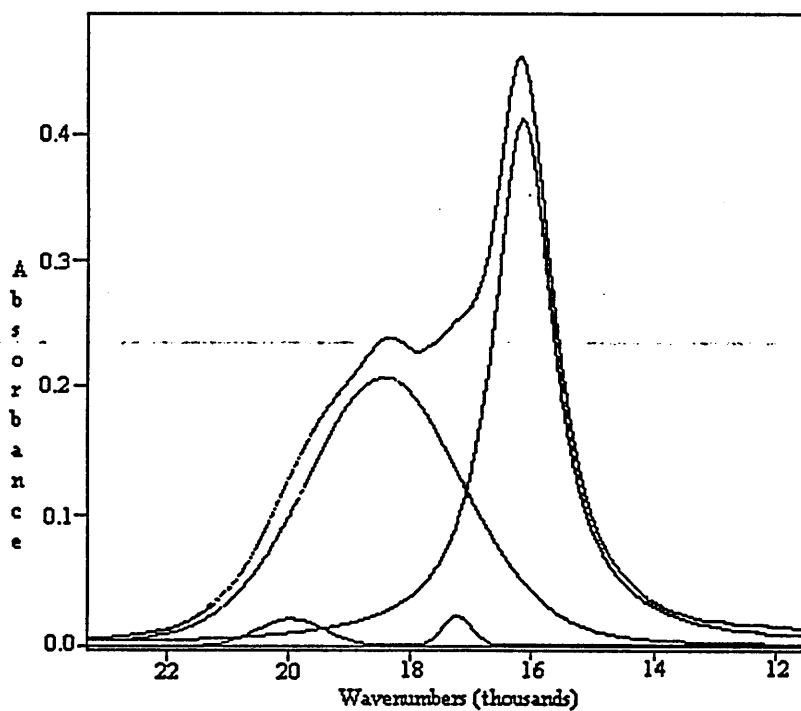
Figure 4.10 The Gaussian-Lorentzian approximation of the absorbance spectra for A406.

94

The two main bands of the absorption spectra correspond to the Davydov doublet in molecular crystals with two un-equivalent molecules per unit cell. This system is referred to as the "herringbone" arrangement, as shown in figure 4.12.
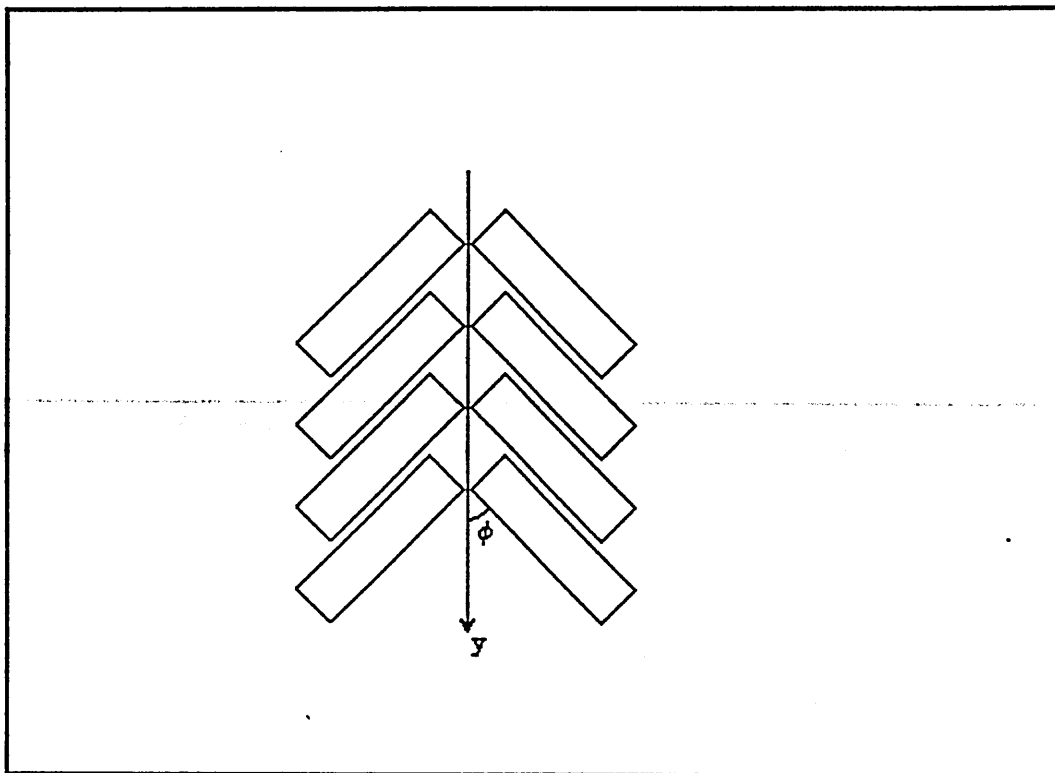
Figure 4.12 The "herringbone" molecular arrangement, viewed from above

the substrate. Y is the dipping direction.

Such arrangement is seen in molecular crystals of the α and β form of phthalocyanine (Cook et al 1993).

The angle ϕ can be calculated using the following expression (Kirstein and Mohwald 1992).

$$\tan^2 \phi = \frac{f_{\parallel}}{f_{\perp}}$$

4.4

Where $f_{//}$ and $f_{\perp}$ are the oscillator strength components directed parallel and perpendicular to the stack axis (y). According to Kashas' model for molecular dimers (Pope and Swenberg 1982), the $f_{//}$ and $f_{\perp}$ components correspond to the "blue" and "red" bands of the Davydov doublet.

Taking into account that the oscillator strength is proportional to the integral of the absorption intensity through the corresponding band (Pope and Swenberg 1982).

$$f \approx \int J(v)dv \qquad\qquad 4.5$$

The final expression can be obtained.

$$\tan^2 \phi = \frac{\int J_{//}(v)dv}{\int J_{\perp}(v)dv} \qquad\qquad 4.6$$

Using the areas under the Gaussian-Lorentzian approximations for the Davydov doublet, the values of ϕ are obtained. A406 has $\phi = 44°$ and A410 has $\phi = 44°$. The values are close to what are expected with the β-form molecular crystal of metal free phthalocyanine at $\phi = 45.7°$ (Cook 1993). This result is in agreement with the results obtained in section 4.4.2, table 4.1 (44°). This suggests that the analysis method of the angle using polarised spectroscopy (as in section 4.4.2) is more accurate when averaged over the whole spectrum and not when split into separate peaks (as in tables 4.2 and 4.3).

4.5 Summary

For both materials (A410 & A406), the Q-band (550-800nm) and B-band (<500nm) are apparent. Davydov splitting is visible from the peak shape incorporating two main peaks under the absorption envelope. The longer wavelength peak at 770 nm is attributed to the aggregates in the film. The peak at 630 nm is attributed to the dimer with parallel planes. The weak sideband at 680 is attributed to the monomer.

The two materials display similar absorbance spectra of the form expected for these materials (Fernandes et al 1995). The differences in peak size are due to the effect of the differing 'tail' groups of these metal free phthalocyanines.

The results confirm the good quality of the Langmuir-Blodgett deposition, with a linear relation between absorbance and thickness.

For A406, the dimer is almost aligned perpendicularly to the substrate face at 82°. However the aggregate dipole is at 49° to the substrate face, suggesting a staggered stacking formation. The monomer is 20° out of alignment with the dimer at 62°. However the monomer orientation is between that of the dimer and aggregates. This is reasonable as the dimer and aggregates are made up of monomers. The dipoles are oriented at an average angle of 57° from the dipping direction, this would agree with the herringbone alignment as described by Nabok et al (1995).

For A410, the dimer and aggregation dipole fields are both at 66° from the substrate face indicating a strong columnar stacking of the molecules. The

monomer is only fifteen degrees out of alignment at 51°. The dichroism values correspond very well with Fernandes et al (1995) (1.38 @ 772nm and 0.8 @ 636nm). The results are within five percent agreement. The dipoles are also oriented at an average angle of 40° from the dipping direction, this also corresponds to the herringbone alignment (Nabok et al 1995).

Using the areas under the Gaussian-Lorentzian approximations for the Davydov doublet, the values of ϕ are obtained. A406 has $\phi = 44°$ and A410 has $\phi = 44°$. The values are close to what is expected with the β-form molecular crystal of metal free phthalocyanine at $\phi = 45.7°$ (Cook 1993). This result suggests that the analysis method of the angle using polarised spectroscopy (section 4.4.2) is more accurate when averaged over the whole spectrum as in table 4.1 (44°) and not when split into separate peaks as shown in tables 4.2 and 4.3 (57° and 40° respectively).

Chapter 5

SURFACE PLASMON RESONANCE (SPR)

CHARACTERISATION OF THIN FILMS.

5.1 Introduction to SPR Issues with Thin Films

The interaction of electromagnetic fields with a polarising medium generates polarisation excitons known as Plasmons. These excitons may propagate either through the bulk of a medium, halted by the interface to another medium, or they propagate along the interface between two differing dielectric materials. Such interface excitons are called Surface Polaritons. Surface polaritons propagate in a wave-like manner along the interface and their electromagnetic fields can either be evanescent away from the surface or oscillatory depending on the dielectric properties of the media. Surface plasmon polaritons (or surface plasmons) occur at the interface between a metal and a dielectric. (Kovacs 1982).

Surface plasmons can be defined as coupled localised transverse magnetic (TM) electromagnetic field charge density oscillations that may propagate along an

interface between two media with dielectric constants of opposite signs such as with a metal and a vacuum (Raether 1977). The intensity of the electromagnetic fields associated with these waves is at a maximum at the interface and decays exponentially on both sides. Therefore their wave vector (k_{sp}) is very sensitive to any modification occurring at the interface. These waves are optically excited using a suitable optical arrangement such as the prism. The evanescent waves result from total internal reflection on the inner face of the prism. This optical arrangement is known as the Kretchmann configuration (Kretchmann & Raether 1968) and is termed as the attenuated total reflection or (ATR) method. However, the double grating method has been investigated and suggested as an improvement over the prism in terms of experimental integrity (Nemetz et al 1994)

The experimental principle is to coat the base of the prism with a thin evaporated layer of a metal (e.g. silver or gold). For a particular value of the angle of incidence θ_I inside the prism, the tangential component of the wave vector of the evanescent wave matches that of the surface plasmon, which is then excited. When the coupling is optimum (a silver thickness of approximately 50nm) the total incident energy is dissipated through diffusion of the plasmon wave in silver. As a result of this, the reflection coefficient falls to zero. The resulting dip in the reflection as a function of incident angle is attributed to the surface plasmon resonance.

Truong et al (1994) describe "photonics" as the optical analogue of electronics in which photons, instead of electrons, are used to acquire, store, transmit and

process information. Non-linear optics will play a major part in enabling photonics to develop. Truong et al (1994) state that the recent progress in the field of high-speed optoelectronics and information technology has encouraged the search for materials with good non-linear optical properties. This naturally leads on to further development of the techniques for measuring non-linear optical properties. Some of these techniques are: i) time-resolved third-order non-linear optical susceptibility (Truong et al 1994), ii) second harmonic generation (Isomura et al 1994, Sakaguchi et al 1994), and iii) the Pockel's effect (SPR) (Cresswell 1992). Surface plasmon resonance (SPR) is an optical measurement that has applications with thin films as chemical sensors (Matsubara et al 1988), SPR can measure the dielectric constant of a sample attached to a metal film. If the sample is contaminated by a chemical species, then the dielectric constant would be affected and can be used to obtain the concentration of the chemical species. Matsubara et al (1988) were successful in detecting concentrations as low as 10^{-4} wt./wt. of ethanol in water. Although their sample was water based, the same principle can be used to detect gases with thin films. If a gas sensitive organic film is placed on the metal film, its change in dielectric constant due to the presence of a contaminant gas may be observed. SPR has also been used to create 3-dimensional images of thin films (Morgan and Taylor 1994). It has also been used to investigate the molecular structure of Langmuir-Blodgett films (Cresswell et al 1994) and test the suitability of the film for non-linear device applications.

5.2 Surface Plasmon Principles.

Surface plasmon resonance measures both the dielectric constant of the metal and that of a sample medium coating the metal. It is ideal for measuring the properties of Langmuir-Blodgett films that are deposited on metal coated slides. The plasma surface (metal) may allow group resonant oscillation of free electrons, this produces a charge density wave propagating along the surface. This transverse wave is called the surface plasmon. Its oscillating field vector is normal to the surface. Thus the light to excite the surface plasmon should be polarised parallel to the incident plane (p-polarised). Resonance occurs when the wave vector and frequency of the incident light coincide with those of the surface plasmon. The conditions at which resonance occurs can give the dielectric constant of the sample.

5.2.1 Coupling to and Excitation of Surface Plasmons

The collective electron oscillation constituting the plasmons have a collective wave vector k_{sp} parallel to the metal and dielectric interface. The dispersion (ω-k) relation for these surface modes can be obtained by applying Maxwell's equations and satisfying the appropriate boundary conditions for such an interface.

$$k_{sp} = k \left(\frac{\varepsilon_1 \varepsilon_2}{\varepsilon_1 + \varepsilon_2} \right)^{1/2} = \frac{\omega}{c} \left(\frac{\varepsilon_1 \varepsilon_2}{\varepsilon_1 + \varepsilon_2} \right)^{1/2} \qquad\qquad 5.1$$

Where ω is the eigenfrequency of these modes, and ε_i is the dielectric constant of the ith medium. For k_{sp} to be real, which is the requirement for a propagating mode:

I) ε_0 and ε_1 should be of opposite signs,

II) and $|\varepsilon_1| > \varepsilon_0$

which are the conditions for a metal and dielectric interface.

Therefore k_{sp} is always greater than the light wave vector component, along the interface that travels through vacuum.
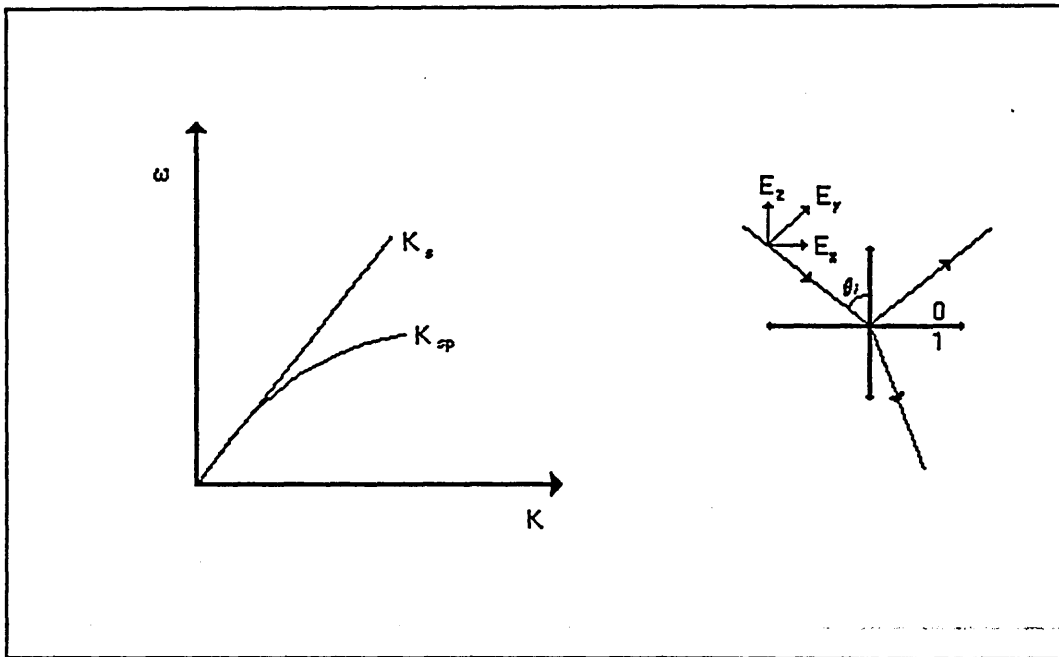
Figure 5.1 Dispersion of light in sample (Ks) and surface plasmon (Ksp). The ordinate is frequency, the abscissa is wave vector.

Note: 1) ε_0 and ε_1 should be of opposite signs, 2) and $|\varepsilon_1| > \varepsilon_0$

Figure 5.1 shows that the energy and momentum of the incident light and the surface plasmons (SP's) cannot be the same simultaneously as the two curves do not cross. This means that the excitation can only be achieved if the x-component of the light momentum can be enhanced to match that of the SP's. This is done by embedding the metal between two different dielectric media such as glass and vacuum. Total internal reflection of light in a glass prism occur when light is incident at internal angles beyond the critical angle, on an interface of higher to lower refractive index media (Kretchmann and Raether 1968). This totally reflected beam evanescently decays away from the surface of the prism and travels along the interface with a momentum enhanced by the high refractive

index of the prism. This enhanced energy allows the light to match the energy of the SP's at a metal / dielectric interface.
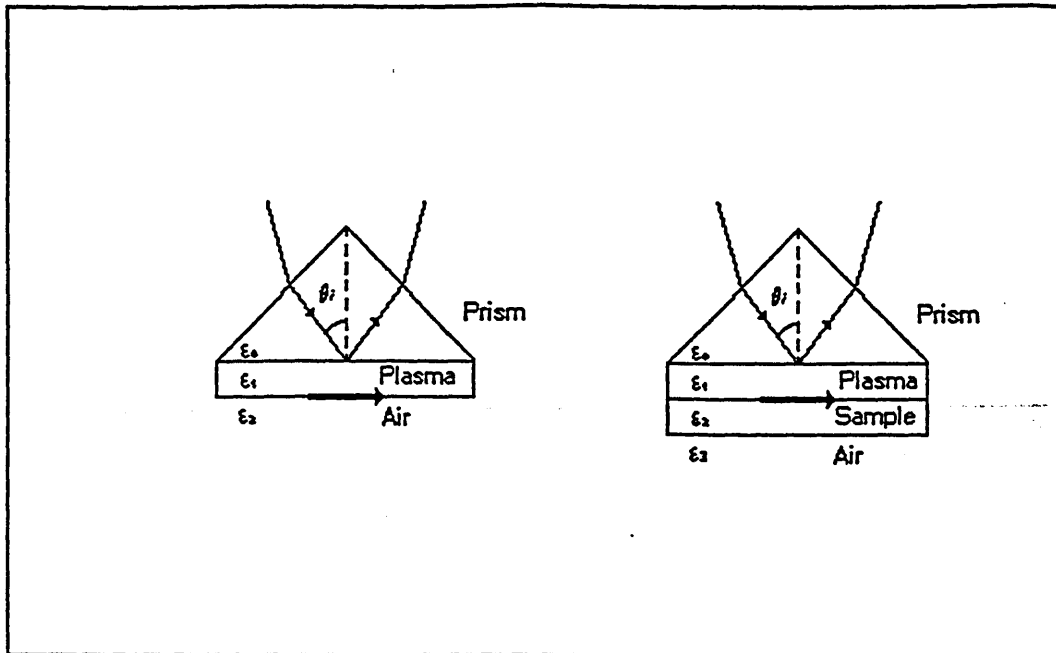
Figure 5.2   Kretschmann's configuration for observing SPR.

Figure 5.2 shows the Kretchmann configuration for light coupling to SP's across a thin metal plasma. The metal film thickness is chosen to be thick enough to reduce re-radiation into the prism but thin enough to permit the field to penetrate to the opposite surface. Typical film thickness' of gold or silver are in the region of 50nm (Hassan et al 1995).

5.2.2 Surface Plasmon Imaging Issues

The SPR technique may be used to produce visible images of the sample. This is a useful technique for quality checks of the structure of Langmuir-Blodgett films. The principle is that the light responsible for the surface plasmon generation is expanded into a wider parallel beam to interrogate the whole sample surface. The collimated nature of the wide beam is very important as the angle of incidence must remain the same for all the sample surface. The reflected light is then focused back down to the size of the (video) camera aperture. The camera monitor will display the illuminated image. If the sample is a composite of a number of films, then as the various parts of the film undergo the SPR resonance angle, the resonant part of the film appears dark. This darkness corresponds to the low reflectivity trough in the SPR curve. The amount of resolution available with this large change in reflectivity is clearly visible on the image, the films appear similar to the naked eye, but under SPR imaging, the different thickness' are clearly visible. This method has clear advantages over normal optical microscope imaging, as the resolution available with this technique can easily identify the interface between films on a nanometer scale.

5.3 Experimental Techniques

5.3.1 Equipment

A monochromatic plane polarised Spectra Physics He-Ne ($\lambda = 632.8$nm) gas laser is used to illuminate the prism. To ensure that the light beam is of an optimum collimation, intensity and polarisation, it is passed through an aperture, a neutral density filter, and a polariser. The beam is modulated using a mechanical chopper to produce a step signal (on / off) at a frequency of 1.6 kHz. This frequency is chosen to help eliminate noise from sources of lower frequency such as laboratory light sources. A beam splitter is then used to divert a small fraction of the beam intensity to a reference photo-detector. The reflected beam is detected by a photo-detector and the reflected signal is passed together with the reference signal to a Stanford Research Systems SR830 DSP Lock-in Amplifier. The use of a reference beam compensates for any drift in the light source intensity and removes the background dc level from the modulated signal, leading to highly reduced noise in the data. Figure 5.3 shows the experimental configuration.
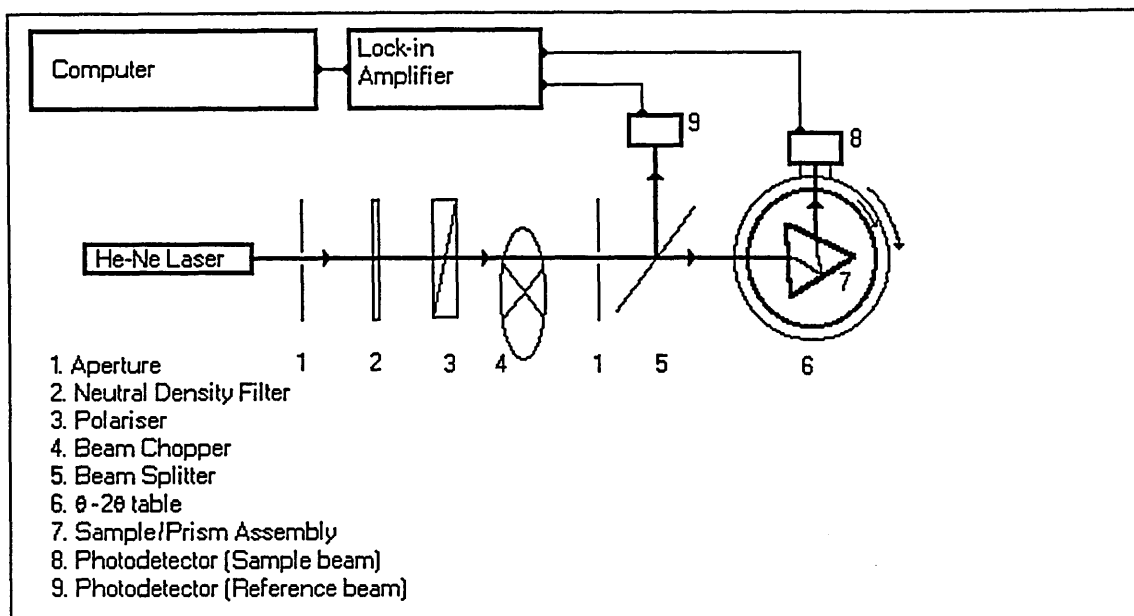
Figure 5.3   *A schematic representation of the components used to obtain*

SPR.

The prism-sample assembly consists of the glass prism, of equilateral triangle configuration, with a refractive index of around 1.51. The equilateral configuration is ideal for this experiment as it is the most flexible in terms of range of incident light angles and permitting effective reflection using the θ / 2θ angle table. The prism is also readily available in optical laboratories. The θ / 2θ angle table is essential as it permits the prism to be rotated by an angle θ whilst the reflected beam can be tracked using a photodetector rotating through 2θ. The two stages of the table are independently motorised with a pair of computer controlled stepper motors. The motors are geared such that as the prism rotates through θ, the photo detector arm rotates through 2θ, in the same direction.

5.3.2 Sample Preparation

The sample slides are ultrasonically cleaned with high purity organic solvents (such as aristar chloroform), prior to coating. An approximate metal thickness of 50nm is obtained with a metal evaporation rate of around $1nm.s^{-1}$. The evaporation process for depositing metals on glass slides is detailed in Chapter 6. A number of slides are subsequently coated with Langmuir-Blodgett layers of phthalocyanines. These are used to investigate the effect organic films have on the surface plasmons and to obtain the properties of these films. The prism was cleaned at regular intervals with an organic solvent to avoid contamination.

The slide is joined to the backside of the prism using regular glass index matching fluid. This method is convenient in that the prism remains separate from the metal. The metal is easily deposited on a clean slide.

5.3.3 Prism Location

It was found that the ideal position of the prism is so the centre of the prism is on the centre of rotation of the table. Previous attempts used the back of the prism (as the centre of rotation), as it was thought that light would only interrogate a single spot on the back. However refraction was not taken into account and the reflected beam appeared to move at a greater rate than expected (2θ). Positioning the prism, centred on the centre of rotation permitted true single-spot interrogation, and a properly tracked reflected signal.

5.3.4 Calibration

To calibrate the angle table, the normal incidence must be known. This can be obtained by rotating the prism table until the first face reflection returns back down the optical path. This position is the zero position. The detector is also calibrated from this zero angle, by positioning the detector in the second face (inside back of the prism) reflection path. The angle range to be covered should start before and continue after the Total Internal Reflection (TIR) angle. The first set of measurements gives the angle at which TIR occurs.

5.3.5 Data Capture and Analysis

The whole set-up is interfaced to a computer. The photo diode voltage is detected by the lock-in amplifier as the rotation stages are moved (by the computer controlled stepper motors). The data set is obtained by the computer via an IEEE488 interface, permitting software calculation of reflectivity as a function of the angle of incidence.

The data set is plotted using the Easyplot graphic software. Curve fitting is performed using software based, least square fit to the reflection Fresnel equations. The curve fit parameters allow values to be obtained for the complex dielectric constant and thickness of both the metal layer and any phthalocyanines films coated on the metal.

To obtain images of the metal and deposited films, a video camera is placed in the normal position of the detector (on the 2θ arm). The beam splitter, chopper and photodetectors are not used. The beam is collimated by using a small divergent lens to expand the beam. At the location at which the beam is expanded to the size of the prism, a collimating lens is positioned. This is a lens with a focal length equal to the distance between it and the first (divergent) lens the experimental configuration is shown in figure. 5.4. The beam collimation is checked using a scaled background in the beam path at various positions between the lens and the prism. The whole prism is now illuminated with a collimated plane-polarised light source. The reflected signal is also collimated and therefore too large to be read by a typical video aperture, so it is reduced with a further lens to obtain the whole prism image within the video camera aperture.

Monitor and Data Capture

He-Ne Laser

1. Aperture
2. Neutral Density Filter
3. Polariser
4. Divergent Lens
5. Collimating Lens
6. θ-2θ table
7. Sample/Prism Assembly
8. CCD camera
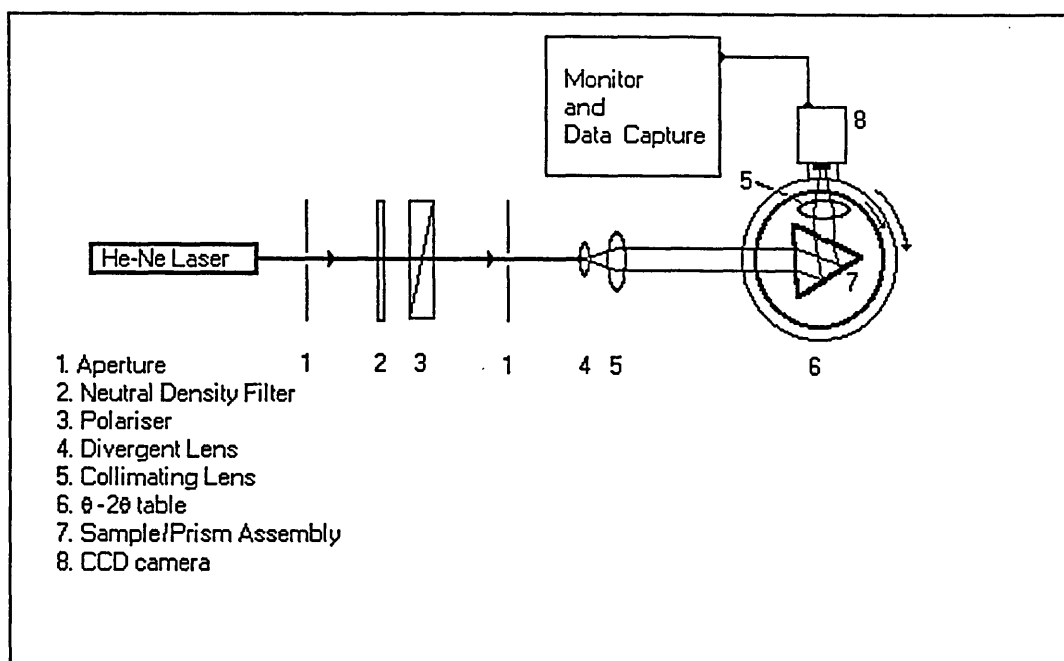
Figure 5.4   *A schematic representation of the components used to obtain SPR Images.*

112

As the prism is rotated, the angle of incidence varies over the range that the resonance angle is expected to occur. As the material (metal or organic film) resonance angle is obtained, the material is expected to appear dark. This is due to the dip in reflectivity described previously. The image is recorded with VIDI image capture software. This technique has been used to observe defects (striations) in Langmuir-Blodgett films (Merle et al 1992).

5.4 Experimental Results and Discussion

Results are presented for the A410 metal free phthalocyanine deposited by the Langmuir-Blodgett technique on gold coated glass substrates.

Figure 5.5 shows the surface plasmon resonance results. The curves clearly show the change in the resonance angle due to the deposition of the phthalocyanine film on the gold. The A410 on gold sample result could have been improved (the dip extended to zero reflectivity) by using a thinner layer of gold (Shirshow 1994). However, the accuracy of the results would not be significantly improved as the reflectivity obtained in this work is of sufficient size to permit accurate calculation using the software supplied by Leeds University.
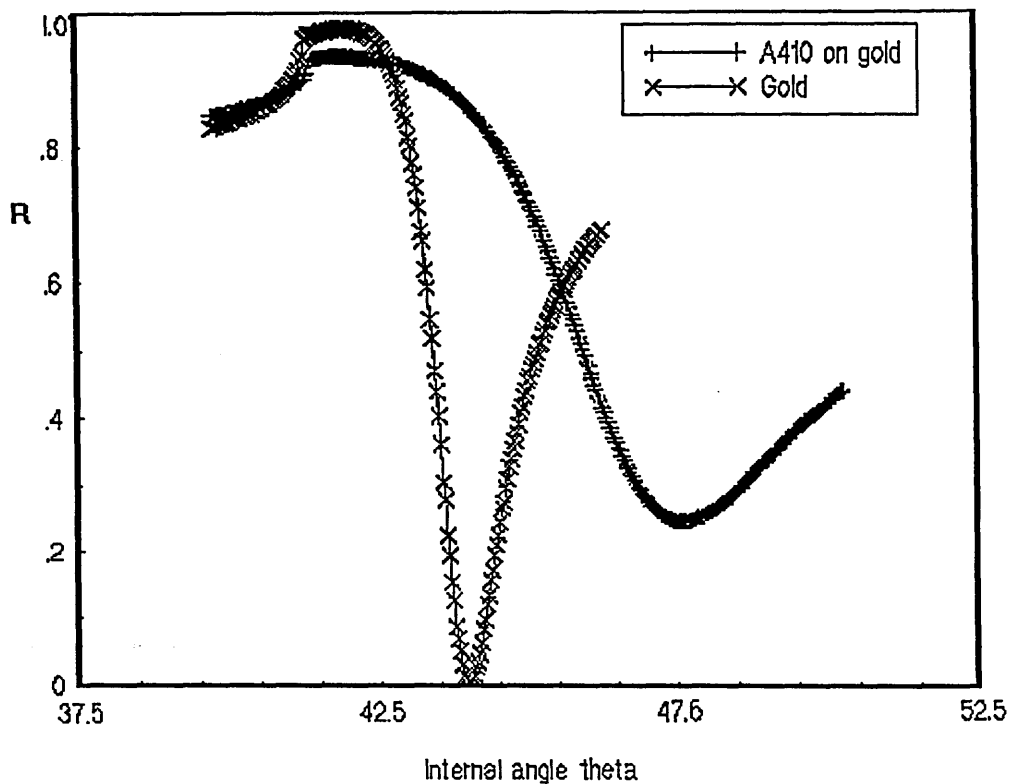
Figure 5.5   *The surface plasmon resonance curves from the gold coated*

reference slide and a phthalocyanine on gold coated slide.

Internal angle vs. Reflectivity. The shift in the angle at which

total internal reflection occurs is apparent as is the difference

in sharpness of the trough.

From figure 5.5, the change in internal angle at which total internal reflection occurs is apparent, and the change in the depth of the reflectance trough can be clearly seen. These changes are caused by the addition of the phthalocyanine film, on top of the gold. The phthalocyanine has a different refractive index, extinction coefficient and thickness to gold. This is why it produces the large change.

114

Film Material	Gold	Pc
Refractive index n	0.185	1.679
Extinction coefficient k	-3.4	-0.3423
Thickness, d	462 Å	172 Å

Table 5.1 Results from fitting the model to the experimental results.

The values in table 5.1 were obtained using computer software incorporating the equation for reflectivity at total internal reflection: (Chen and Chen 1981)

$$R = \left| \frac{\gamma_{31} + \gamma_{12} \exp(i2k_{z1}d)}{1 + \gamma_{31}\gamma_{12} \exp(i2k_{z1}d)} \right|^2 \qquad 5.2$$

with

$$\gamma_{31} = \frac{\varepsilon_3 k_{z1} - \varepsilon_1 k_{z3}}{\varepsilon_3 k_{z1} + \varepsilon_1 k_{z3}}$$

$$\gamma_{21} = \frac{\varepsilon_1 k_{z2} - \varepsilon_2 k_{z1}}{\varepsilon_1 k_{z2} + \varepsilon_2 k_{z1}}$$

and

$$k_{jz} = \left(\varepsilon_j \frac{\omega^2}{c^2} - k_x^2 \right)^{1/2} \qquad \text{for } j = 1,2,3, \qquad 5.3$$

$$k_x = n \frac{\omega}{c} \sin\theta \qquad 5.4$$

Where the subscripts 1,2,3, designate the quantities in the metal, air, and the prism respectively. ε_j and k_{jz} are the dielectric constants and the wave-vector components perpendicular to the interface of the medium j; d is the thickness of the metal film, and $\lambda = 2\pi c/\omega$ is the wavelength of light in a vacuum.

The software was supplied by Leeds University for this purpose and the validity of the software has been verified.

The Langmuir-Blodgett phthalocyanine film was seven monolayers thick, by using the angle of tilt for the A410 material, $\theta \approx 67°$ (from chapter 4), with the thickness obtained (172Å) and by basic trigonometry the molecular length can be obtained.

$$l_1 = (172/7) / (Sin\ 67°)$$
5.5

A molecular length of 26.7 Å is obtained. This is of the order expected for this molecule (25Å, from chapter 3, table 3.5).
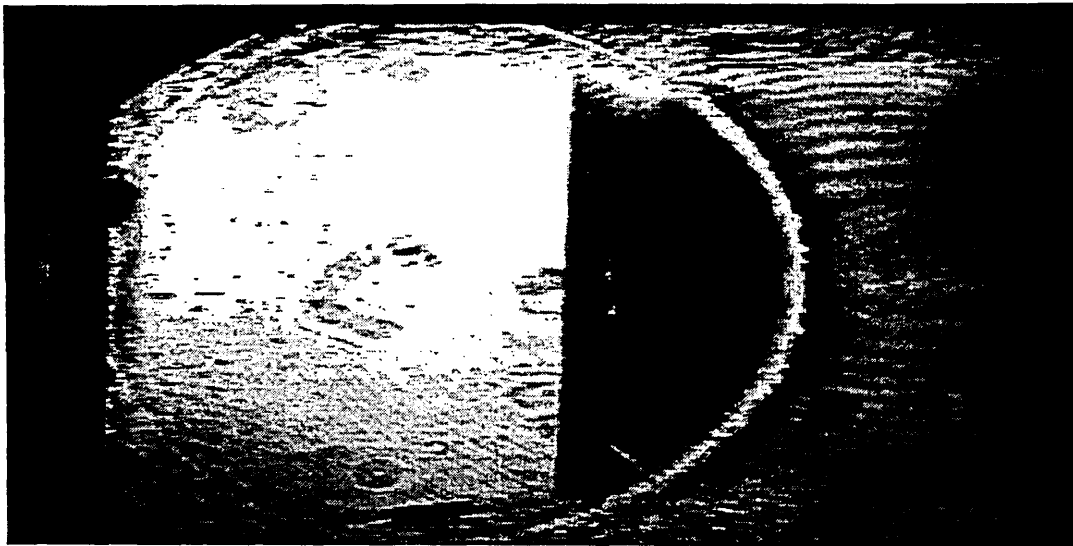
Figure 5.6   *This is a computer captured image from a CCD camera. The*

picture shows the prism with the phthalocyanine on the gold

coated slide. There are clearly two different regions. The

light portion to the left is the phthalocyanine film. The darker

region to the right is the gold film. The prism is positioned

with an internal angle of 44°.
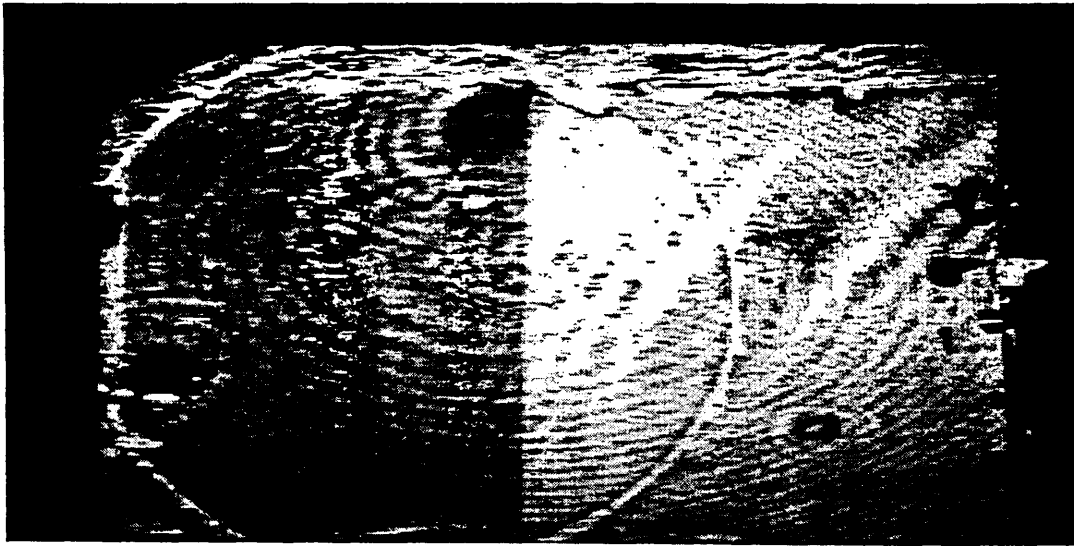
Figure 5.7. This image was produced using the same technique as Figure 5.6, The prism is positioned with an internal angle of 47.6°. This time the phthalocyanine is in resonance with a low reflectivity and so appears dark. The gold on the right side is brighter.

The accompanying images, figures 5.6 & 5.7, taken with a video camera clearly display the surface plasmon effect. The first is taken at the gold resonance angle and the gold part of the image is the darkest. This is due to the low reflectance of the gold at this angle. The phthalocyanine section is the central strip and this appears lighter as it is not under resonance and has a higher reflectivity at this angle. The second picture was taken at the phthalocyanine resonance angle and this picture displays the reverse effect with the phthalocyanine appearing dark and the gold appearing light. These pictures are directly related to the SPR curves showing the trough in the reflection value at the resonance angle, which corresponds to the dark appearance of the film at that angle. The resolution available is clearly apparent, however the quality of the pictures presented is not sufficient to use them as an investigative tool. Too much distortion resulted from lens effects and the imaging software and hardware used. Spatial filtering of the light source to remove the noise element of the lasing source, and high quality optics would improve the image. A four-bit image acquisition system was used giving sixteen grey shades. Ideally an eight bit (256 shades) system should be used together with higher quality optics. Using a grey scale 3D plot, (with grey shade representing the z axis) a visual representation of the topography of the sample film can be obtained.

5.5 Summary

The refractive index of the A410 metal free phthalocyanine was calculated to be 1.679, and a film of seven monolayers was found to have a thickness 172 $\overset{\bullet}{A}$ by the SPR technique. By using the angle of orientation for the A410 material, $\theta \approx$ 67° (from chapter 4), a molecular length of 26.7 $\overset{\bullet}{A}$ is obtained. This is of the order expected for such a molecule.

The images produced, although showing potential, are not of a suitable quality to use for investigating the quality of the Langmuir-Blodgett film deposition. Better quality optics, spatial filtering of the light source, and the use of eight-bit image acquisition software are expected to greatly improve the usefulness of SPR thin film imaging.

Chapter 6

ELECTRO-OPTICAL

CHARACTERISATION OF THIN FILMS.

6.1 Introduction to Electronic Applications of Thin Films

The use of organic materials in electronic devices has increased greatly over the last few decades. The availability of a thin film that has non-linear optical

properties, photo voltaic properties or even gas sensitivity, incorporated in an electronic device, would indicate the potential that these films could have in commercial applications. The Langmuir-Blodgett (LB) technique has been increasingly utilised over the last 20 years to produce thin organic films and prototype devices. The ability to produce a highly ordered film of a precise thickness, in the order of a few molecules thick, has many applications within the electronics industry. Their photo conductive properties have been utilised for solar cells (Yanagi et al. 1994) and their gas sensitivity has been used to make gas sensors (Cole et al 1993).

Photo voltaic devices, in particular solar cells, can be made with thin organic films as an insulating layer between a metal and a semiconductor as a metal - insulator-semiconductor (M.I.S.) device (Roberts et al. 1981). The photo-conductive properties of thin phthalocyanine films have been studied by a number of workers, (Twarowski et al. 1982, Yoneyama et al. 1986, Brynda et al. 1991 and Yanagi et al. 1994). Yoneyama et al. (1986), Brynda et al. (1991) and Yanagi et al. (1994) have studied phthalocyanine films in a sandwich structure. The method of testing a device was to measure the IV characteristics in dark conditions and then under illumination, and subsequently compare the difference. The open-circuit voltage (with no externally applied voltage) under illumination indicates the degree of photo-voltaic activity and thus the suitability of the device as a solar cell or photoreceptor. The range of values obtained is shown in table 6.1.

Reference	Cell structure	Film deposited by:	Open circuit voltage, Voc
Yoneyama et al 1986	Al / 15 asy-CuPc / Ag	Langmuir-Blodgett	~0.2 V
Brynda et al 1991	Al / CuTTBPc / Ni	Langmuir-Blodgett	0.4 V
Yanagi et al 1994	Au / AlPcCl / n-Si	Vacuum deposition	0.45 V

Table 6.1 A selection of open circuit voltages obtained.

Vincent & Roberts (1980) produced a review paper that covered the issues concerning Langmuir-Blodgett films with regard to their application in devices. In particular, they outline the photo conductive properties of these films as caused by incident photons creating electron-hole pairs. These e-h pairs are made to separate and stay apart for long enough to allow photochemical reactions to take place. Vincent & Roberts (1980) also bring together the results of many other workers and describe the electronic conduction mechanisms in more detail.

6.1.1 Solar Cells and Photovoltaic Devices.

Couts (1978), put forward a good case for solar power as an alternative energy source to fossil fuels. Couts also described the solar cell issues in detail covering device structure conversion efficiency, photo conduction mechanism and practical devices. The summary from the paper included a list of requirements, that solar cells should meet to permit their large scale application:

a) The whole array should have a greater efficiency than 10%

b) This efficiency should be maintained for 20 years

c) The cost of the power generated should be less than $1000 kW^{-1}

(Note: in 1978)

d) There should be a virtually unlimited supply of the materials utilised.

Point d) would be irrelevant if recovery of materials is possible from spent cells. The two main types of cell at the time: Silicon cells and CdS/Cu_2S cells were expected to meet these requirements. By the early eighties (Roberts et al. 1981), thin Langmuir-Blodgett films of anthracene were being tested in Schottky (Metal Insulator Semiconductor) structure solar cells. With a noted improvement of 20% to 40% over simple Schottky devices without the thin insulating film. This work has been confirmed by Yanagi et al. (1994) who compared the effect of adding an insulating layer between the metal and semiconductor in Schottky

124

structures. Although Yanagi et al. (1994) observed deteriorated performance in some of the M.I.S device structures, an improved photo conduction was observed in the devices that had heated substrates during film deposition. The chloroaluminium phthalocyanine film was deposited by evaporation. Xu et al. (1994) fabricated triple junction solar cells without any organic polymer, but have achieved a conversion efficiency of 11.5%. These amorphous silicon solar cells are currently the most promising for practical devices. One problem with the type of semiconductor used with these devices is their lack of sensitivity to the visible light spectrum. The introduction of a thin layer of a photo-active dye (i.e. phthalocyanine) on the semiconductor electrode surface to act as a sensitiser to the visible light spectrum, could improve the photo response. Phthalocyanine compounds have been considered for this purpose as they have the required chemical properties (stability, high visible light absorption coefficient, semiconducting properties and the wide variety of synthetic variations). PC's can also be selected so that the excited state of the phthalocyanine is above the conduction band edge and their ground state is within the band gap. This is important as it separates the charge carriers at the semiconductor /dye interface. Care must be taken to ensure that the dye is not too thick, which could reduce the light intensity (Yanagi et al. 1994).

6.1.2 Field Effect Transistor (FET) Devices

Thin organic films have been successfully utilised to make FET devices (Pearson et al. 1994). FET characteristics were observed from the device and the characteristics were used to calculate the mobilities of the charge carriers. The mobility was found to increase after doping with iodine. No reasons for this were suggested in the paper, but it is likely that the donor material introduces charge carriers of a higher mobility than the recipient charge carriers.

6.1.3 Gas Sensors

Phthalocyanines have been successfully utilised to make NO_2 Gas detectors (Cole et al. 1993), (O'Rourke et al. 1993). The film is deposited by the Langmuir-Blodgett technique onto a quartz substrate that has thin interdigitated platinum electrodes already in place. The electrode pattern is shown in figure 6.1.
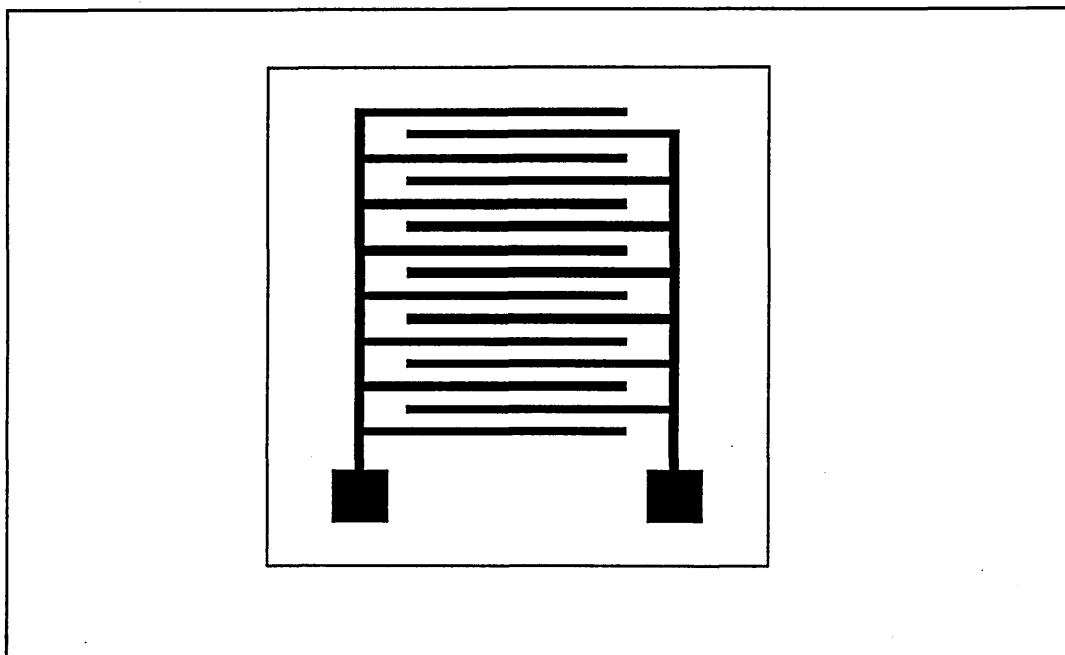
Figure 6.1　　　*The Yoshi platinum electrode pattern (not to scale) each*

sample is approximately 5mm square.

The metal substituted phthalocyanine is sensitive to NO_2 and displayed a change

in conductivity due to the presence of the gas. The phthalocyanines are sensitive,

selective and stable, and are considered suitable for gas sensing devices.

A disadvantage of raised electrodes, is the possibility of film detachment.

Langmuir-Blodgett films of C16H33-BEDT-TTF molecules suffered from

detachment of the film from microelectrodes, resulting in a tunnelling

conductivity. The film having been deposited on raised electrodes (Carrara et al

1995). Although not a phthalocyanine film, this phenomena is possible with

many organic films and demonstrates the importance of the design of devices.

6.2 Theoretical Issues.

Within organic semiconductors such as phthalocyanines, steady state transport properties are largely controlled by the amount and energy distribution of trapping sites for charge carriers. The current is believed to be predominantly carried by holes.

To integrate an organic material into a device or measurement system, electrical contacts need to be made onto the material. There are three types of contact, i) neutral, ii) ohmic, and iii) blocking. The difference between these types of contact is in the work function ratios between the metal contact and the organic semiconductor. The work function (ϕ) is the energy difference between the Fermi level and the lowest energy level of an electron in a vacuum. A neutral contact is obtained when the work functions are equal. An ohmic contact is found when the metal work function is larger than the organic semiconductor, resulting in zero impedance. A blocking contact occurs when the metal has the lower work function. The resulting junction is a Schottky or rectifying junction, with a carrier depletion layer.

There are two types of dc conduction, ohmic and space-charge limited conduction. Ohmic conduction is characterised by Ohms' law with current proportional to applied voltage. Space-charge limited conduction is due to carrier injection at an ohmic contact. The ohmic junction creates an excess of carriers or

"space charge" at the contact. The current is independent of the space charge but the space charge eventually limits the current.

$$J \propto V^n \qquad \text{where } n \leq 2 \qquad\qquad 6.1$$

J is the current density and V is the applied voltage.

The well-known expression for the conductivity of an intrinsic semiconductor is:

$$\sigma_i = \sigma_{o_i} \exp\left(\frac{-\Delta E_g}{2kT}\right) \qquad\qquad 6.2$$

For extrinsic semiconductors, the excitation of carriers from the impurity levels must be allowed for, so:

$$\sigma_E = \sigma_{o_E} \exp\left(\frac{-\Delta E_i}{kT}\right) \qquad\qquad 6.3$$

In general, the conductivity of a semiconductor is made up of two terms, however due to the temperature dependence of the terms E_g and E_i predominate in different temperature regions.

At high temperatures the intrinsic term (6.2) dominates (2kT).

At low temperatures the extrinsic term (6.3) dominates (kT), (Rudden and Wilson 1980).

The activation energy (ΔE) can be obtained from the slope of $\ln(\sigma)$ versus $1/T$.

6.3 Experimental Procedures.

When electrical measurements are performed on thin films, the measurements can be performed with a number of electrode configurations. The configurations that are practical are: a) with the film deposited on thin electrodes, b) electrodes deposited by evaporation on the top of the film, (both a and b configurations to give an in-the-plane-of-the-film measurement). Or: c) the film sandwiched between two electrodes to give a through-the-film measurement.

N.B. For case c, the base electrode deposited on the substrate before deposition of the film, the top electrode deposited on the film afterwards.

All instruments are linked up to a computer with an IEEE bus system. The system can then be used automatically to obtain the large amounts of data required for electrical measurements. The sample is mounted on a cryostat probe which is in turn placed in a liquid nitrogen cryostat as shown in figure 6.2.

1. Insulating Jacket
2. Liquid Nitrogen Tank
3. Temperature control space
4. Sample space
5. Nitrogen fill / vent
6. Insulating Jacket valve
7. Sample space valve
8. Nitrogen gas flow valve
9. Sample and feed wires
10. Sample window
11. Electrical feed through
12. Heater and Thermocouple
13. Heat exchange blocks
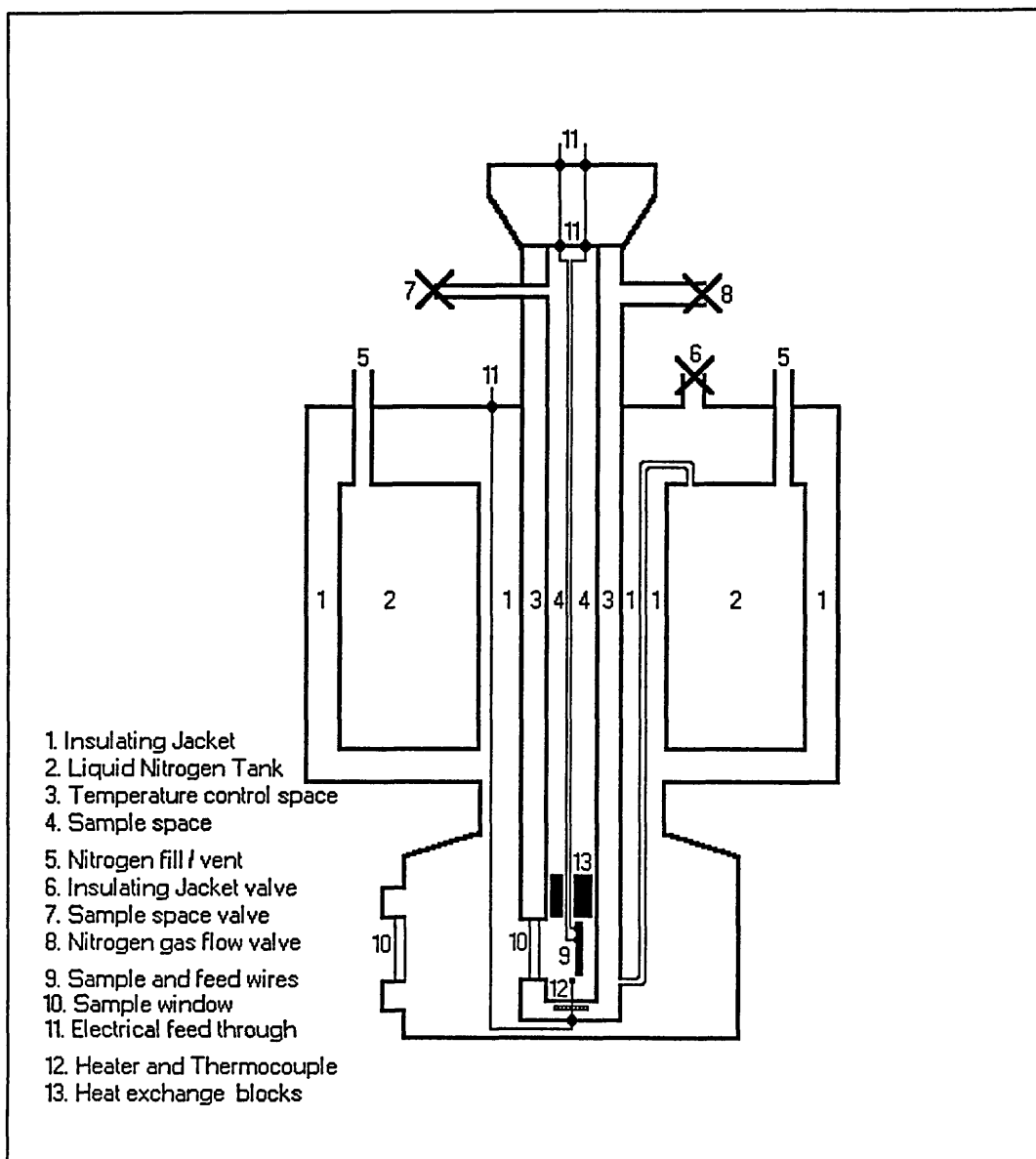
Figure 6.2   *The liquid nitrogen cryostat in sectional view displaying the internal chambers.*

This cryostat allows control of the sample environment, parameters such as temperature (78-300 K), vacuum (or choice of gas), and illumination (with a monochromator), can be controlled. The effect of these parameters on the electrical properties of the film can thus be investigated. Vincent (1980 p143) concluded that electrical measurements were preferably performed under a dry
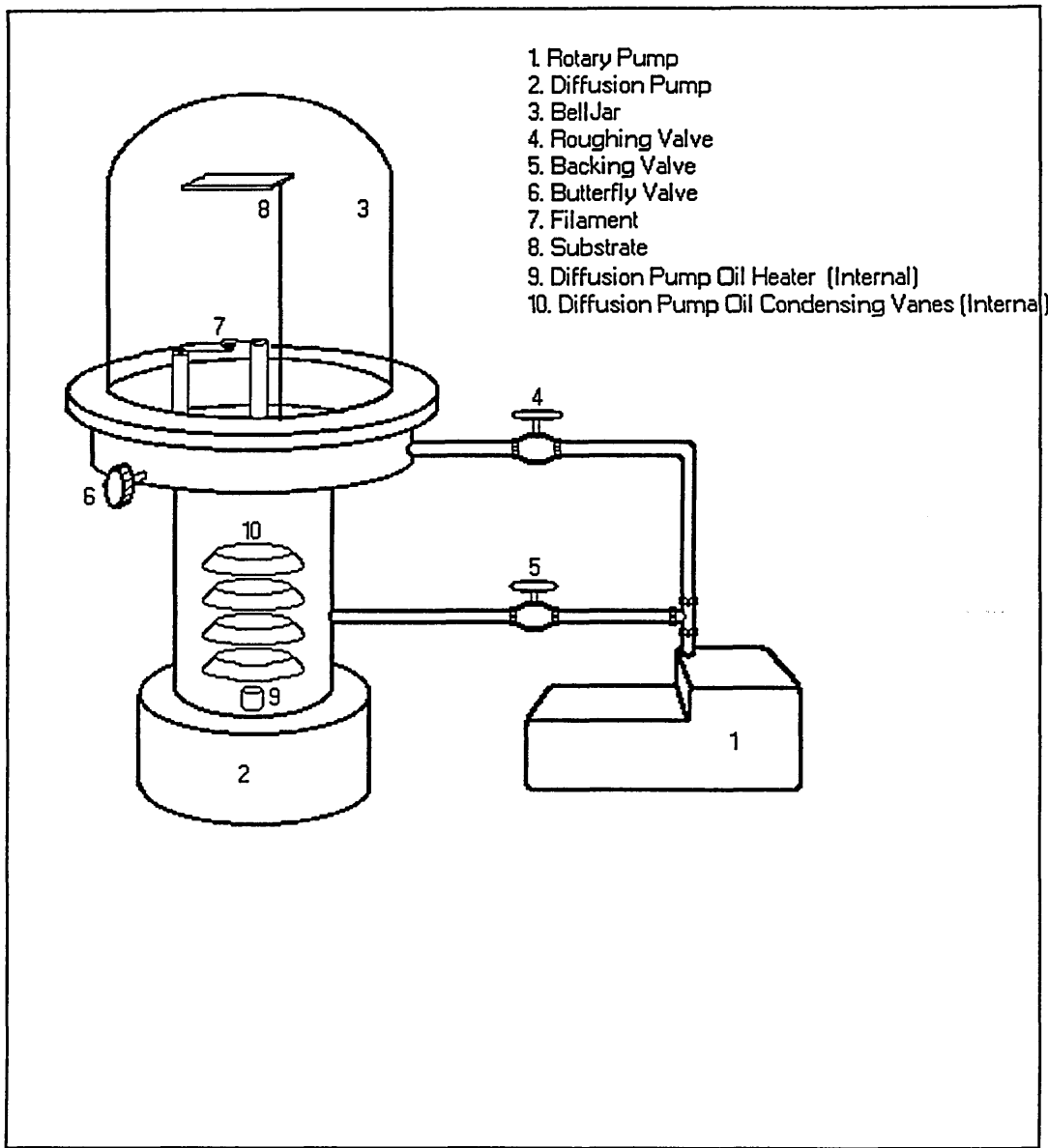
nitrogen environment. This prevents the humidity affecting the sample that would occur if air is used as an ambient and reduces the probability of molecular evaporation that is possible if the tests are carried out under vacuum. A dry nitrogen environment also allows faster temperature response of the sample than would be possible with a vacuum. This is due to the fact that the nitrogen convects heat, whereas a vacuum would not. However, the cryostat is suitable for use with samples in a vacuum, as the design is optimised for radiative heat transfer. The gaps between the temperature controlled face, the sample probe, and the sample are small.

6.3.1 Deposition of Electrodes by Evaporation.

6.3.1.1 Evaporation Principles and Techniques.

This process relies on the principle that if a solid is melted and then evaporated, it condenses on the surrounding surfaces. If this is carried out in a high vacuum (10^{-5} -10^{-6} Torr) then the condensing metal will be largely free from contaminants and the coating thickness should be uniform. The vacuum system that is commonly used is a combination of a rotary mechanical pump and an oil diffusion pump, as shown in figure 6.3. The rotary pump is used to initially create a vacuum of approximately 10^{-1} Torr, "roughing" the sample chamber and "backing" the diffusion pump. When this vacuum is attained, the diffusion pump

can be switched on to draw the vacuum down to 10^{-6} Torr. The oil diffusion pump operates with a heating element in the base, boiling the oil. The oil then condenses on metal plates that are water cooled. The diffusion process pulls the vacuum down to around 10^{-6} Torr. The diffusion is a slow process. The pump cannot operate at atmospheric pressure, because the oil becomes overloaded with air. This is why the diffusion pump is only used between 10^{-1} and 10^{-6} Torr. The rotary (mechanical) pump is responsible for the initial pumping. Because of the heat of the vaporised metal, care must be taken to avoid damage to the film. Substrate cooling may be used. A crystal film thickness monitor is used to ensure the rate of evaporation is controlled. This instrument measures the change in oscillating frequency of a crystal (due to the change in mass) placed next to the sample. The amount of metal deposited on the crystal is proportional to the change in oscillating frequency. The instrument can be calibrated to read accurate values for the rate of deposition and the thickness.

1. Rotary Pump
2. Diffusion Pump
3. Bell Jar
4. Roughing Valve
5. Backing Valve
6. Butterfly Valve
7. Filament
8. Substrate
9. Diffusion Pump Oil Heater (Internal)
10. Diffusion Pump Oil Condensing Vanes (Internal)

Figure 6.3   *The vacuum pump configuration of rotary and diffusion*

pumps for vacuum evaporation.

6.3.1.2 Evaporation Technique for Depositing Electrodes.

This process is used to deposit metal electrodes on the film surface. It involves boiling and then evaporating a small amount of the metal from a heating element. The substrate and heating element are enclosed in a bell-jar (as per figure 6.4) which is located on top of a vacuum system. The process is performed under high vacuum (10^{-6} Torr is typical). The element is heated and the metal evaporates from the element and condenses on all surrounding surfaces. The vacuum system that is used is a combination of a rotary mechanical pump and an oil diffusion pump.

The system has a valve combination that allows new samples to be loaded in the bell jar whilst the diffusion pump is kept at operating conditions. Electrode patterns are achieved by using a mask placed directly in front of the substrate. The mask is a thin metal plate with holes cut in the locations where electrodes are required on the substrate. The mask is made thin enough to avoid shadowing the substrate electrode locations. The experimental configuration is shown in figure 6.4.
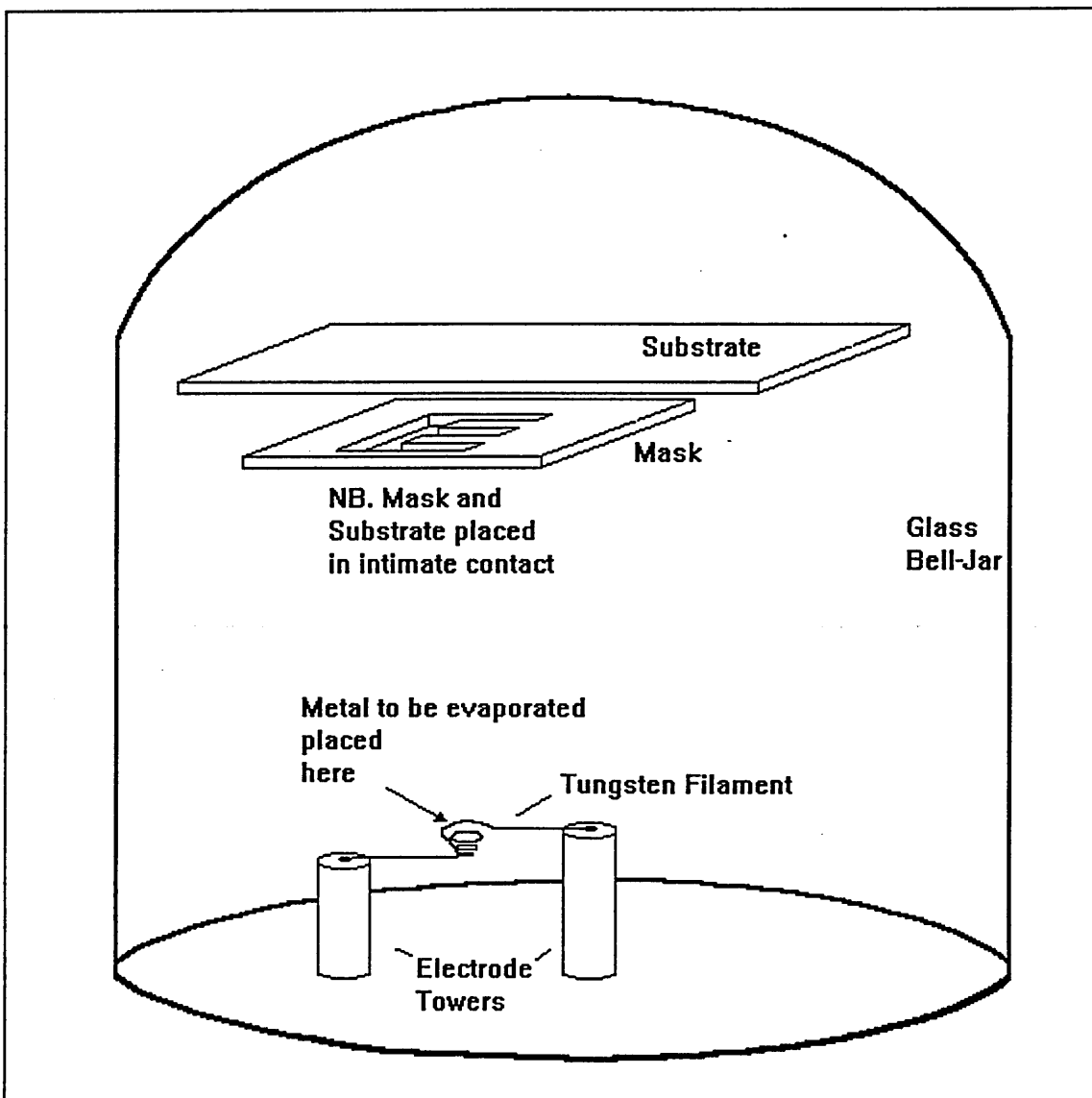
Figure 6.4   *The Evaporation components enclosed within a bell-jar.*

As the film is very thin, there is a high probability that the molten metal can damage or even burn through the film. To avoid film damage the metal is evaporated very slowly. "Flashing" of the heating element power allows time for the heat to dissipate between flashes. Substrate cooling can be implemented to reduce the possibility of film damage. Cooling is possible in a vacuum with the

136

use of a Peltier array heat pump. The array is operated using a power supply and requires a heat sink.

6.3.2 Current -Voltage (IV) Measurements.

IV measurements involve applying a voltage across the film, via electrodes, and measuring the current in the circuit. A range of voltages from 0.1 V up to 100 V depending on the conductivity of the sample, can be used. The choice of applied voltage depends on the current handling capacity of the sample or device, and ultimately is limited by the electrometer that has a current limit of 2mA and a maximum voltage output of 100V. A Keithley 617 electrometer is used to perform these measurements. The electrometer has the facility of supplying a stable voltage to a circuit whilst measuring the current.

6.3.3 Photocurrent Measurements.

Photo-current effects are measured using a monochromator to shine light of a desired wavelength onto the sample. The sample is mounted inside the Oxford Instruments cryostat to control the environment (choice of ambient gas, level of illumination, temperature). The experimental configuration is as shown in figure 6.5.
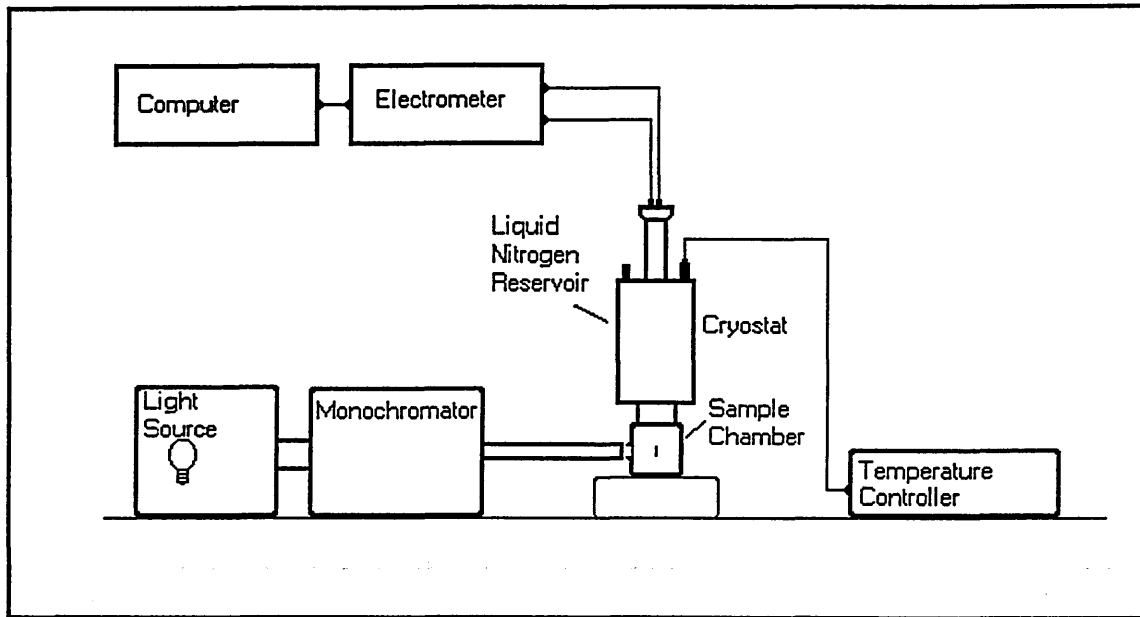
Figure 6.5 *The photo-current experimental schematic representation.*

An IV test is performed in the dark and then under illumination, the difference between the two values is the photo-current.

$$I_{ph} = I_{ill} - I_d \qquad\qquad 6.4$$

Where: I_{ph} = photocurrent, I_{ill} = current under illumination and I_d = dark current.

The Keithley 617 electrometer is used for these measurements. Photo-current measurements can be time dependent, the facility to monitor the time as the sample undergoes different environmental parameters, is used to obtain the experimental time dependence.

6.4 Electrical Characterisation Results and Discussion.

The Electrical measurements have been carried out to measure the effect of film thickness, light wavelength, film temperature and applied voltage on the photo conduction. This information is fundamental to being able to model the conduction process under a variety of conditions and for assessing the performance of the materials in a range of applications. The samples were deposited on Yoshi electrodes by the Langmuir-Blodgett method. These samples were used for all the electrical tests reported in this thesis.

The Yoshi electrodes were supplied by Sheffield Health and Safety Executive, they were prepared using lithography. With reference to figure 6.1, these are the electrode array details:

Number of electrodes, N = 15. (Number of gaps = N-1)

Electrode interspacing (gap width), D = 60μm.

Length of electrode overlap, P = 3.125mm.

Thickness of the Langmuir-Blodgett film, T ≈ 2 nm/layer.

The Yoshi electrode configuration measures the planar electrical response. Measurement of the electrical response using a sandwich electrode configuration was not performed as attempts to deposit electrodes on the thin organic film using

the evaporation technique resulted in a short circuit when electrically tested. The heat of the evaporated electrode material was believed to damage the film. Another possibility is electrical shorting through pin-holes in the Langmuir-Blodgett film.

6.4.1 Current-Voltage

To confirm the conduction process as ohmic, the relation between current and applied voltage was investigated. Figure 6.6 confirms the conduction mechanism obeys Ohms' law for voltages in the range 0-9 volts for the A410 material.

Figure 6.7 confirms the A406 material as ohmic below 60 volts but above 60 volts, the mechanism is sub-ohmic indicating a limited current above 0.3nA.
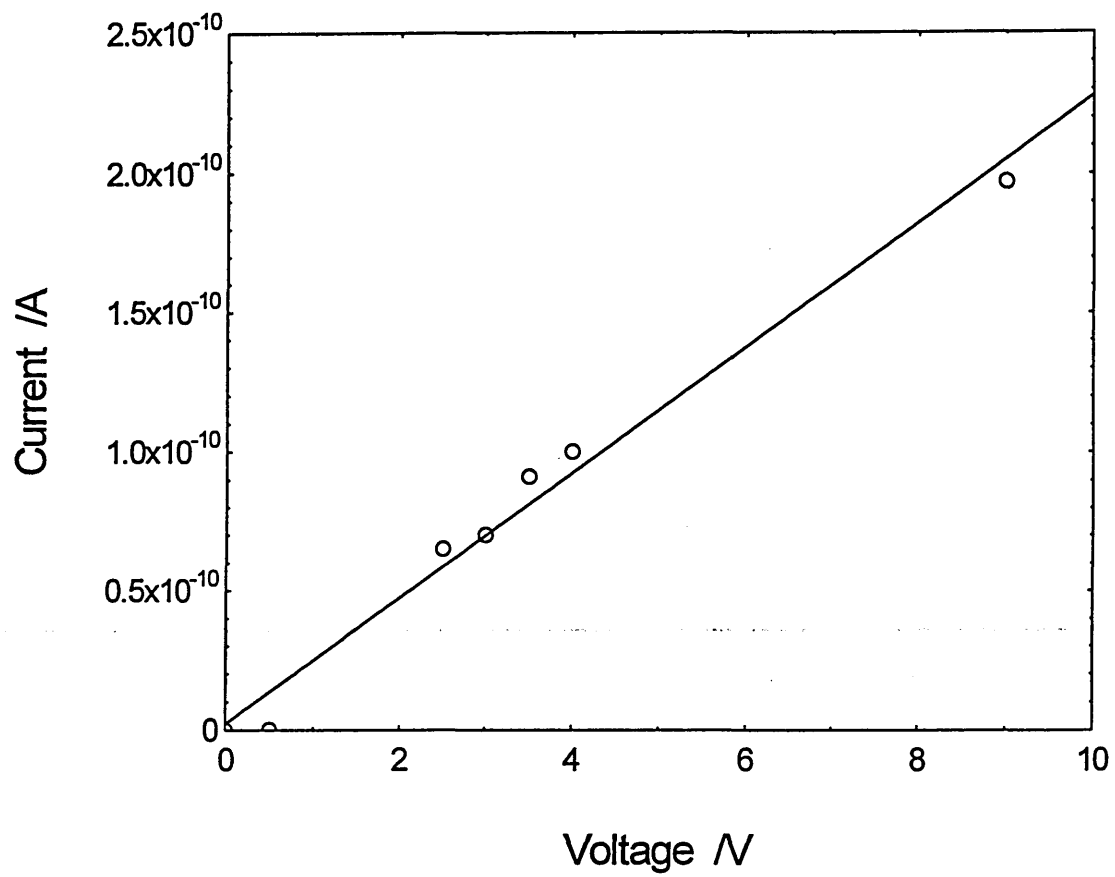
Figure 6.6   *Current Voltage plot for material A410 (30 monolayers thick)*

with linear, ohmic relation.
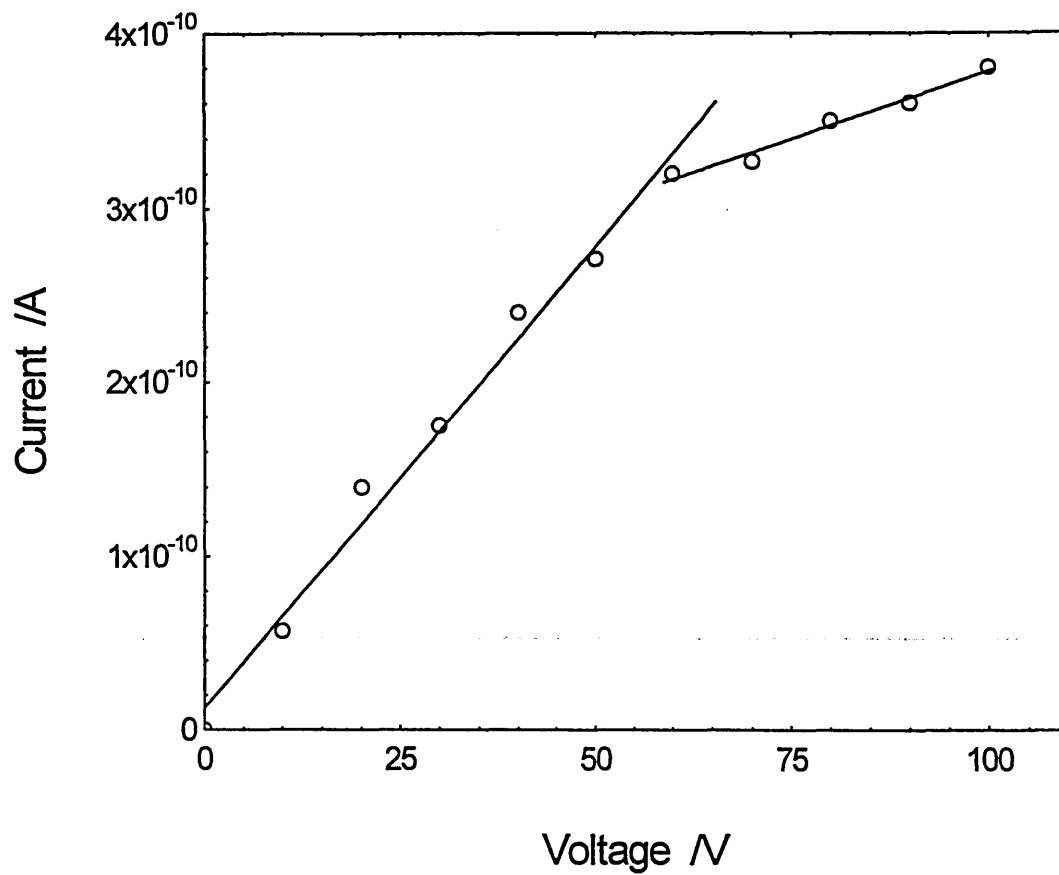
Figure 6.7   *Current Voltage plot for material A406 with linear, ohmic*

relation up to 60 volts and a sublinear region above 60 volts.

6.4.2 Photocurrent Characterisation.

To ensure that the light from the monochromating light source was of constant intensity over the output wavelength range, a calibration was performed. Figure 6.8 indicates that the output was reasonable steady over the range 500-800nm.
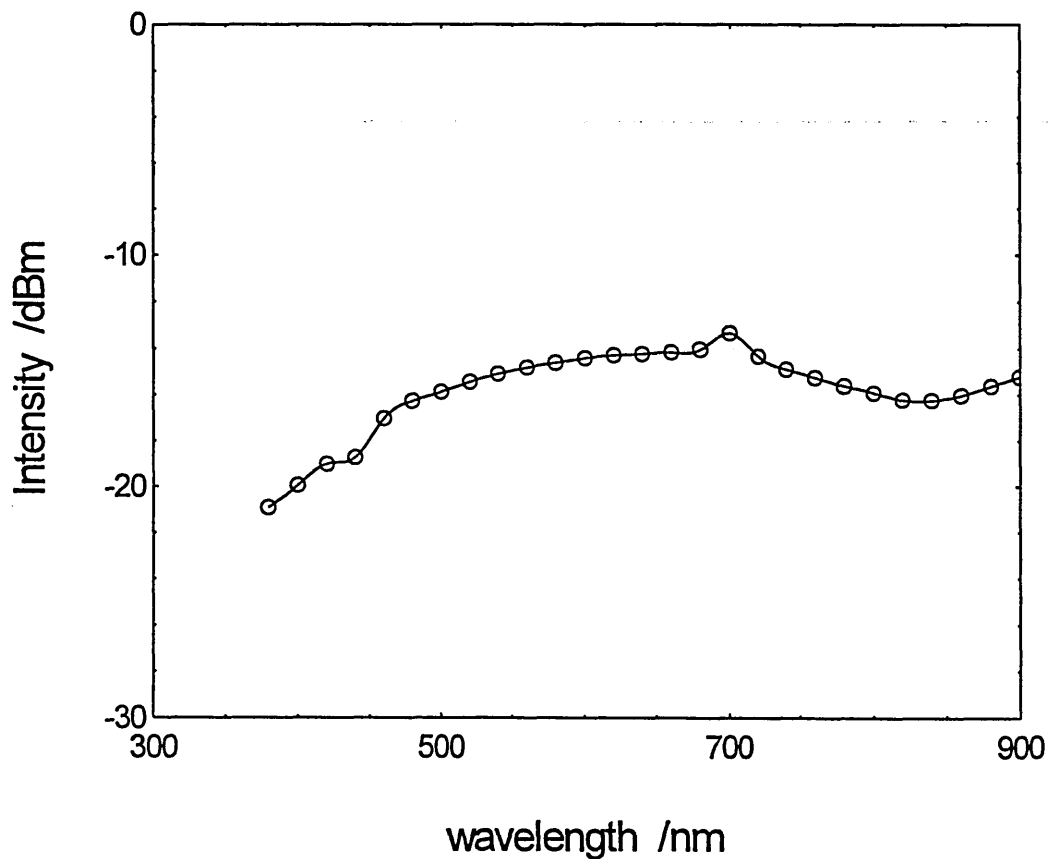
Figure 6.8   The monochromator output intensity spectrum.

After application of 100V potential difference across the electrodes, measurements were taken. The Initial observation was of the very low conduction of the films in a darkened environment (dark current, Id). Under illumination, the

photo current became apparent. The photo current was dependent on wavelength

in a similar form to the optical absorbance.
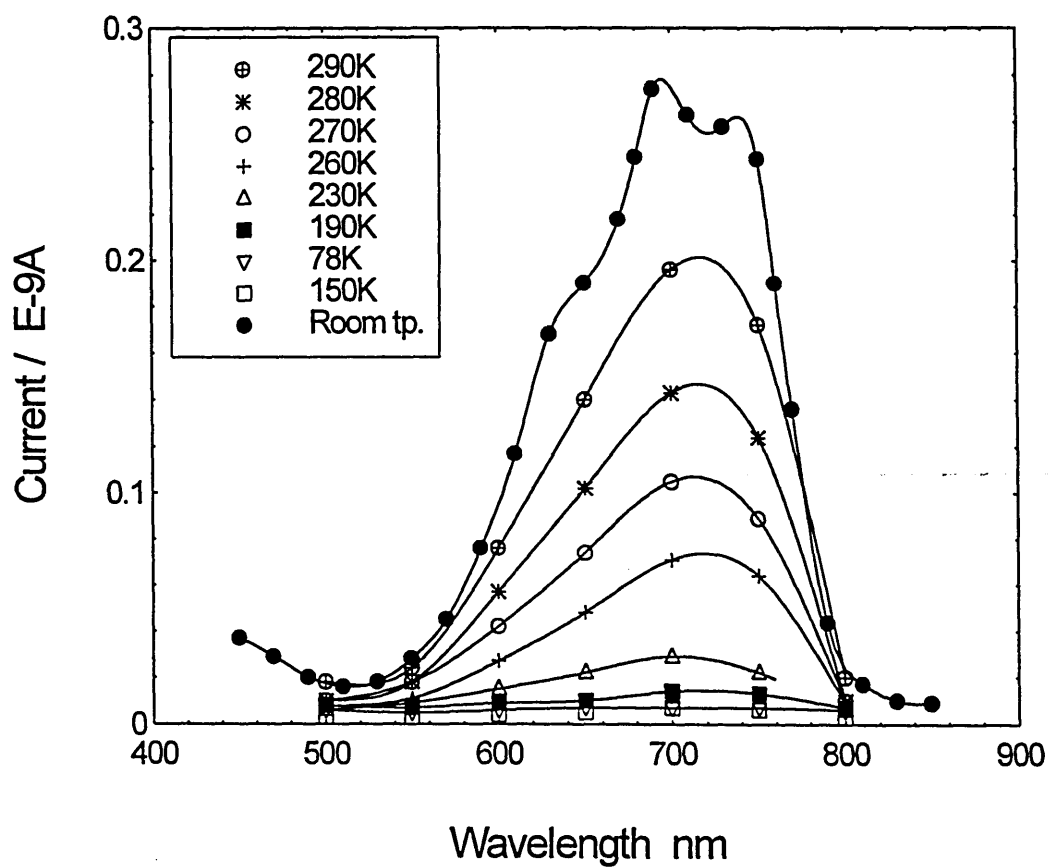
Figure 6.9   Photo-current as a function of wavelength over a range of

temperatures for A410, twenty monolayers thick with an

applied voltage of 100V.

144

Peak photo current at around 700nm was observed for the samples tested (A410, A406). The relation between photo current and light wavelength show a marked similarity to the optical absorption spectra. This is not surprising as the process of optical absorption is of photons releasing charge carriers (electron hole pairs). This will occur during illumination of the sample. An increase in the photo current is expected with the increase in charge carriers under illumination. The relation of photo current to wavelength mirrors the absorption spectra.

The lack of detail (i.e. fewer intermediate wavelengths, but still a good overall effect) on the photo current graph was due to the instability of the readings. It was considered more valuable to have a smaller number of accurate, repeatable readings than a large number of readings, possibly showing misleading and unnecessary detail. However when a smaller gap between wavelengths is used, the peaks (as on the absorption spectra) are just visible in the Room temperature measurement on figure 6.9 The shape of the graph is reproducible and the values are obtained after a stabilisation period of not less than one hour.
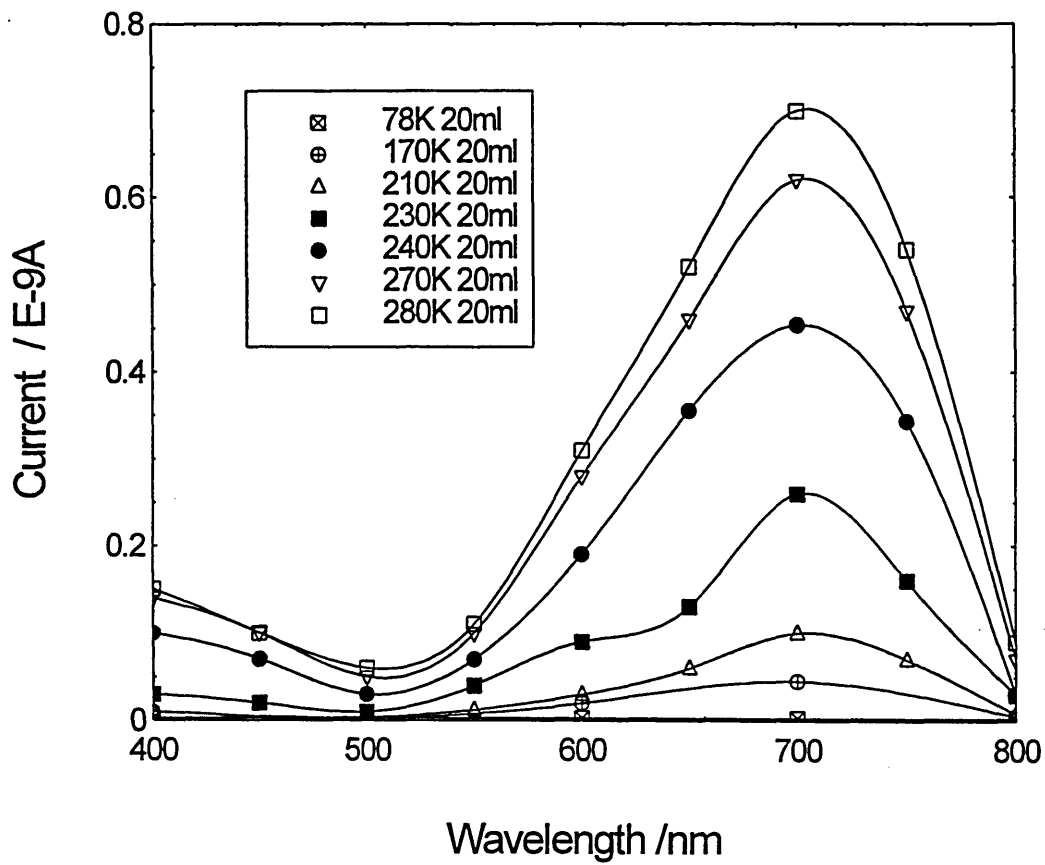
Figure 6.10   *Photo-current as a function of wavelength over a range of*

temperatures for A406, twenty monolayers thick with an
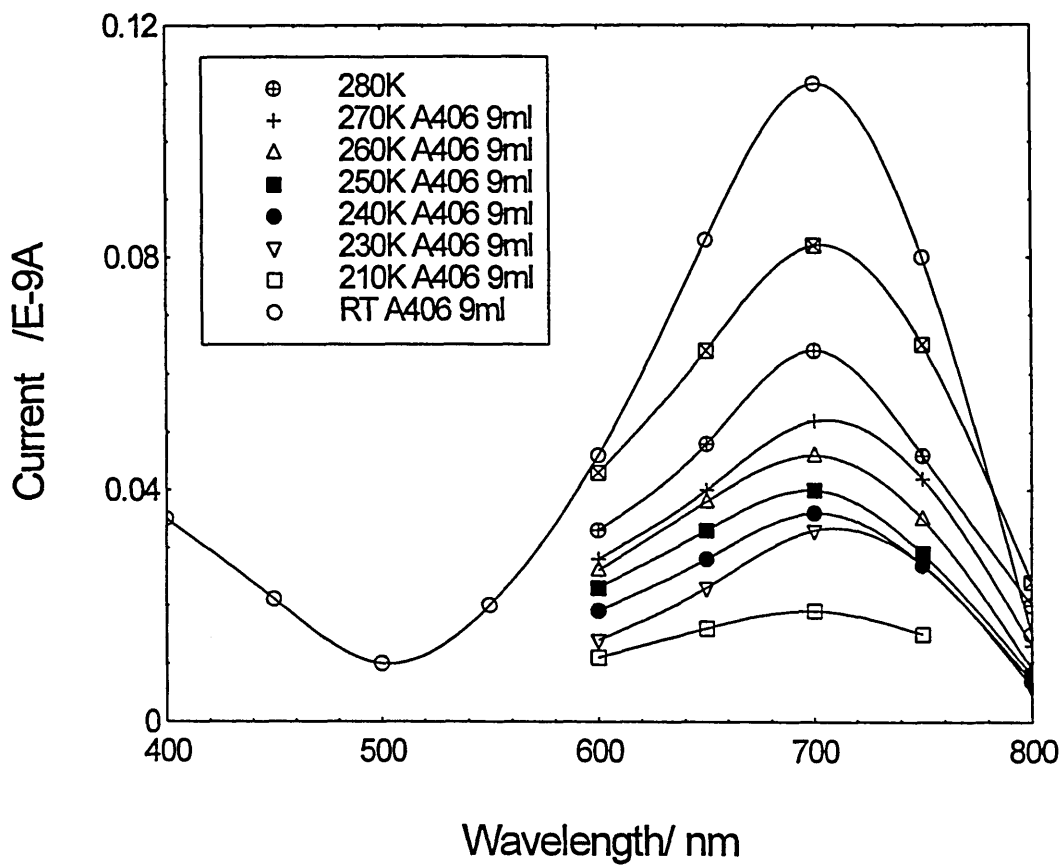
applied voltage of 100V.

Figure 6.11 *Photo-current as a function of wavelength over a range of*

temperatures for A406, nine monolayers thick, with an

applied voltage of 100V. *(Note: RT indicates Room*

Temperature)

147

The intrinsic conductivity σ, of these phthalocyanines was estimated from the following equation (6.5). This calculation is based on the operation used by Kutzler et al (1987).

$$\sigma = \frac{SD}{TP(N-1)} \qquad\qquad 6.5$$

Where:

$S = I / V$ (Ω^{-1})

D = gap between the electrodes (cm)

T = thickness of the film (cm)

P = electrode overlap (cm)

N = number of electrodes

Values obtained for the photo-conductivity at room temperature are:

$0.434nScm^{-1}$ for A410 (20 monolayers thick),

$1.6nScm^{-1}$ for A406 (20 monolayers thick) and

$0.366nScm^{-1}$ for A406 (9 monolayers thick).

The variation in the values obtained for the A406 material suggest the photo conduction is a bulk process The thicker film, with correspondingly higher absorbance would result in a higher carrier photogeneration, this could account for the higher photoconductivity when measured in planar configuration. The same effect could not be assumed for the sandwich configuration of electrodes, as an increase in the thickness of the film would also increase the distance between the electrodes and so reduce the electric field strength, counteracting the apparent benefits of thicker films. The sheer scale differences between planar and sandwich electrode configurations incorporating film thicknesses around twenty nanometers, means that the electric field is much greater in sandwich devices. However, on the negative side, a sandwich device is limited because the light has to pass through the electrodes to reach the film. Any further comparative analysis would require measurement of the film in sandwich configuration.

From this result, the Langmuir-Blodgett films of A406 with their higher photoconductance (at equal thickness to A410) would be the better choice of the two materials, for optoelectronic devices where a high quantum yield is required.

Using relation (6.2):

$$\sigma_i = \sigma_{o_i} \exp\left(\frac{-\Delta E_g}{2kT}\right)$$

and plotting $\ln\sigma$ versus $1/T$ enables the activation energy ΔE to be obtained from the slope.
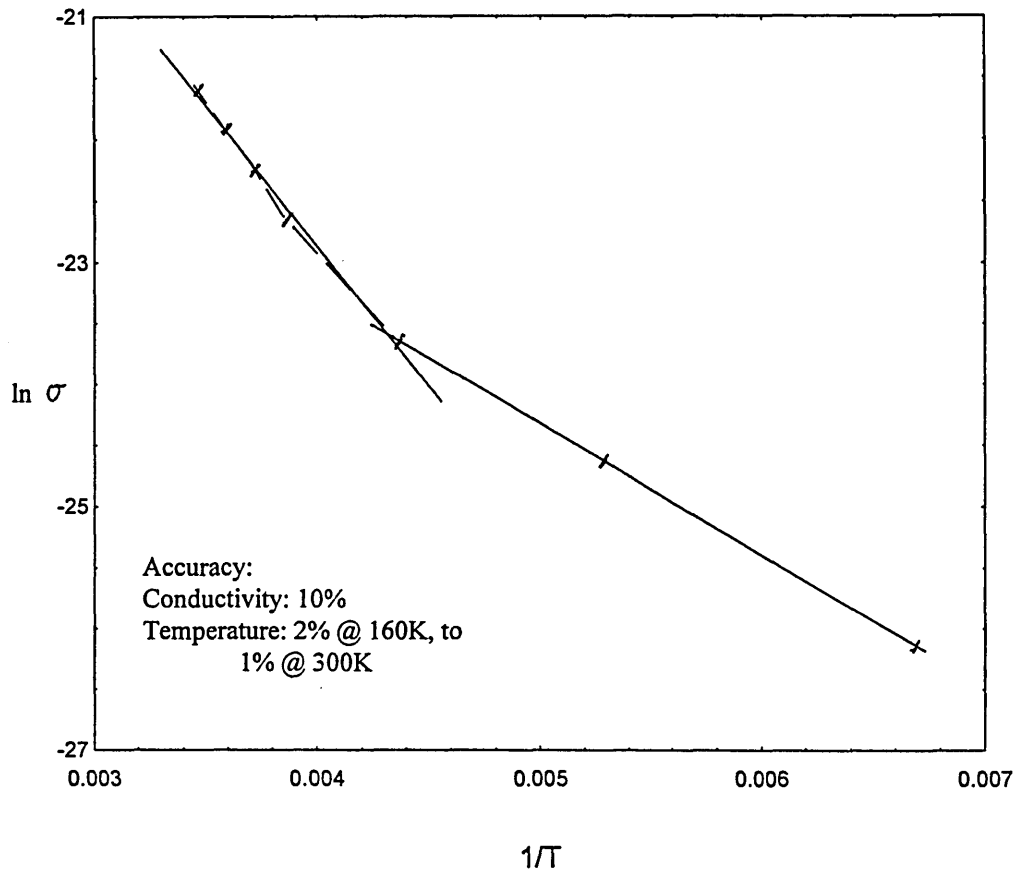
Figure 6.12 ln σ as a function of 1/T for A410, twenty monolayers thick. There are two regions, corresponding to two activation energies the transition temperature is around 250K.

Figure 6.12 corresponds to the expected response (Rudden and Wilson 1980), with two slopes, the steeper portion at higher temperatures corresponding to term (2), the shallower at lower temperatures (3) (from section 6.2). See Appendix B for accuracy notes.
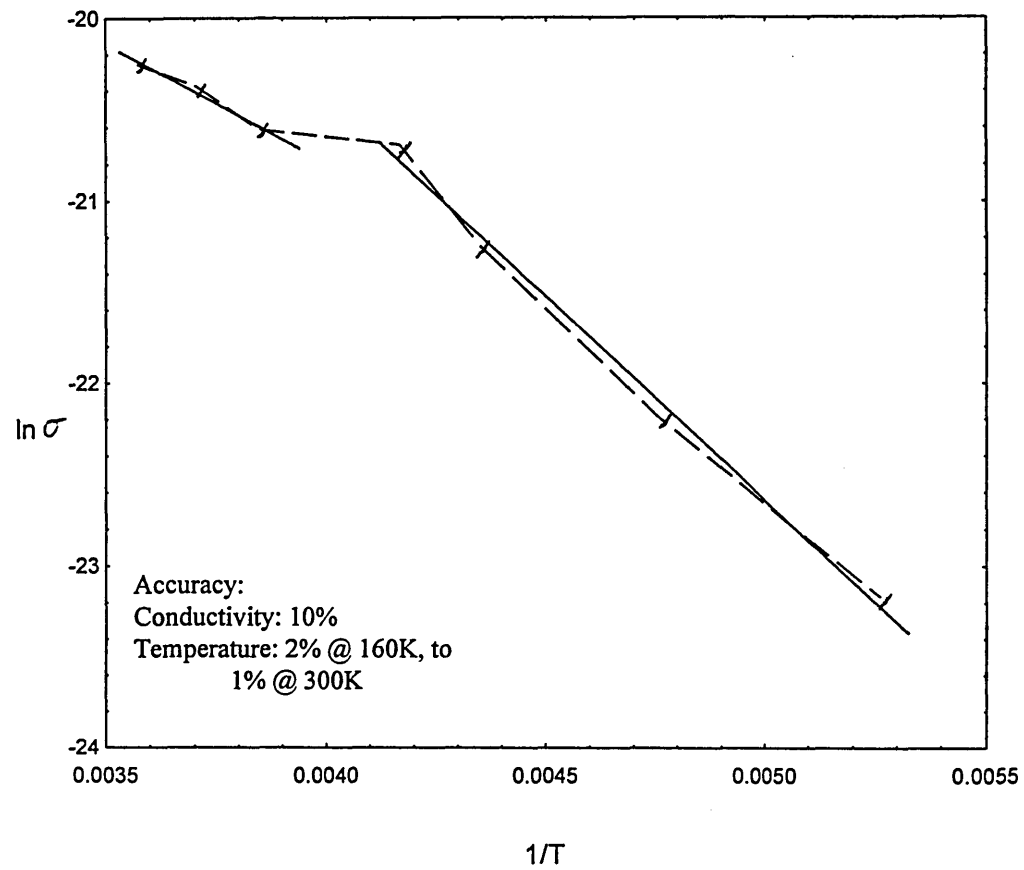
Figure 6.13 *ln σ as a function of 1/T for A406 twenty monolayers thick. There are two regions, corresponding to two activation energies the transition temperature is around 250K.*
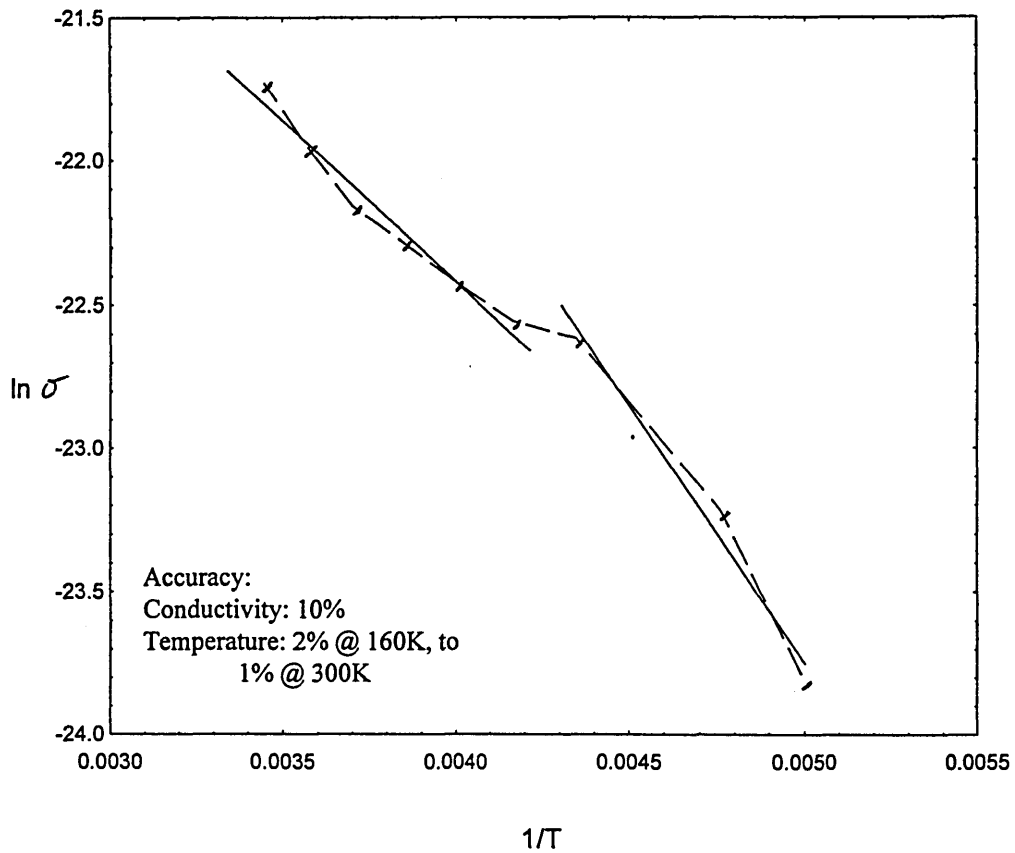
Figure 6.14 ln σ as a function of 1/T for A406 nine monolayers thick. There

are two regions, corresponding to two activation energies the

transition temperature is around 250K.

The three figures, 6.12, 6.13 and 6.14 all show two activation energy regions, the transition temperature was in the region of 250K in all cases. The activation energies calculated using function (2) are presented in table 6.2.

	Activation energy (eV) At temperature > 250K	Activation energy (eV) At temperature < 250K
A410, 20 monolayers	0.197	0.092
A406, 20 monolayers	0.112	0.191
A406, 9 monolayers	0.096	0.150

Table 6.1 Activation energies for photo-current at 700nm. Calculated using the

gradients obtained from figures 6.12, 6.13 and 6.14.

The activation energies were not calculated for dark conduction as the current was too low to resolve any difference over the temperature range.

The two regions for the A410 material follow the expected pattern with the low temperature region having a shallower gradient. The A406 material has a steeper region at low temperatures this was an unusual result but could be explained as the photocurrent at low temperatures is significantly lower than that at room temperature, the thermally activated conduction process would suggest that the activation energy should be higher at lower temperatures.
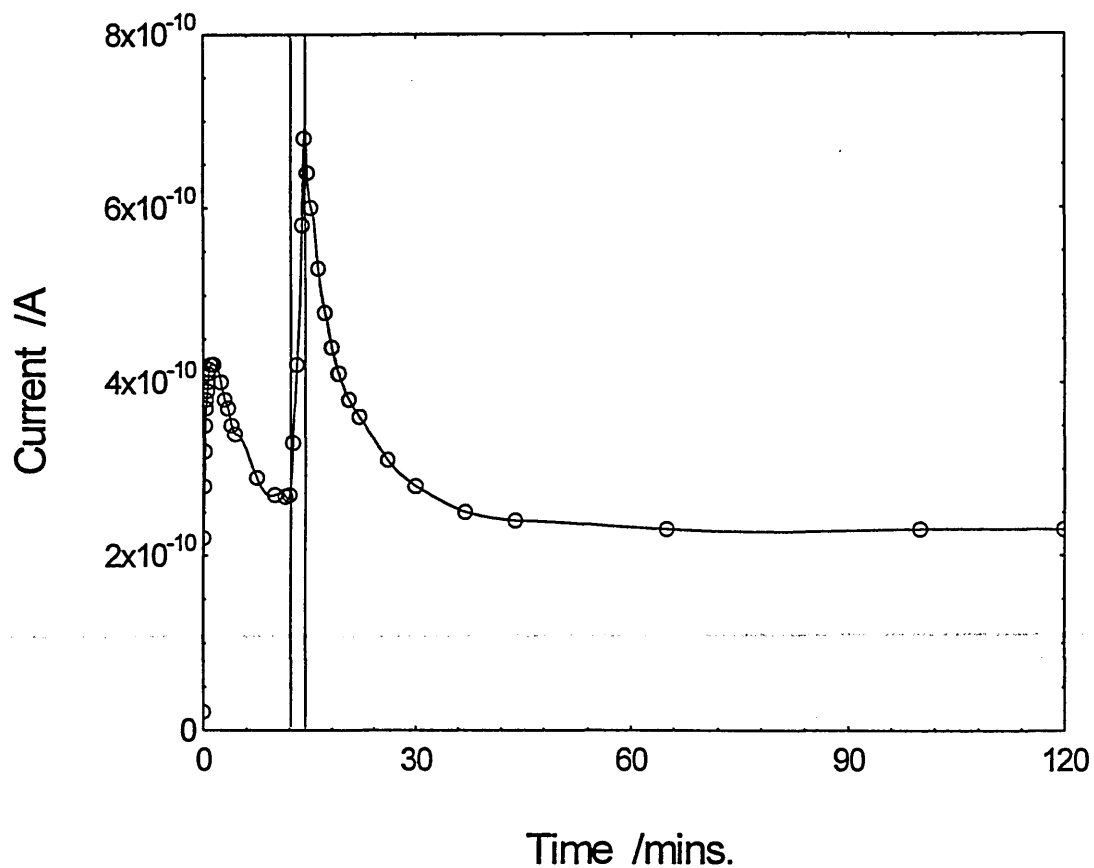
Figure 6.15   *Photo-current at 700nm (100V) as a function of time for*

A406, twenty monolayers thick. Initially in a vacuum, air

was admitted at 12mins for two minutes duration. The

recovery is shown, the recovery is complete after a further

35mins in vacuum. Note: The increase of current in air is

only halted by the resumption of vacuum pumping. Currents

of 16 nA are observed after 1hour in air.
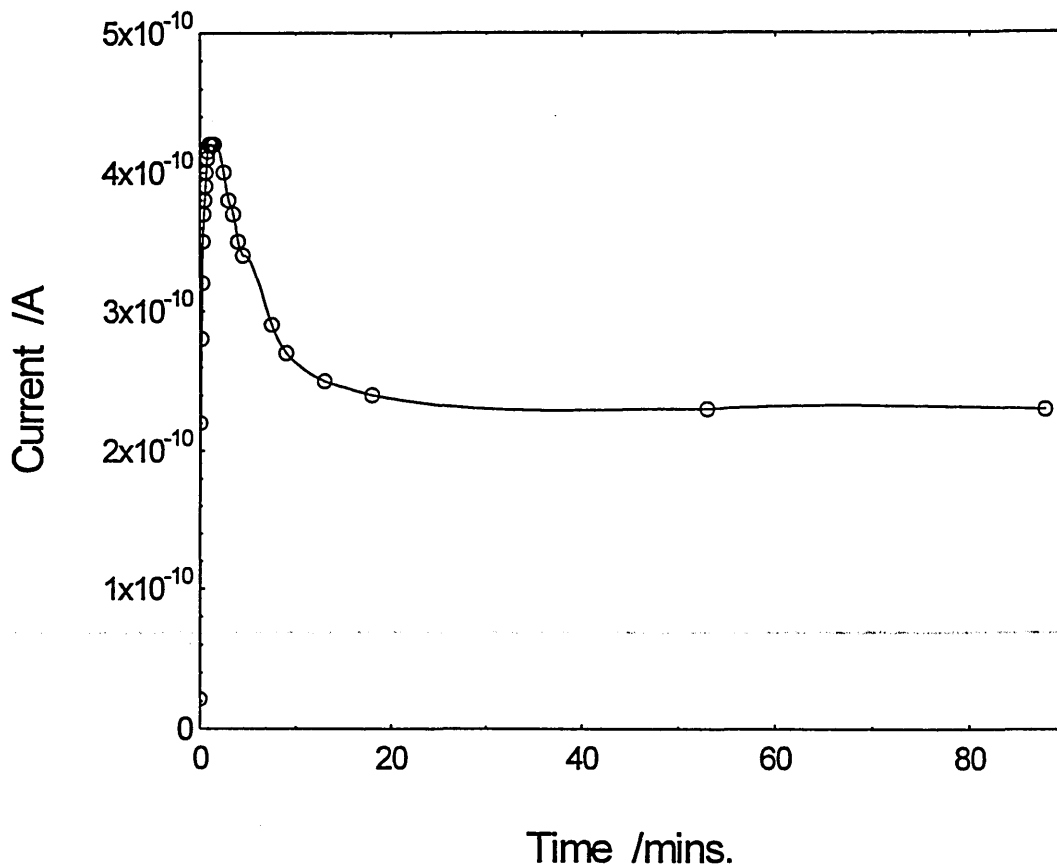
Figure 6.16   *Photo-current response at 700nm as a function of time for*

A406, twenty monolayers thick, in a vacuum with an applied

voltage of 100V. The light is switched on at time =0 mins, and

remains on until time > 90mins.

Figures 6.15 and 6.16 show the photoresponse in relation to time. The effect of

the admitting air into the vacuum is indicated on figure 6.15. As the

photoresponse was found to take much longer to reach a stable value in air, all

measurements were performed under vacuum. The response time to incident light

in a vacuum initially forms a peak photocurrent followed by a gradual reduction

to a stable value after thirty minutes.

In Langmuir-Blodgett films, conductivity processes are determined by traps which are supposed to be connected with the microcrystaline boundaries that occur in Langmuir-Blodgett films. The kinetics of current changes with applied voltage after switching on the light, are usually observed in organic semiconductors and explained by the process of carrier capturing at different traps in the film (Ray et al 1995).

6.4.3 Accuracy and Repeatability.

Accuracy depends on the instrument, the sample environment and the experimental set-up. The electrometer has a greater accuracy than required and thus is not a problem. The environmental effects were reduced to a level where they could be controlled or ignored. The interconnects were shielded for their entire length. The greatest error was due to the ambient gas in which the sample was contained. The film was extremely sensitive to gases, this was apparent in that when the sample chamber was evacuated of air to a pressure of 10^{-1} Torr, the conductivity was greatly affected.

Figure 6.15 shows the study, the effect of the vacuum over air, is to reduce the maximum photo current by a few orders of magnitude. When nitrogen was introduced, the maximum photo current increased. Indicating that the introduced gas (nitrogen), affected the conductivity, or that the gas was contaminated with another active element such as oxygen.

To ensure maximum repeatability and to reduce the effect of external environmental factors, in the experiments, the sample was maintained under constant evacuation with a rotary pump. The level of vacuum (as long as it was 10-1 Torr or better) had no apparent effect on the current, a diffusion pump was used in conjunction with the rotary pump on a number of occasions, there was no detectable difference due to the increased vacuum. This indicates the small relative benefit from 10^{-1} Torr to 10^{-3} Torr over atmospheric to 10^{-1} Torr.

6.5 Summary

The Phthalocyanine films are electrosensitive to environment gases. The photo current is time dependent. The time dependence alters depending upon the gaseous environment of the sample. The sample in a vacuum has a shorter stabilisation time. The sample in an air environment will take much longer to reach an acceptable stable conductivity.

The films display photo conductive properties, the photo conduction spectrum mirrors the optical absorption spectrum. The twin peaks visible on figure 6.9 are further indicators of the similarity. Due to the time involved in the response time for each reading, the detail of the peaks was missed. However, as this data was intended to be used to calculate the activation energy, the detail is not vital. The photo conduction process is attributed to photon generated charge carriers.

Values obtained for the photo-conductivity (700nm) at room temperature are:

0.434nScm^{-1} for A410 (20 monolayers thick),

1.6nScm^{-1} for A406 (20 monolayers thick) and

0.366nScm^{-1} for A406 (9 monolayers thick).

The variation of the photoconductivity for A406 was attributed to the greater carrier photo-generation of the thicker film. Further investigation of this result is required to verify this, and determine the optimum thickness. A406 was chosen as the most suitable material for optoelectronic devices that require a large photoresponse.

The activation energies are calculated for the two materials, two activation energies are obtained for each material, above and below the transition temperature at 250K.

A410, 20 monolayers 0.197eV (T > 250K), 0.092eV (T<250K)

A406, 20 monolayers 0.112eV (T > 250K), 0.191eV T<250K)

A406, 9 monolayers 0.096eV (T > 250K), 0.150eV (T<250K)

Activation energies were not calculated for dark conduction as the current was too low to resolve any difference over the temperature range.

The two regions for the A410 material follow the expected pattern with the low temperature region having a shallower gradient. However, the A406 material has a steeper region at low temperatures.

Chapter 7

CONCLUSIONS AND

RECOMMENDATIONS

The materials investigated in this thesis are novel metal free phthalocyanines, molecularly engineered to be deposited by the Langmuir-Blodgett method. Their intended application is in the optoelectronics field. The properties of interest to device engineers are centred on the structure of the film, the optical properties of the film and the electrical properties of the film.

The molecular structure and ordering are of importance because the optical and electrical properties partly depend upon the molecule-molecule interactions within the film. The molecular orientation of the film molecules was measured geometrically in chapter 3 from information obtained during the Langmuir-Blodgett deposition. The molecular orientation with respect to the substrate was investigated to a fuller extent in chapter 4 using polarised light optical spectroscopy.

The optical properties of the organic film are especially relevant for optoelectronic applications. This is because the information concerning the interaction of the light with the film is the key to effective implementation of these films in devices. Useful optical information can be gained from the optical spectra, the absorption wavelength range, the electronic transitions in the molecule and the molecule-molecule interactions can be surmised from the spectra. Further to this a measure of the refractive index of the film would be of importance for devices that require index matching of constituent materials and for modelling of the optical path. The Surface Plasmon method was chosen as it allows the measurement of the refractive index of a Langmuir-Blodgett film without knowing its thickness. The Surface Plasmon technique also enables calculation of the film thickness, and has potential as an imaging tool to observe defects in Langmuir-Blodgett films.

The electrical properties are obviously of importance when considering these materials for application in electronic devices. The relation between the conductivity and applied voltage, temperature, wavelength of incident light and presence of ambient gases, together with the time dependence of the film to a change in the conditions, all provide important information. This information would be used to anticipate the performance of the film in a given device situation. In addition to this an investigation into the conduction regime of these materials should be of use for modelling the conduction properties, and for comparison between similar materials.

7.1 Langmuir-Blodgett Deposition

The metal free phthalocyanines (A410 and A406) can be successfully deposited on glass and gold coated glass slides. Both materials preferred hydrophobic substrates indicating a strong polar bias of the molecules. The slightly better isotherm of the A410 material mirrored the slightly easier film forming properties of this material over A406.

A410 showed gradual collapse above 35mN/m and A406 showed no collapse up to 28mN/m. Both pressures are acceptable for film forming materials.

A geometrical analysis revealed a tilt angle for both materials using the area per molecule method. The values obtained for the tilt angle using the areas per molecule calculated in this work do not agree with other workers on these materials. Performing the calculation using the areas per molecule of other workers gives a tilt angle of around 66°, which agrees with the result obtained in chapter 4 (section 4.4.2) . This method also revealed the inaccuracy in the area per molecule calculated in this work. This inaccuracy is attributed to the calculation of the concentration of the sample when performing Langmuir-Blodgett deposition, and to a lesser extent, the calculation of the subphase area. Further deposition of this material using the Langmuir-Blodgett method should be accompanied by a detailed re-calculation of the trough area and the sample concentration.

The optical absorbance versus thickness indicates a linear relation between thickness and absorbance, indicating that the films were deposited in a uniform manner.

Both films were successfully deposited on Yoshi slides (platinum interdigitated electrodes) using the same deposition parameters presented. These samples were used for the electrical tests performed in Chapter 6.

7.2   Optical Absorption Studies

For both materials (A410 & A406), the Q-band (550-800nm) and B-band (<500nm) are apparent. Davydov splitting is visible from the peak shape incorporating two main peaks under the absorption envelope. The longer wavelength peak at 770 nm is attributed to the aggregates in the film. The peak at 630 nm is attributed to the dimer with parallel planes. The weak sideband at 680 is attributed to the monomer.

The two materials display similar absorbance spectra of the form expected for these materials (Fernandes et al 1995). The differences in peak size are due to the effect of the differing 'tail' groups of these metal free phthalocyanines.

The results confirm the good quality of the Langmuir-Blodgett deposition, with a linear relation between absorbance and thickness.

For A406, the dimer is almost aligned perpendicularly to the substrate face at 82°. However the aggregate dipole is at 49° to the substrate face, suggesting a staggered stacking formation. The monomer is 20° out of alignment with the dimer at 62°. However the monomer orientation is between that of the dimer and aggregates. This is reasonable as the dimer and aggregates are made up of

monomers. The dipoles are oriented at an average angle of 57° from the dipping direction, this would agree with the herringbone alignment as described by Nabok et al (1995).

For A410, the dimer and aggregation dipole fields are both at 66° from the substrate face indicating a strong columnar stacking of the molecules. The monomer is only fifteen degrees out of alignment at 51°. The dichroism values correspond very well with Fernandes et al (1995) (1.38 @ 772nm and 0.8 @ 636nm). The results are within five percent agreement. The dipoles are also oriented at an average angle of 40° from the dipping direction, this also corresponds to the herringbone alignment (Nabok et al 1995).

Using the areas under the Gaussian-Lorentzian approximations for the Davydov doublet, the values of ϕ are obtained. A406 has $\phi = 44°$ and A410 has $\phi = 44°$. The values are close to what is expected with the β-form molecular crystal of metal free phthalocyanine at $\phi = 45.7°$ (Cook 1993). This result suggests that the analysis method of the angle using polarised spectroscopy (section 4.4.2) is more accurate when averaged over the whole spectrum as in table 4.1 (44°) and not when split into separate peaks as shown in tables 4.2 and 4.3 (57° and 40° respectively). This is an experimental issue that should be further investigated to confirm the validity of the results.

7.3   Surface Plasmon Resonance Studies

The refractive index of the A410 metal free phthalocyanine was calculated to be 1.679, and a film of seven monolayers was found to have a thickness 172 Å by the surface plasmon resonance technique. By using the angle of orientation for the A410 material, $\theta \approx 67°$ (from chapter 4), a molecular length of 26.7 Å is obtained. This is of the order expected for such a molecule.

The images produced, although showing potential, are not of a suitable quality to use for investigating the quality of the Langmuir-Blodgett film deposition. Better quality optics and the use of eight-bit image acquisition software are expected to greatly improve the usefulness of SPR thin film imaging. This imaging technique has potential for inspecting the quality of the Langmuir-Blodgett film surface. Details such as pin-holes, film-overlap and the presence of foreign particles, are difficult to investigate, and are not detected by other film quality tests presented in this thesis. This method is already being developed by other workers as a Langmuir-Blodgett film quality inspection tool (Merle et al 1992, and Morgan et al 1994).

7.4   Electro-optical Studies

The Phthalocyanine films are electrosensitive to environment gases. The photo current is time dependent. The time dependence alters depending upon the gaseous environment of the sample. The sample in a vacuum has a shorter stabilisation time. The sample in an air environment will take much longer to reach an acceptable stable conductivity. The presence of humidity in the air could have a detrimental effect on the results.

The films display photo conductive properties which mirror the optical absorption spectrum. Due to the time involved in the response time for each reading, the detail of the peaks was missed. However, as this data was intended to be used to calculate the activation energy, the detail is not vital. Further tests could be used to investigate this observation. The photo conduction process is attributed to photon generated charge carriers.

Values obtained for the photo-conductivity (700nm) at room temperature are:

$0.434nScm^{-1}$ for A410 (20 monolayers thick),

$1.6nScm^{-1}$ for A406 (20 monolayers thick) and

$0.366nScm^{-1}$ for A406 (9 monolayers thick).

The variation of the photoconductivity for A406 was attributed to the greater carrier photo-generation of the thicker film. Further investigation of this result is required to verify this, and determine the optimum thickness. A406 was chosen as the most suitable material for optoelectronic devices that require a large photoresponse.

The activation energies are calculated for the two materials, two activation energies are obtained for each material, above and below the transition temperature at 250K.

A410, 20 monolayers 0.197eV (T > 250K), 0.092eV (T<250K)

A406, 20 monolayers 0.112eV (T > 250K), 0.191eV T<250K)

A406, 9 monolayers 0.096eV (T > 250K), 0.150eV (T<250K)

Activation energies were not calculated for dark conduction as the current was too low to resolve any difference over the temperature range.

The two regions for the A410 material follow the expected pattern with the low temperature region having a shallower gradient. However, the A406 material has a steeper region at low temperatures. This feature could be due to the higher resistivity expected with materials undergoing thermally activated conduction.

7.5   Suggestions for Future Work

The characterisation of new materials is a task that has no end in terms of the range of measurements, test conditions and number of new materials. Characterisation should be selected to meet the requirements of the application with due regard to cost and time limitations. The investigations carried out in this thesis are to find out the basic information required when considering materials for electro-optic devices. Any further measurements should be the result of a need to find out a property. However there are a few investigations presented in this thesis that could be improved upon. The SPR imaging test was not of a suitable standard to permit its practical application as an imaging tool for thin films. The Langmuir-Blodgett technique is not fully explored in terms of range of deposition pressures, substrate treatments, process temperature, and pH of the subphase. Further tests should be performed to fully characterise the film forming and transfer properties of these materials. The electrical properties were only measured using interdigitated planar electrodes, with limited range of thickness films. Variations in the forming parameters of the Langmuir-Blodgett film may have an influence on the conduction process. Further measurements should also investigate the films photoelectric-response in a sandwich configuration, after a suitable method of depositing an electrode on top of the Langmuir-Blodgett film has been found. Possible techniques include evaporation of the metal, but the substrate should be cooled so that the condensing metal will not heat-damage the film.

Further investigations to those presented in this thesis should be oriented to device applications. The manufacture of devices and testing under the influence of a range of light wavelengths and intensities and under a range of temperatures should be performed to asses the true device potential. These materials sensitivity to the gaseous environment could also be exploited with a view to their application as gas sensors. Characterisation of any devices should include a lifetime study to investigate the deterioration of the film under operating conditions.

These two materials A410 and A406 metal free phthalocyanine are only two of a whole range of possible organic materials that could have the required properties for use in electronic devices. Many of these materials have not been investigated. As long as the chemists still produce new materials, there will be a need for characterisation. To produce the devices that have been predicted as possible using organic materials, more work is needed to find the optimum material and improve the characterisation methods.

References

Armand F., Sakuragi H., Tokumaru K., Okada S., Yase K., Matsuda H., Nakanishi H., Yamada T., Kajikawa K., Takezoe H., **1994.**Thin Solid Films, 245, 202-205.

Ashwell G.J., Jeffries G., Dawnay E.J.C., Kuczynski A.P., Lynch D.E., Gongda Y., Bucknall D.G., **1995** J. Mater. Chem., 5 (7), 975-980.

Baker S., 1985, PhD thesis, Durham University, England.

Baker S., Roberts G.G., Petty M.C., **1983.** IEE Proc. 130, 1(5), 260.

Barger W., Dote J., Klusty M., Mowery R., Price R., Snow A., **1988,** Thin Solid Films 159, 369.

Bliznyuk V., Mohwald H., **1995** Thin Solid Films, 261, 275-279.

Brynda E., Kminek I., Nespurek S., **1989,** J. Mater. Sci, 24, 4164-4167.

Brynda E., Koropecky I., Kalvoda L., Nespurek S., **1991,** Thin Solid Films, 199, 377-384.

Bryne J.F., Kurz P.F., **1967** (to Xerox Corporation), U.S. Patent, 3, 357.

Bryne J.F., Kurz P.F., **1971** (to Xerox Corporation), U.S. Re-issue, 27, 117 of U.S. Patent 3, 357.

Carrara S., Gussoni A., Erokhin V., Nicolini C., **1995** J. Mater Sci. Mater in Elec. (6) 79-83.

Chadderton L.T., 1963, J. Phys. Chem. Solids. 24, 751-757.

Chamberlain G.A., 1971, "Organic Solar Cells - A Review"

Chamberlain G.A., Cooney P.J., **1979,** Chem. Phys. Lett. 66, 88.

Chau L., England C.D., Chen S., Armstrong N.R., **1993**, J.Phys Chem, 97, 2699-2706.

Chen W.P., Chen J.M., **1981,** J.Opt. Soc. Am. 71, 2, 189-191.

Chen Q., Gu D., Gan F., **1994,** Solid state electronics, 37, 10, 1768-1770.

Cheung J.H., Fou A.F., Rubner M.F., **1994,** Thin Solid Films, 244, 985-989.

Cole A., McIlroy R. J., Thorpe S. C., Cook M. J., McMurdo J. and Ray A. K., **1993,** Sensors and Actuators B, 13-14, 416-419.

Cook M.J., Daniel M.F., Dunn A.J., Gold A.A., Thomson A.J. **1986,** J.Chem. Soc. Chem Commun. 863.

Cook M. J., Daniel M. F., Harrison K. J., McKeown N. B., and Thompson A. J. **1987,** J.Chem. Soc., Chem. Commun. Com. 437, 1148-1150.

Cook M.J., Dunn A.J., Gold A.A., Thompson A.J. Daniel M.F., **1988** J.Chem. Soc. Dalton Trans. 1583-1589.

Cook M. J.. 1993, spectroscopy of new Mater. Adv. in Spectroscopy 22(3) 87-149.

Cook M. J.. 1994, J. Materials Sci.:Materials in Electronics. 5, 117-128.

Cook M. J., McMurdo J., Miles D.A., Poynter R.H., Simmons J.M., Haslam S.D., Richardson R.M., Welford K., **1994,** J. Mater Chem., 4(8), 1205-1213.

Cook M.J., 1995 Personal communication to Prof. A.K.Ray.

Couts T. J., 1978, Thin Solid Films, 50, 99-117.

Cresswell J.P., 1992, PhD Thesis, University of Durham.

Cresswell J.P., Petty M.C., Shearman J.E., Allen S., Ryan T.G., Fergusson I., **1994** Thin Solid Films, 244, 1067-1072.

Crockett R.G.M., Campbell A.J., Ahmed F.R., **1990** Polymer 31, 602-608.

Donovan K. J., Scott K., Sudiwala R.V., Wilson E.G., Bennett R., Wilkins R.F., Paradiso R., Clark T.R., Batzel D.A., Kenney M.E., **1994** Thin Solid Films. 244, 923-927.

Eley D.D., 1948 Nature 162, 819.

Fernandes I., Cook M.J., Russell D.A., **1995,** A report produced as part of the DTI LINK programme for Langmuir-Blodgett films.

Fowler M.T., Petty M.C., Roberts G.G., Wright P.J., Cockayne B., **1985,** J.Mol. Elec 1, 93.

Fujiki M., Tabei H., **1988,** Langmuir, 4, 320.

Fuqua P.D., Dunn B., Zink J.I., **1994,** Proceedings of the SPIE Vol 2288, Sol-Gel Optics III San Diego.

Ghosh A.K., Morel D.L., Feng T., Shaw R.F., Rowe C.A. ., **1974,** J.Appl. Phys. 45 (1).

Gould R.D., Hassan A.K., **1993.** Thin Solid Films, 223, 334-340.

Grieve M.B., 1995, PhD thesis, University of Sheffield.

Grunfeld F., Martin P., Szablewski M., **1993.** "Langmuir-Blodgett Systems" Users Manual, NIMA Technology, 3rd Edition.

Grunfeld F., 1994, NIMA technology, Coventry, England, Personal communication.

Gutmann F., Lyons L.E., **1967,** "Organic Semiconductors" Wiley, New York.

Hann R.A., Gupta S.K., Fryer J.R., Eyres B.L., **1985,** Thin Solid Films. 134, 35.

Hassan A.K., Ray A.K., Ghassemlooy Z., Cook M.J., Jennings J., **1995.** A report produced as part of the DTI LINK programme for Langmuir-Blodgett films

Hassan A.K., Ray A.K., Travis J.R., Ghassemlooy Z., Cook M.J., Abass A., 1995. Submitted to J. Phys. D.

Hush N.S., Woolsey I.S., 1971. Mol. Phys. 21, 465.

Isomura K., Takehara K., Kobayashi K., Funakoshi G., Taniguchi H., Era M., Tsutsui T., Saito S., 1994, Thin Solid Films, 244, 939-942.

Iwamoto M., Fukuda A., Itoh E., 1994. J. Appl. Phys. 75(3) 1607-1610.

Jones T.A., Bott B., 1985, Transducers IEEE PA USA 414.

Jones R., Hunter R.A., Davidson K., 1994, Thin Solid Films, 250, 249-257.

Kirstein S., Mohwald H., 1992. Chem.Phys. Lett. 189, 4-5, 408-413.

Kovaks G.J., 1978 Surf. Sci. 78.

Kretchman E., Raether H., 1968, Z. Naturf A, 23, 2135.

Kutzler F.W., Barger W.R., Snow A.W., Wohltjen H., 1987 Thin Solid Films. 155, 1-16.

Langmuir I., 1917, J.Am. Chem. Soc. 39, p1848.

Langmuir I., 1934, J. Franklin Inst. 218, p143.

Lou T., Zhang W., Gan F., 1993, Thin Solid Films 223, 368-370.

Loufty R.O., Sharp J.H., Hsiao C.K., Ho R., 1981, J. Appl. Phys. 52 (8) 5218.

Matsubara K., Kawata S., Minami S., 1988, Applied Optics, 27, 7, 961-965.

McCullough R.D., Williams S.P., 1993, J.Am. Chem. Soc. 115, 11608-11609.

McKeown N.B., Cook M.J., 1988, Thin Solid Films, 159, 469.

Merle H. J., Alberti B., Schwendler M., and Peterson I. R., 1992, J.Phys. D. Appl. Phys. 25. 1556-1558.

Morgan H., Taylor D., 1994. Appl. Phys.Lett. 64,(11) 1330-1331.

Moser F.H., Thomas A.L., **1983**, "The Phthalocyanines - Properties", CRC Press Inc.

Mukhopadhyay S., 1990, PhD thesis, South Bank Polytechnic, London.

Mukhopadhyay S., Ray A.K., Cook M.J., Simmons J.M., Hogarth C.A., **1992.** J.Mater. Sci.: Mater. in Elec. 3, 139-143.

Nabok A., Ray A.K., Hassan A.K., Ghassemlooy Z., Cook M., **1995.** To be submitted for publication.

Nemetz A., Fernandes U., Knoll W., **1994** J.Appl. Phys. 75(3) 1582-1585.

Nespurek S., 1984, Czech J. Phys B. 34.

Nespurek S., Hart R.H.G., Bonham J.S., Lyons L.E., **1984,** Aust. J. Chem. 38, 1061.

Nespurek S., Podlesak H., Hamann C., **1994,** Thin Solid Films, 249. 230-235.

NIMA 1994, "The NIMA 600 Series Langmuir-Blodgett Instruments" NIMA Technology Ltd. Coventry, England.

O'Rourke J. K., Brooks J. S., Bell N. A., and Cawley J., **1993,** Sensors and Actuators B, 15-16, 90-97.

Pearson C., Moore A.J., Gibson J.E., Bryce M.R., Petty M.C., **1994,** Thin Solid Films, 244, 932-935.

Peterson I.R., Girling I.R., **1985.** Sci. Prog. Oxf. 69, 533-550.

Peterson I.R., Russell G.J., **1985.** British Polymer Journal. 17, 4, 364-367.

Petty M.C., 1987 "Polymer surfaces and Interfaces", John Wiley & Sons Ltd. p163-187

Pope M., Swenberg C.E., **1982.** "Electronic Processes in Organic Crystals" Clarendon Press, Oxford Uni. Press, New York.

Popovic Z.D., Sharp J.H., 1977 J.Chem. Phys. 66. 5076.

Poynter R.H., Cook M.J., Chesters M.A., Slater D.A., McMurdo J., Welford K., 1994, Thin Solid Films. 243, 346-350.

Raether H., 1977 Phys. Thin Films. 9, 145.

Ray A.K., Mukhopadhyay S., Cook M.J., 1993, Thin Solid Films. 229, 8-10.

Ray A.K., Hassan A.K., Nabok A., Ghassemlooy Z., Cook M., 1995. Submitted to: IEE Devices, Circuits and Systems.

Ricco A.J., Martin S.J., Zipperian T.E., 1985, Sensors and Accutators, 8, 319.

Roberts J.D., Caserio M.C., 1965 "Basic Principles of Organic Chemistry" Benjamin.

Roberts G.G., Petty M.C., Dharmadasa I.M., 1981, IEE proc.,Vol.128(1) 6, 197-201.

Roberts G.G., 1985 Advances in Physics, 34, 4, 475-512.

Roberts G.G., Petty M.C., Baker S., Fowler M.T., Thomas N.J., 1985. Thin Solid Films, 132.

Rothenhausler B., Knoll W., 1988. Nature. 332, 615-617.

Rudden M.N., Wilson J., 1980. "Elements of Solid State Physics" John Wiley & Sons Ltd.

Sadaoka Y., Sakai Y., Yamazoe N., Seiyama T., 1980. The Chem. Soc. of Japan, 1263.

Saito M., Sugi M., Fukui T., Iizima S., 1983. Thin Solid Films, 100, 117.

Saito M., Sugi M., Iizima S., 1985. Jpn. J. Appl. Phys. 24, 379.

Sakaguchi H., Nagamura T., Penner T.L., Whitten D.G., 1994, Thin Solid Films, 244, 947-950.

Schmeißer D., Rager A., Thonke K., Pilkuhn M., Fröhlich D., Gauglitz G., Schäfer M., Oeikruk D., **1991**. Synthetic metals. 41-43, 1457-1463.

Shirshow Y., **1994** (Academy of science, Ukraine) Personal Communication.

Simmons J.G., **1971.** J. Phys D: Appl. Phys., 4, 623-657.

So F.F., Forrest S.R., **1988.** J.Appl. Phys. 63(2) 442-446.

Stabenow J., **1968**, Der Bunsenges Phys. Chem.72 (3) 374.

Sussman A., **1967**(a) J.Appl. Phys. 38(7) 2738-2747.

Sussman A., **1967**(b) J.Appl. Phys. 38(7) 2748-2752.

Tennent R.M., **1971**, "Science Data Book", Oliver and Boyd, p62.

Thorpe S.C., Broughton R., **1994** Personal communication.

Tokito S., Sakata J., Taga Y., **1995.** Thin Solid Films, 256, 182-185.

Travis J., Ray A.K., Thorpe S.C., Cook M.J., James S.A., **1995.** Meas. Sci. Technol. 6, 1-7.

Tredgold R.H., Jones R., **1981.** IEE. Proc. Vol.128, (1) 6, 202-206.

Tredgold R.H., Smith G.W., **1982** IEE Proc. 129(1) 4, 137-140.

Tredgold R.H., El-Badawy Z.I., **1985**, J.Phys. D: Appl. Phys.18, 2483-2487.

Truong K.D., Bandruauk A.D., Tran-Thi T.H., Grenier P., Houde D., Palacin S., **1994**, Thin Solid Films. 244, 981-984.

Tsibouklis J., Petty M., Song Y., Richardson R., Yarwood J., Petty M.C., Feast W.J., **1991**, J.Mater. Chem., 1(5), 819-826.

Twarowski A.J., **1982.** J.Chem Phys. 76(5) 2640-2645.

Van Ewyk R.L., Chadwick A.D., Wright J.D., **1981**, J. Chem. Soc. Faraday Trans. I 77, 73.

Valarian H., Nespurek S., **1993**, J.Appl.Phys. 73(9), 4370-4377.

Vartanyan A.T., **1948**, Zhur Fim. Khim. 22, 769.

Vincent P. S., Roberts G.G., **1980**, Thin Solid Films. 68, 135-171.

Vincent P.S., Popovic Z.D., McIntyre L., **1981**, Thin Solid Films. 82, 357.

Williams G., Moore A.J., Bryce M.R., Petty M.C., **1994**. Thin Solid Films. 244, 936-938.

Wilson A., Collins R.A., **1987**, Sensors and Actuators. 12, 389.

Winter C.S., Tredgold R.H., **1983**, IEE Proc. Vol 130. (1) 5, 256-259.

Winter C.S., Tredgold R.H., Hodge B., Khoshdel B., **1984**, IEE Proc. Vol.131, (1), 4, 125-128.

Xiao Y., Yao Z., Jin D., **1993**, Thin Solid Films, 224, 237-241.

Xu Z., Zou X., Zhou X., Zhao B., Wang C., **1994**, J.Appl Phys. 75(1) 588-595

Yan W., Zhou Y., Wang X., Chen W., Xi S.. **1992**. J.Chem. Soc. Chem. Commun., 873-875.

Yanagi H., Kataura H., and Ueda Y., **1994**, J.Appl. Phys. 75 (1), 568-576

Yamamoto N., Tonomura S., Tsubomura H., **1981**, J. Appl. Phys. 52(9) 5705.

Yoneyama M., Sugi M., Saito M., Ikegama K., Kuroda S., Iizima S. **1986**, Japanese Journal of Applied Physics, 25, 7, 961-965.

Zhu Y.M., Chen H., Wei Y., Yan W., **1994** Appl. Phys. B., 59, 617-619.

Appendix A

THE LANGMUIR-BLODGETT PRESSURE

AREA ISOTHERM

This appendix describes the isotherm, the practical uses, and a series of examples are presented showing good isotherms and some interesting effects apparent from the shape. A poor isotherm is presented with the likely reasons for failure.

During the Langmuir-Blodgett deposition process, the material chosen to form the film is dispersed on an enclosed water surface. The material is spread, using an organic solvent, so that all the film molecules are in contact with the water, the hydrophobic and hydrophillic terminations of the molecule (also known as amphiphillic molecules) ensure that the molecules all align in the same direction. By using sliding barriers the enclosed surface area of the water is reduced forcing the film molecules into closer contact. The compression process is analogous to the compression of a two dimensional gas into a liquid and then into a solid as shown in figure A.1.
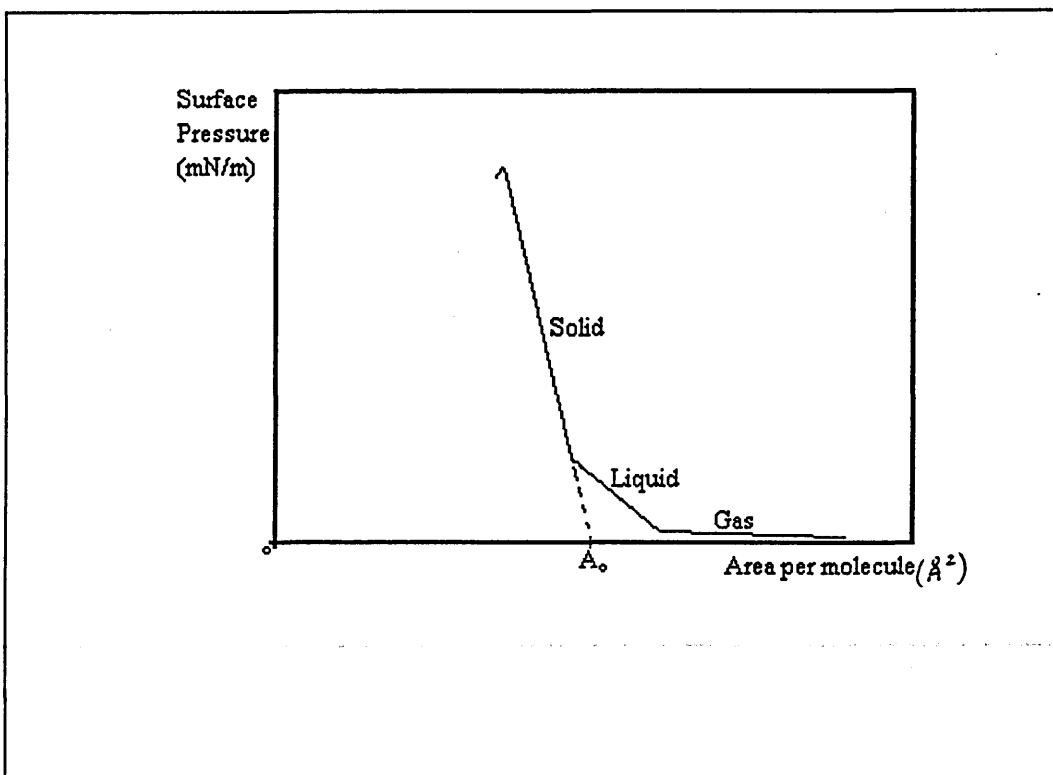
Figure A.1 The idealised isotherm, showing gaseous, liquidous and solidous compression and the area per molecule extrapolation.

By measuring the surface pressure (section 3.2) and the area of the enclosed water surface, a plot of the increase in surface pressure due to the reduction in area can be observed. This plot is referred to as an isotherm from thermodynamic science notation as the temperature is constant whilst the pressure and area change. As the L-B compression is a two dimensional process, the surface pressure is measured in force per unit length (not force per unit area). Usually the enclosed area is used with details about the quantity of sample, the concentration if the sample and the molecular weight of the film to calculate the area per (film) molecule. This calculation is done by the NIMA trough software in real time so that an isotherm

of area per molecule verses surface pressure can be monitored during compression.

It is possible to determine from an isotherm the area taken up on the water surface by each molecule. By knowing the quantity of the film material, the enclosed area and the compression properties revealed by the isotherm, the linear part of a compression isotherm can be projected to zero pressure and thus the area per molecule on the water surface can be obtained by reading the value of the x axis at the projected intercept (A_o on figure A.1).

One feature that occurs with some organic molecules is a kink in the compression curve as shown in figure A.2. This feature is due to the molecules moving from one, quasi-stable, two-dimensional packing to another, closer packed, alignment. The two different phases have different densities and it is usually the higher density (and higher surface pressure) phase that is deposited.
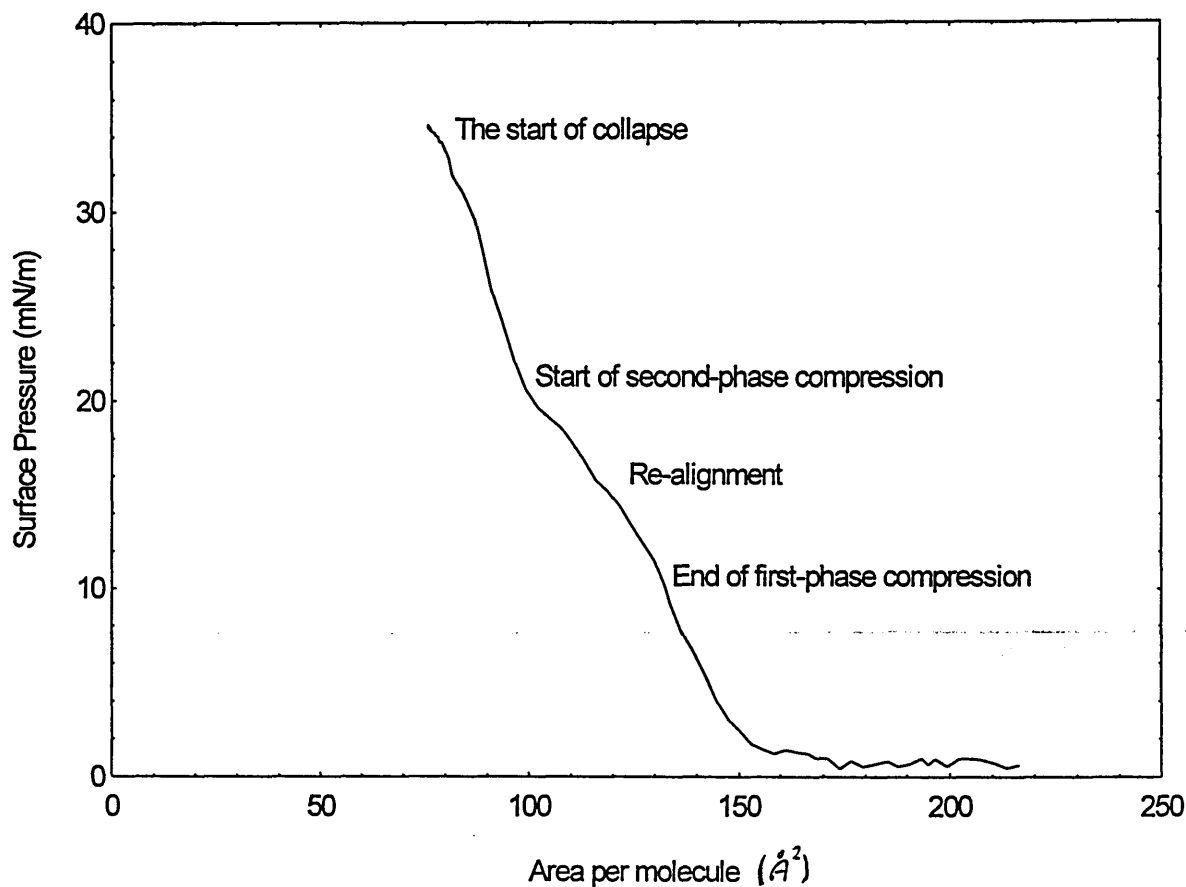
Figure A.2 An actual isotherm showing a two-phase compression.

(Not A410 or A406)

As the surface area reduces, the surface pressure increases, due to the film molecules being compressed. Eventually, the pressure is greater than can be sustained by the film and collapse occurs. Depending on the stability of the film, the collapse is either catastrophic or gradual (or something in-between). Highly stable films collapse or shatter completely and subsequent compression results in the surface pressure decreasing dramatically. Flexible or less stable films fold along domain boundaries resulting in a stabilisation of the pressure with further

compression, as the film gradually folds over its self as shown in figure A.3. The

pressure at which all types of collapse occur, depends on the stability of the film.
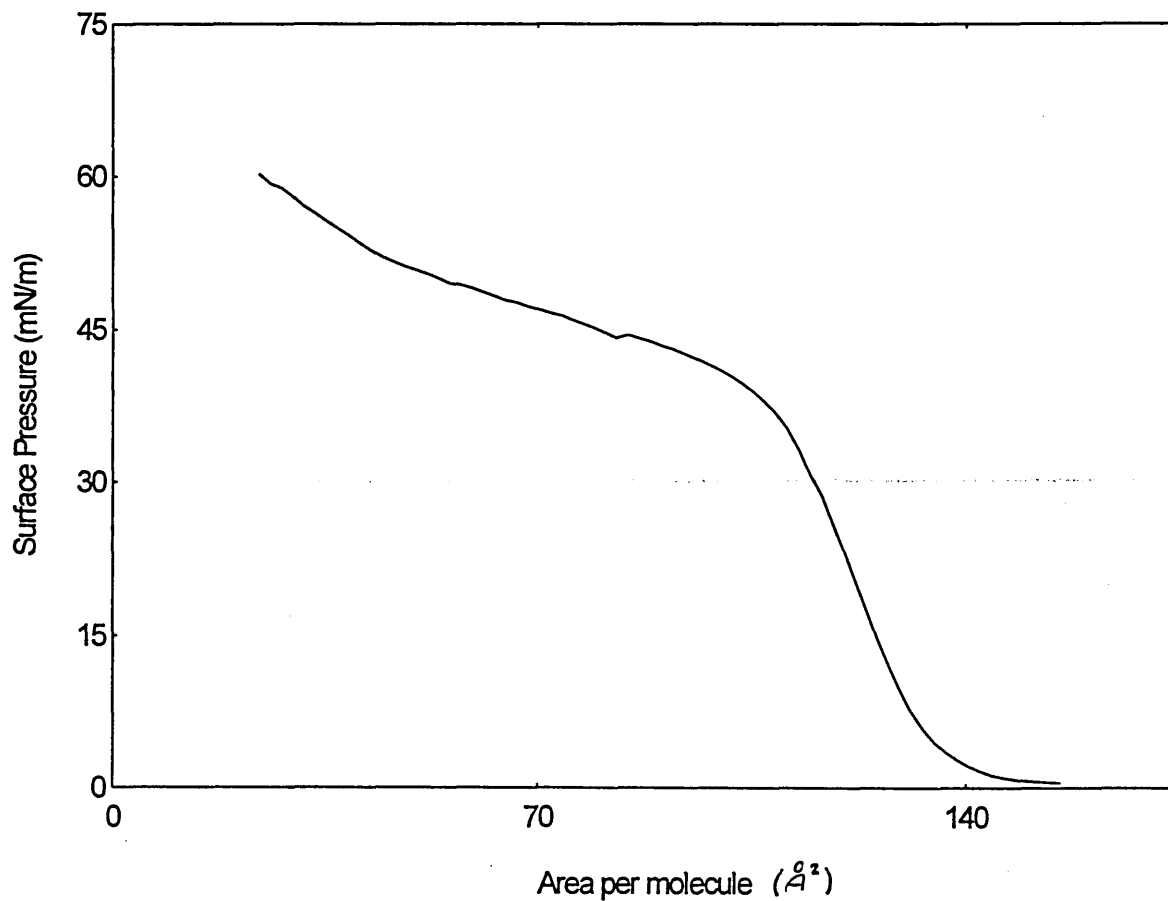
Figure A.3 Showing gradual increase of pressure above the collapse point as

the film gradually folds. (A410)

If the film or water surface is greatly contaminated, or the film material will not

form a stable monomolecular film, the isotherm resembles the result presented in

figure A.4.
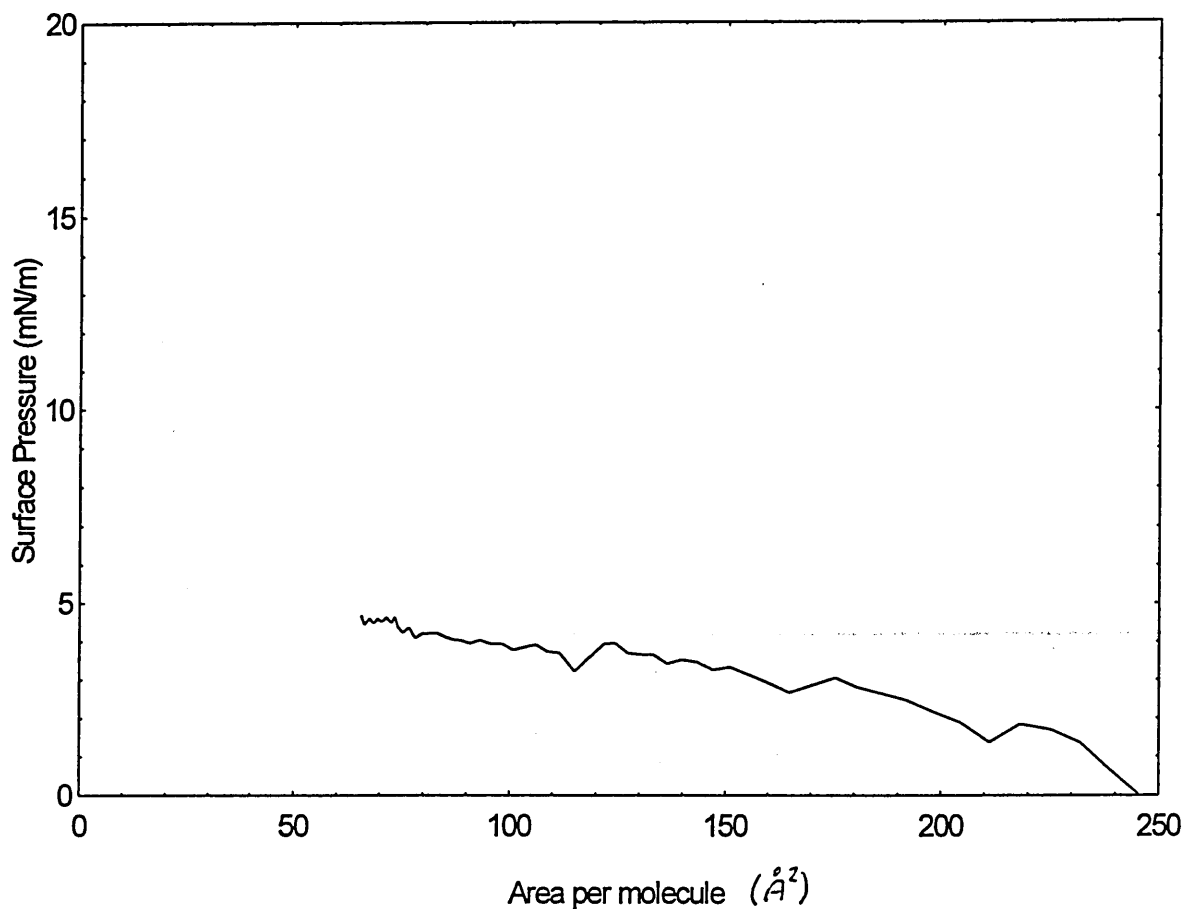
Figure A.4 A poor isotherm, showing little capability of the film to hold a

surface pressure.

As the presence of contaminants reduces the structural integrity of a monomolecular film, further compression does not produce a large increase in surface pressure. The resultant isotherm is shallow and sometimes roughness is apparent where the film collapses in stages. However some materials do not readily form a good isotherm. This is usually due to the materials having weak amphiphillic properties, and thus not having the required stability.

Appendix B

ACCURACY ESTIMATION

It is rare to find an estimate of the error margins in published work in the field of this thesis. However with many of the measurements presented, information about the expected error would be useful for subsequent workers to compare published work to their own results. It is with this in mind that the following brief resume of the measurements is presented with estimated error margins. On certain graphs in this thesis, an estimate is provided of the likely accuracy of the result.

The Langmuir-Blodgett technique is difficult to perfect. The causes of variations in the film quality are contaminants and, fundamentally, the care taken by the operator to ensure good conditions. The resulting film is often non-uniform and may not even transfer from the subphase. However, there are numerous checks to confirm the thickness and quality of the film. Even before the transfer of film material, the isotherm can be used to verify that the area per molecule corresponds to the predicted value (from the synthetic chemist). This depends on accurate measure of the film-to-solvent concentration. Solvent evaporation should be taken into account on older solutions, but a solution should not be kept for more than a week. The amount of material deposited on the water is a small

source of error, but as the loss of material whilst using a micro syringe is dependant on the skill of the operator, the error can be reduced. The enclosed water surface area is also used to calculate the area per molecule. The software is calibrated to the open and closed barrier positions, and the barrier speed, so the change in area will be more accurate than the absolute measure. Which means the isotherm will have the correct shape even if the scale is inaccurate. The first check of deposited film quality is the transfer ratio. This relies on accurate measure of the enclosed water surface area, which is made difficult as the enclosed area is complex due to curved corners, variations due to the meniscus of the water at the trough edges, and the substrate and Wilhelmy plate areas. From statistical variations noted during this programme of work, the area per molecule varies by 10% and the collapse pressure has a 15% range. However as the sample concentration was not measured to great accuracy (due to the limited quantity of film material available), a further error of as much as 30% in the absolute value of area per molecule could be possible. A transfer ratio (TR) of 100% is rarely achieved. This is due to a number of physical reasons. The film could be unstable or leaking around a barrier resulting in gradual collapse giving rise to higher TRs than expected. An area-time plot at constant pressure will reveal unwanted collapse. Film deposition and peel are likely with films that have low attraction to themselves, resulting in positive then negative TRs. Monitoring the meniscus can give indications of when this is happening. If the meniscus is in the opposite direction to the substrate motion, then peeling of the monolayer is likely. A related problem is uneven deposition, caused by poorly cleaned substrates. This effect causes uneven TRs and the unevenness can be visibly seen on thicker films.

The meniscus direction change that occurs during L-B deposition also gives rise to a variation in the effective substrate area. This last reason is small but unavoidable, the ideal TRs are alternately slightly above and below 100% (a 5% variation is common for a glass slide, but this does depend on the height to width ratio of the substrate).

The optical absorption measurements utilise industry standard measurement equipment incorporating reference samples and software baseline compensation to provide reliable results. The optical molecular orientation measurements are an approximation, but due to the low statistical variation (2%) between samples the measurement itself is repeatable.

The surface plasmon technique is experimentally effective, provided the dip in the reflectivity curve gets as close to zero as possible. Modelling of the curve can result in very close fitting between experimental and theoretical points thus indicating the model provides accurate results.

The electrical measurements are performed using an accurate electrometer, nominally capable of measurements of 10^{-12}A. However electrical currents much below the nanoampere (nA = 10^{-9}A) range are notoriously difficult to measure due to stray electric fields, leakage through contaminants and environmental conditions. Currents below 0.03nA were ignored, due to the noise levels of this magnitude. The measurements were prone to poor time stability. The time dependence of the readings was compensated for by taking all readings after

1hour stabilisation. Atmospheric effects were reduced by performing all measurements with the sample held under a moderate vacuum (10^{-1} Torr). The temperature of the sample was measured with a thermocouple of high accuracy, however the thermocouple is not placed on the sample but at the heat exchange block. The temperature of the sample compared to the reading, would then depend on the temperature gradient between the thermocouple and the sample. This was estimated at 2% at 160K decreasing linearly to 1% at 300K. The results measured under these optimised conditions were repeatable to within 10%.